UNIVERSITY OF NOTTINGHAM

Using Physiological MRI to Estimate Dynamic Cerebral Autoregulation Metrics

Functional MRI Feasibility Study

Negar Hawezi

30/04/2015

Contents

1.1 Background 15

1.2 Physiological aspects of Cerebral Autoregulation 18

1.2.1 Static and dynamic cerebral autoregulation 20

1.3 Cerebral circulation 23

1.3.1 Circle of Willis 23

1.3.2 Blood Brain Barrier BBB 26

1.4 Impairment in cerebral auto regulation 27

1.4.1 Cerebrovascular reserve and misery perfusion 27

1.4.2 Cerebral Autoregulation and Hypertension 28

1.4.3 White matter hyper intense lesions (Leukoaraiosis) 30

1.4.4 Stroke risk association with auto regulation 32

1.5 Measuring dynamic cerebral autoregulation 34

1.6 Functional magnetic resonance imaging 37

1.6.1 Calibrated BOLD and hypercapnia method 39

1.6.2 Phase contrast magnetic resonance angiography (PC MRI) 41

1.7 Non invasive methods to induce blood pressure fluctuations 43

1.7.1 Sudden release of inflated thigh-cuff 43

1.7.2 Respiratory challenges 44

1.8 Conclusion 46

2 Systematic Review of Literature 47

2.1 Introduction 47

2.2 Methods 49
2.3 Results 51
2.4 Methods to quantify CA metrics 54
2.4.1 Magnetic resonance imaging (MRI) studies 54
2.4.2 Trans-cranial Doppler ultrasound studies (TCD) 58
2.5 Cerebral autoregulation indices 60
2.6 Discussion 64
2.6.1 Non invasive physiological method to measure CA 64
2.6.2 Consistency of CA metrics 65
2.6.3 Regional heterogeneity 66
2.6.4 Interventions to fluctuate blood pressure 69
2.6.5 Limitations 72
2.7 Conclusions and future directions 74
3 Obtaining beat-to-beat Arterial Blood Pressure Measurements using Non invasive methods 75
3.1 Background 75
3.2 Plethysmographic arterial blood pressure recording devices 78
3.2.1 MR compatible arterial blood pressure monitoring device (NIBP-MRI/Caretaker; Biopac®) 78
3.2.2 Non invasive Continuous Arterial Blood Pressure Monitoring Device from (Finometer ®) 79
3.2.3 Technical issues 82
3.3 Monitoring beat-to-beat arterial blood pressure measures 83

3.3.1 Methods and materials 83
3.3.2 Data Analysis 88
3.3.3 Thigh-cuff release method 90
3.3.4 Inspiratory and non-inspiratory BH 95
3.3.5 Cued Deep Breaths 100
3.4 Conclusions 103
Chapter 4 105
4 Using Physiological MRI to Estimate dCA Metrics 105
4.1 Introduction 105
4.2 Methods and materials 107
4.3 Data Acquisition 109
4.4 Data analysis 112
4.4.1 Pre-processing 112
4.4.2 Regional time series extraction 113
4.4.3 Non invasive interventions to induce BP fluctuations 116
4.5 Results 125
4.5.1 Thigh –cuff release 125
4.5.2 Inspiratory breath-hold method iBH 128
4.5.3 Statistical analysis 131
4.6 Discussion 133
4.7 Limitations 137
Chapter 5 141

5 Time Resolved Phase Contrast Angiography (4D PC MRI) and Breath-Hold method 141

5.1 Background 141

5.2 Methods and Materials 143

5.3 Data acquisition 143

5.4 Data Analysis 144

5.5 Results 147

5.6 Discussion 152

5.7 Conclusion 156

6 Summary of the work presented in this thesis 157

7 References 161

Table of Figures

Figure 1 Classic cerebral autoregulation curve [32] **22**

Figure 2 Circle of Willis (CoW), Time of Flight Angiography (ToF) **25**

Figure 3 Chart of search results (PRISMA statement) **53**

Figure 4Methods to simulate dynamic cerebral auto regulation **57**

Figure 5 Summary of non invasive BP fluctuation methods **77**

Figure 6 Caretaker finger cuff, port and graphical user interface GUI **81**

Figure 7 Finometer finger cuff and device **81**

Figure 8:Schematic representation of cued deep breathing test (CDB) and observed BP response. **87**

Figure 9: Blood pressure (BP) response curve to thigh-cuff release (TCR) method **91**

Figure 10 Mean arterial blood pressure (MAP) from Caretaker device **97**

Figure 11 :Sequential representation (from left to right) of iBH protocol instruction slides **111**

Figure 12: Watershed areas segmentation **115**

Figure 13: Thigh-cuff release test (TCR) in the scanner **119**

Figure 14: Breath-hold test (modeling different variables) **120**

Figure 15 Reactivity analysis of brain, for iBH challenge (23 years, male subject) **130**

Figure 16 Bland-Altman plots **132**

Figure 17 Graphical representation of the relationship between CBF and PaCO2 [131]. **136**

Figure 18: 4D PC MRI data analysis from GT-flow **145**

Figure 19: Average flow velocity **148**

Figure 20 Flow curve through three different arteries **149**

Figure 21: Peak systolic and end diastolic velocities **150**

Figure 22 Mean arterial blood pressure (MAP) during BH and iBH protocols **155**

Table of Tables

Table 1 Summary of the autoregulation indices used to estimate dCA 63

Table2 Summary of the volunteers who participated in each protocol. TCR, Thigh-cuff release, iBH, deep-inspiratory breath-hold test. BH, non-inspiratory breath-hold test. CDB, cued deep-breathing. BOLD, Blood oxygen level dependent MRI, 4D PC, Time resolved Phase-contrast MR angiography.....86

Table 3: Mean arterial blood pressure measures (MAP) at the baseline from the three devices (Omron-HEM, Caretaker, and Finometer) 92

Table 4 MAP measures from the Caretaker and Finometer devices at different time points after cuff-deflation 92

Table 5: mean arterial blood pressure (MAP) responses to 20-second deep-inspiratory breath-hold (iBH) ...96

Table 6: mean arterial blood pressure (MAP) responses to 20-second non-inspiratory breath-hold (BH) 96

Table 7: summary of mean arterial blood pressure (MAP) measures after cued deep breath test (CDB). 101

Table 8: Summarizing the percentage BP change-responses to non invasive arterial blood pressure fluctuating methods.....104

Table 9: Estimated CA parameters for five accepted TCR measures 127

Table 10: summary of CA parameters calculated for iBH method 129

Table 11 Example of flow velocity output data from GT-flow software (Basilar artery at baseline) (23 years; male).....146

Table 12 Flow velocity for two subjects at averaged 20 phases of cardiac cycle time points. At baseline, at 33% inspiratory breath-hold (iBH), and at 33% non-inspiratory breath-hold (BH) 151

Abstract

Cerebral autoregulation is the homeostatic mechanism that maintains sufficient cerebral circulation despite changes in the perfusion pressure. Dynamic CA refers to the changes that occur in CBF within the first few seconds after an acute MAP change. Assessment of the CA impairment plays important role in the prognosis of many cerebrovascular diseases such as stroke, sub-arachnoid haemorrhage, as well as traumatic brain injury and neurodegenerative disorders.

This thesis investigates the feasibility of using physiological MRI to estimate dynamic cerebral autoregulation (dCA) metrics. In particular, this thesis has an emphasis on measuring beat-to-beat arterial blood pressure inside the scanner to provide better understanding of the physiological aspects of dCA. Further, continuous blood pressure (BP) measures in response to different non invasive BP fluctuating methods are acquired to evaluate the reliability of these methods to induce response changes.

Blood Oxygen Level Dependent (BOLD) fMRI method was used to estimate the expected variations of tissue oxygenation during induced dCA changes in healthy volunteers. The non invasive arterial blood pressure measurements were acquired using MR compatible arterial blood pressure monitoring device (NIBP-MRI/Caretaker; Biopac®). Further, sudden release of inflated thigh-cuffs (TCR) and inspiratory breath-hold (iBH) methods were used in the scanner to induce dynamic autoregulatory changes. These two methods were investigated in a pilot study, to evaluate the reliability prior to the MR study by comparing BP measurements obtained outside the scanner using non invasive methods. This pilot study included monitoring BP changes in response to four types of non invasive BP fluctuating methods. The reliability of NIBP/MRI Caretaker device was examined by comparing the BP response changes with the simultaneously acquired BP data from Finometer plethysmographic device. The cerebral autoregulation metrics were estimated

by calculating the rate of regulation (RoR) following dynamic BP fluctuating events. Rate of regulation defines the rate at which the BOLD signal changes depending on MAP changes at a particular time. Further, the tissue specific regulation parameters were obtained for grey matter (GM), white matter (WM) and water shed areas (WS). The effect of iBH method on cerebral blood flow (CBF) and velocity (CBFV) was explored in a preliminary study by quantitative measures using time resolved 4D PC MRI angiography in two subjects.

The mean arterial blood pressure (MAP) changes in response to TCR and iBH method were comparable. The fMRI data demonstrated BOLD signal amplitude change in response to the induced fast MAP changes. The GM and WS areas showed similar rates of regulation, and these were nominally higher than WM RoR in both TCR and iBH methods. Further, the 4D PC MRI data suggested 29% CBF-increase in response to 33% iBH in four minutes acquisition time.

The acquired non invasive arterial BP measures concurrent with the BOLD signal amplitude response, allowed deriving the rate of regulation as a metric of dCA. It is not known whether this information is clinically relevant to gauge the haemodynamic risk association to cerebrovascular disease. However, BOLD signal change and CBF changes after iBH are confounded by the extent to which the CO2 gradually accumulate in response to iBH and causes an overshoot in the CBF response-change.

In conclusion, the presented study indicates the feasibility of using physiological MRI to measure dCA in response to non-invasively induced MAP changes. Estimation of the dCA metrics could be improved by using advanced data fitting methods as well as controlling for physiological parameters such as PECO2.

Declaration

I hereby declare that this thesis is my own work and effort and that it has not been submitted anywhere for any award. This thesis is my own original research undertaken at the Departments of Radiological Sciences and Anaesthesia, Division of Clinical Neuroscience, School of Medicine, University of Nottingham, Queens Medical Centre, Nottingham from Oct 2012 to Sep 2014.

The ethics permission was obtained after the approval for minor amendments from Nottingham Ethics Committee to the developmental Ethics approval for novel MR techniques within Radiological Sciences (B12012012A).

I was responsible for the recruitment of volunteers, informed consent provision, organisation, scanner set up, BP measurement and BP stimulation interventions. I have assisted and run the MR scanning under the supervision of qualified MR technician (Anita French) at 3T GE scanner, Queens Medical Centre. Subsequent to the MRI scans I was responsible for all the post processing and interpretation of the MRI data. I compiled all the datasets and performed analysis and statistical tests.

Acknowledgment

This feasibility study on using MRI to estimate CA metrics could not have been made possible without the contribution and help from my esteemed colleagues.

First and foremost I wish to express my gratitude towards my supervisor Professor Dorothee Auer for her support, attention to detail and continuous guidance throughout the study. I am also indebted to Professor Ravi Mahajan for all his experienced advices and certain availability to help through my work. I would like to thank Dr Nishath Altaf for his support and motivating advices that helped enormously through my study.

I wish to acknowledge the help I have received from Dr Mark Horsfield and Professor Ronney Panerai from the University of Leicester for setting up TCR method. I would also like to convey thanks to Dr Amir Awwad for helping on 4D PC MRI and his valuable guidance and advice throughout the project. Special thanks to Maryam Abaei and Dewen Meng for helping on FSL FEAT and I would like to thank William Cottam, Tom Welton for answering all my questions. Very special thanks to my best friend and sister Dr. Afaf El Saraj, without you I would be lost. I would like to thank Dr. Arshak Aram for tackling all those digital problems and keeping me always motivated. In addition I would like to thank all the staff and students in the Division of Radiological Sciences at University of Nottingham, they have enthusiastically contributed as participants during the development of this study, without their cooperation this project would not have been possible. A Special thanks goes to the staff at the University of Nottingham MR-unit for scanning all my study participants. Exceptional thanks for Dr Azad Hawezi for his continuous

support and understanding, thank you for being there for me unconditionally.

I wish to express my love and gratitude to my beloved family for their understanding and endless love, through the duration of my study and for being there for me always. My greatest gratitude goes to my mum, thank you for keeping me motivated and positive. ACRAD office the fish-tank gang, thank you for providing plenty entertainment and making studying enjoyable time. Special thanks for who are probably bored of hearing "once I've finished my thesis!" (Sorry Seno!).

Abbreviations

2D PC MRI Two-dimensional phase contrast magnetic resonance imaging

4D PC MRI Time resolved three-dimensional phase contrast magnetic resonance imaging

ABP Arterial blood pressure

ACA Anterior cerebral artery

ACoA Anterior communicating artery

ASL Arterial Spin Labelling

BA Basilar Artery

BBB Blood brain barrier

BH breath-hold

BOLD Blood oxygen level dependent magnetic resonance imaging contrast

BP Blood pressure

CA Cerebral autoregulation

CBF Cerebral blood flow

CBFV Cerebral blood flow velocity

CBV Cerebral blood volume

CCA Common Carotid artery

CD Compressed disk

CI Confidence Interval

CMRO2 Cerebral metabolic rate of oxygen

CNS Central nervous system

CoW Circle of Willis

CVR Cerebrovascular reactivity

dCA Dynamic cerebral autoregulation

DVD Digital Video Disk

ECF Extra cellular fluid

EDV End Diastolic Velocity

FEAT Functional Expert Analysis Tool

fMRI Functional Magnetic Resonance Imaging

fNIRS Functional Near-Infrared Spectroscopy

FOV Field of View

FMRIB Oxford Centre for Functional Magnetic Resonance Imaging of the Brain

FSL FMRIB Software Library, a collection of functional and structural brain image analysis tool

GM Grey Matter

GT-flow Gyro-tools flow analysis software

GUI graphical user interface

HRF Haemodynamic Response Function

iBH Inspiratory Breath-Hold

ICA Internal Carotid Artery

IHGT Isometric hang grip test

MAP Mean Arterial Pressure

MCA Middle Cerebral Artery

MCA v Middle Cerebral Artery velocity

MNI Montreal Neurological Institute

MR Magnetic Resonance

MRI Magnetic Resonance Imaging

MW Mental Work

PCA Posterior Cerebral Artery

PCoA Posterior communicating Artery

PET Positron emission tomography

ETCO2 End Tidal CO2 concentration

PSV Peak Systolic Velocity

ROI Region of Interest

RoR Rate of Regulation

R-rec rate of recovery

SD Standard Deviation

T Tesla, the standard unit of magnetic flux density, it is equivalent to one weber per meter squared

TCCD Trans-Cranial colour Doppler

TCD Trans-cranial Doppler

TCR Thigh-cuff Release

TE Time of Echo

ToF Time of Flight

TR Repetition Time

VA Vertebral Artery

WM White matter

WMHL White Matter Hyper Intense Lesions

WS Watershed

WS1 Anterior Boarder Zone

WS2 Internal Boarder Zone

WS3 Posterior Boarder zone

Chapter one Introduction

1.1 Background

Autoregulation refers to the changes occurring in an organ during fluctuations in perfusion pressure to keep the blood flow relatively constant. Because of the high metabolic demands of the brain, cerebral autoregulation (CA) is one of the most important autoregulation mechanisms in the body that allows the brain to match its metabolic demands [3]. During physiological conditions such as low and high perfusion pressure, CA protects the brain from cerebral hypoxia and brain edema [1]. Cerebral autoregulation is impaired in many cerebrovascular diseases such as stroke and sub-arachnoid hemorrhage, as well as in traumatic brain injury and neurodegenerative disorders[2-5]. Understanding CA alterations may help to understand the neuronal damage related to cerebrovascular diseases, hence it has an important prognostic value. Establishing a simple diagnostic tool to estimate CA metrics is necessary in order to assess the haemodynamic risk association of cerebrovascular disorders [9]. Several physiological factors contribute to maintaining sufficient blood supply to the brain such as blood pressure (BP), partial pressure of end-tidal CO2 ($ETCO_2$), and sympathetic tone [6]. CA metrics could be estimated by measuring the underling CBF and CBV changes [7]. Furthermore, the CMRO2 is another dynamic factor that should be accounted for when estimating CA [8]. Measuring CA metrics should include physiological aspects associated with the underlying CBF changes. Recent literature has shown the necessity of

including all derivatives when estimating CA metrics, particularly the arterial BP [9]. Recent studies suggest that including BP measures improves time varying estimates of CA [10]. Techniques with high temporal resolution such as trans-cranial Doppler (TCD) allow for continuous recording of CBFV. This allowed the identification of transient responses of CBFV to sudden changes in BP, and hence estimation of dynamic CA (dCA) [6]. This thesis focuses on measuring the dynamic CA metrics only, using non invasive methods.

Estimating the dCA metrics requires high spatial and temporal resolution techniques. Increasing the temporal resolution of the dCA estimation parameters is important for two reasons; first, CA is, like other physiological processes, modulated by several biological factors that change over time [11]; and secondly, the vasoactive mechanisms that modulate cerebrovascular resistance, show variable degrees of non-stationarity [9].

Various techniques have been used to measure dynamic cerebral autoregulation such as Trans-cranial Doppler ultrasound (TCD), magnetic resonance imaging (MRI) and functional near infrared spectroscopy (fNIRS) [12-16]. Quantitative measures of cerebral blood flow (CBF) and velocity (CBFV) are dependent variables of autoregulation parameters. MRI and TCD measures of these parameters have been used in clinical and research settings to estimate CA metrics. The TCD measures of cerebral blood flow velocity (CBFV) have been a standard way of measuring CA metrics [12]. However, wider clinical application of TCD measures may be affected by the limited spatial resolution of the technique [17]. In the last two decades, the developments in the analysis and applications of functional magnetic resonance imaging (fMRI) have improved CA measurements with high temporal and spatial determinations [18-20].

Furthermore, quantitative MR-imaging techniques have opened the way for non invasive and more reliable methods of quantifying cerebral haemodynamic metrics, such as dynamic susceptibility contrast measures of cerebral blood volume (CBV)[21], phase contrast magnetic resonance imaging [22] and arterial spin labelling (ASL) [23]. Determining the autoregulation parameters in a healthy brain is an important factor in establishing a physiological diagnostic tool to measure dCA metrics. In this chapter, the physiology of intact cerebral autoregulation will be discussed first, including the anatomy and histological compartments of cerebral circulation. Second, two types of cerebral autoregulation, dynamic and static autoregulation, will be described and then the impaired autoregulation and some pathological conditions will be discussed. Finally the MR diagnostic tools used to measure dCA metrics will be discussed.

1.2 Physiological aspects of Cerebral Autoregulation

Cerebral blood flow remains relatively constant despite changes in the cerebral perfusion pressure (CPP) throughout the process of autoregulation [24]. Normally the CBF is estimated as about 20% of the total cardiac output, which measures about 700-850 ml per minute [24, 25]. When CPP increases, this leads to vasoconstriction, the process of narrowing the vascular diameter to increase the vascular resistance. Increasing the resistance protects the brain against the risk of hyperperfusion. Vasodilatation occurs in response to a drop in CPP; the vasodilatation lowers the vascular resistance and decreases the risk of hypo perfusion[24].

The resistance arteries' smooth muscles will dilate and constrict, responding directly to decreases and increases in perfusion pressure, respectively [26]. Changes in the oxygen extraction fraction (OEF) preserve tissue oxygenation during changes in CPP [27]. Thus the cerebral blood flow is preserved through a complex mechanism of metabolic and vascular motor function.

Cerebral autoregulation provides sufficient blood supply to match the metabolic rate of brain. When the metabolic rate elevates in response to neural activation, the CBF increases to reach the metabolic demands, and thus the concept of cerebrovascular reactivity (CVR) arises [28, 29].

Neurovascular coupling is a term used to describe the process of coupled neural activity and cerebral metabolism activity that is facilitated by vasoactive mechanisms. Multiple mechanisms participate in maintaining a constant CBF such as myogenic, metabolic and local neurogenic factors [9].

Cerebrovascular reactivity provides the basics for neurovascular coupling, which may interfere with the autoregulation of cerebral blood flow. Cerebral autoregulation is abolished if vessels fail to dilate and constrict in response to neural activations [30].

1.2.1 Static and dynamic cerebral autoregulation

Cerebral autoregulation comprises cerebral arteriolar vasodilatation and vasoconstriction in response to fluctuations in the mean arterial blood pressure. This could be described as "static" cerebral autoregulation, which is the ability of CBF to respond to longer lasting changes in MAP, and "dynamic" CA, which refers to the changes that occur in CBF within the first few seconds after an acute MAP change [31]. Thus there are two types of CA evaluation, the static and the dynamic approach. The steady-state (static) evaluation of cerebral autoregulation is the basis for the classical autoregulation curve (Figure 1). The static autoregulation metrics are estimated by measuring CBF at a constant baseline arterial pressure, followed by another CBF measurement that is taken after the ABP manipulation and the corresponding autoregulation response have been completed [32]. Lassen et al (1959) were the first to describe the static CA in humans, by measuring CBF using the Kety-Schmidt technique [33]. This method of CA evaluation usually requires invasive and long-term pharmacological interventions to alter arterial blood pressure [34]. During static CA testing, autoregulation is said to be impaired, if the CBF changes significantly with either an increase or decrease in MABP [35]. In the case of intact CA, the blood flow is maintained at or near the baseline level.

The vasomotor control of cerebral circulation is mediated by metabolic, myogenic and neurogenic mechanisms including the excretion of chemical mediators and metabolites that require a finite time-interval to effect changes in vascular response [6]. Therefore, it is predictable that the CBF response to sudden ABP changes also takes a finite amount of time to complete [36]. The development of high temporal resolution techniques that

allow continuous recording of CBF changes has opened the door for developing a dynamic approach to CA estimation. Dynamic CA testing includes measuring CBF changes in response to rapid concomitant ABP changes. Evaluating the dynamic CA response provides information about the latency as well as the efficiency of autoregulatory action, which may be relevant to some clinical conditions such as traumatic brain injury [34]. A variety of pathological conditions including brain trauma, sub arachnoid haemorrhage and ischaemic attack affect the autoregulatory abilities to variable extent[6].

Classic cerebral autoregulation studies are performed in a semi-steady state in which the CBF values reflect the results of a cerebrovascular response that is adapted to a gradually increased level of BP [24]. In other words, the static CA study assesses the outcome of autoregulation performance rather than the process. Autoregulatory capacity may be partially or totally lost after a stroke or sub-arachnoid haemorrhage [6]. Therefore, it might be important to evaluate and even monitor the effectiveness of cerebral autoregulation in such patients. Dynamic cerebral autoregulation assessment could be non invasive and less prolonged, pharmacological BP interventions are not required and it could be performed at the bedside using trans cranial Doppler ultrasound [24, 34].

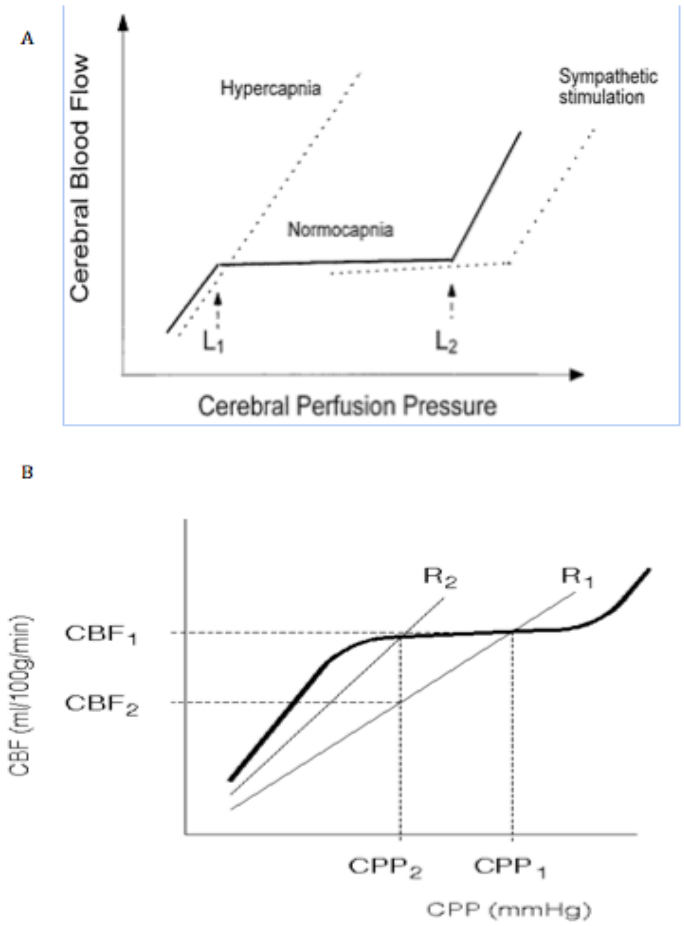

Figure 1 Classic cerebral autoregulation curve [32]

A: Schematic representation showing the characteristic autoregulation curve of cerebral blood flow against changes in perfusion pressure adopted by Panerai et al 1998 from the original CA curve by Aaslid R et al. Points L1 and L2 represent the limits of autoregulation. The effects of hypercapnia and sympathetic nerve activation are also shown as examples of interventions that can shift CA curve. B: Pressure flow resistance graph, assuming CBF1 at CPP1, the dynamic linear curve R1 would drop an equal percentage amount of CBF2 if pressure drops to CPP2. After some delay autoregulation becomes effective and changes the resistance to R2, whereby flow is restored to very near its original value [37].

1.3 Cerebral circulation

Structural and functional properties of the cerebral circulation allow the brain to match the high metabolic demand and the need for tight water and ion homeostasis. Tight water regulation is necessary in the brain because it has limited capacity for expansion within the skull. The unique cerebral endothelium, known as the blood brain barrier (BBB), has specialized tight junctions that do not allow the free transfer of electrolytes and metabolites.

Large extracranial and intracranial arteries contribute significantly to vascular resistance in the brain, unlike in the peripheral organs, where the majority of vascular resistance resides in small arteries and arterioles. The following two sections briefly discuss the distribution of cerebral vasculature and physiological aspects of the blood brain barrier.

1.3.1 Circle of Willis

Blood is supplied to the brain mainly through a complex network of arteries called the Circle of Willis (CoW). This is divided into three types of arteries: afferent, efferent and communicating arteries. [38, 39]. The afferent arteries, namely the internal carotid (ICA) and vertebral arteries (VA), are those arteries that supply blood to the circle. The efferent arteries take blood from the circle to the brain and they can be divided into the anterior, middle and posterior cerebral arteries (ACA, MCA, and PCA). They are connected to each other by anastomosing arteries, which consist of the anterior and posterior communicating arteries (ACoA, PCoA) [40] (Figure 2). The composition of the Circle of Willis varies from person to person; only half of the population have a complete circle [41].

Cerebral venous drainage is through superficial sinuses and deep veins. The superficial system is mainly composed of dural venous sinuses. Walls of sinuses consist of dura mater, which is a thin and valveless wall. Superior sagittal sinus flows over the sagittal plane inferiorly and superiorly to join with the deep drainage system, which comes from the straight sinus, in the confluence of sinuses. Eventually the venous blood will drain into the jugular vein to be finally drained into systemic circulation via the superior vena cava [42, 43].

As the arterial system of the brain is not anastomosed directly with the venous system, the leptomeningeal network covers the entire brain with a network of non-anastomosed arteries and veins in between the surface of the brain and the arachnoid membrane. The arterial network consists of arteries, arterioles and arterio-arterial anastomoses. There are small muscle sphincters located in the junction between cortical arteries and the parenchyma, which are known to control the blood flow. The blood flow is controlled directly by vaso-motility (dilatation or constriction) of pre-capillary sphincters [25].

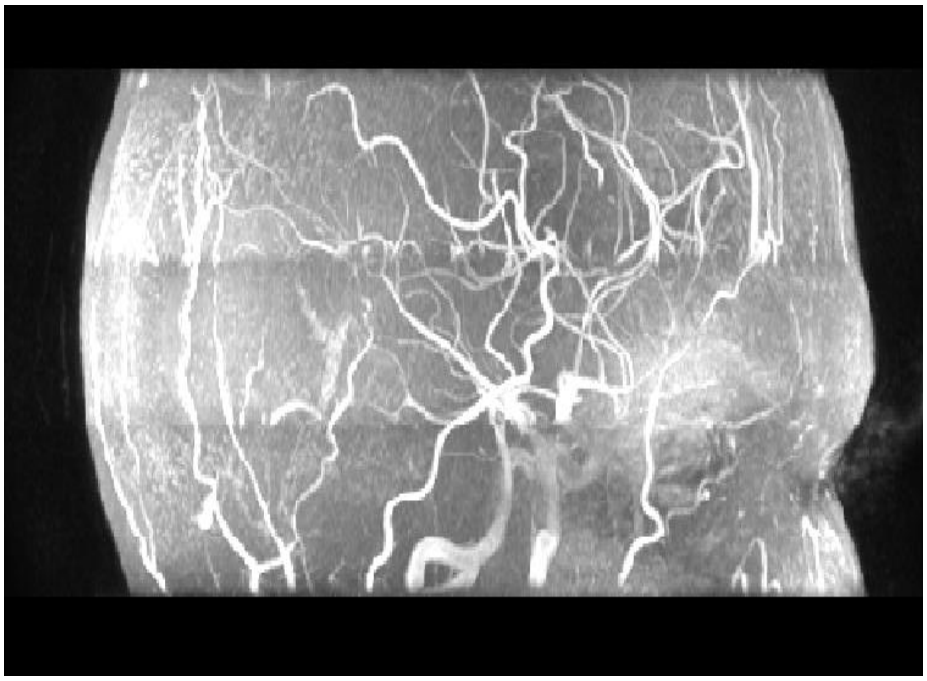

Figure 2 Circle of Willis (CoW), Time of Flight Angiography (ToF)

Time of flight (ToF) sequence (23 years male subject), multiple 2D slices are reconstructed by maximum intensity projection (MIP) technique to show 3D image of circle of Willis prior to 4D phase contrast MR angiography

1.3.2 Blood Brain Barrier BBB

In contrast to the systemic circulation, cerebral vasculature does not allow the free transfer of metabolites and electrolytes through capillary beds. A combination of physical and metabolic barriers protecting the brain, it consists of tight junctions and enzymatic barriers called the blood brain barrier (BBB). The BBB allows necessary nutrients to pass through the barrier whilst it restricts the permeability of non-necessary metabolites and toxic substances. This selective permeability is controlled by the central nervous system's (CNS) need for nutrients. The CNS capillary beds act as a blood- extra cellular (ECF) barrier. The tight junctions surrounding the endothelial cells, similar to the choroid plexus endothelium, characterize it. Pericytes available in capillary walls act as receptors for the vasoactive mediators such as angiotensin II, vasopressin, norepinephrine (noradrenalin) and phagocytosis. These cells adapt to pathological conditions by undergoing morphological and histological changes. They adapt to chronic hypertension by hypertrophy, hyperplasia and the production of cytoplasmic contractile protein filaments. The BBB breaks down in many diseases such as hypertension, tumour, trauma and infection [44].

1.4 Impairment in cerebral auto regulation

1.4.1 Cerebrovascular reserve and misery perfusion

Misery perfusion is a condition of cerebral circulation in which regional blood flow is reduced relative to the regional metabolic demand for oxygen, which might be caused by arterial stenosis or occlusion. It is defined by increased oxygen extraction fraction (OEF) [30]. Such a state of inadequate cerebral metabolism may result in some critical pathology including irreversible changes in cerebral white or grey matter. Misery perfusion was described for the first time in 1981 by Baron [45]. Misery perfusion occurs during several chronic cerebrovascular pathologies. The literature data show the association between increased risk of stroke and misery perfusion. In symptomatic major cerebral artery disease misery perfusion is a predictor of subsequent stroke [46]. Thus, the identification and management of patients with misery perfusion is essential to further improve their prognosis. Aoi et al (2012) used the phase relationship between MABP and CBFV to assess dCA in elderly patients with chronic ischaemic infarction. Their results showed that better dynamic cerebral perfusion regulation is associated with less atrophy and better long term functional status [47].

1.4.2 Cerebral Autoregulation and Hypertension

Hypertension is defined as a blood pressure level of more than 140/90 mmHg over several repeated measures. This is according to the Seventh Report of the Joint National Committee on Detection, Prevention, Evaluation and Treatment of High Blood Pressure (JNC 7) [48]. Malignant hypertension, which is defined as a BP of ≥ 180/120, has direct effects on cerebral autoregulation [49]. Chronic hypertension may shift the upper and lower limits of cerebral autoregulation. Immink et al (2004) observed a simultaneous decrease in the middle cerebral artery blood velocity (MCA V) with a reduction in the arterial blood pressure induced by an intravenous antihypertensive drug (sodium Nitroprusside SNP). They suggested that the static as well as the dynamic CA are affected by high arterial blood pressure levels [50]. Recent study findings suggest that the duration and rate of fluctuation of BP should be targeted in the prevention and treatment of cerebrovascular complications [51]. A chronic state of high blood pressure is a predisposing factor for a number of cerebrovascular diseases including hemorrhage, atherosclerosis, BBB dysfunction, carotid stenosis and lipohyalinosis [51]. It is established that acute and chronic hypertension are predisposing factors for severe cerebrovascular diseases. There are multiple underlying parameters that detect the severity of hypertension effects on cerebrovascular circulation. Hypertension alters the structure of cerebral blood vessels by producing vascular hypertrophy and remodeling [44]. Furthermore, it promotes atherosclerosis in larger arteries and lipohyalinosis in penetrating arteries [52]. These structural changes can compromise cerebral perfusion or alter cerebral autoregulation [53]. Ischaemic damage to the cerebral tissue probably occurs during spontaneous dips in arterial

pressure in the presence of arterial narrowing by lypohyaline deposits and atheromatous lesions. Sudden pressure elevations may also provoke ischaemic damage to the brain tissue in long lasting arterial spasm [53]. Local factors such as disturbed cerebral perfusion probably determine the site of infarct or the risk of haemorrhagic change.

Several studies depended on pharmacological modifications of ABP to measure steady state CA metrics in patients with cerebrovascular diseases [54, 55]. However, developing non invasive physiological diagnostic tools that are applicable for hypertensive patients is necessary in order to avoid pharmacological induced complications in this group of patients.

1.4.3 White matter hyper intense lesions (Leukoaraiosis)

White matter hyperintense lesion (WMHL) is a clinical condition that consists of subcortical small ischaemic lesions, also known as leukoaraiosis [56]. These hyperintensities are observed on T2 weighted and fluid attenuated inverse recovery sequence (FLAIR) MR images. They are usually considered as an incidental finding in normal aging but are also associated with neurological and cognitive disorders [57]. Recent literature indicates the presence of hyperintense lesions in subcortical grey matter regions and brain stem [57]. The collective term should be subcortical hyperintensities if the grey matter and brain stem lesions are included. White matter hyperintensities are indicative and a consequence of small vessel disease, and are thus associated with a high risk of stroke, dementia and mortality [58]. The presence of WMHL in Alzheimer's disease has been associated with reduced cognitive function [58]. The pathophysiology of WMHL is not well established yet. It is thought that in Alzheimer's disease, higher WMHL is associated with higher amyloid beta deposits, which is possibly related with small vessel disease and amyloid clearance [59].

Support for the hypothetical ischaemic origin of Leukoaraiosis could be derived from studies based on estimating CBF changes. Fazekas et al (1988), in a group of WMHL patients, noted higher blood flow frequency in extracranial carotid arteries, and lower mean blood flow velocity in grey matter [60]. Impaired autoregulation is identified as a significant and independent determinant of the severity of leukoaraiosis lesions [61] .

Several studies have reported whole brain or GM alterations in the CBF of patients with WMHL [62-64].

1.4.4 Stroke risk association with auto regulation

Stroke is an acute neurological deficit caused by vascular pathology. There are two types of stroke: ischaemic stroke due to lack of blood flow, and haemorrhagic stroke due to bleeding. Ischaemic stroke is usually caused by athero-thrombotic emboli. Hypertension has been identified as a major predisposing factor for stroke and primary cerebral hemorrhage [45]. Zia et al (2007) observed an increased risk of both ischaemic and hemorrhagic stroke in hypertensive patients [65].

After stroke, the autoregulatory capacity may be partially or completely impaired rendering CBF dependent on BP. Therefore, it could be argued that in post-stroke patients, BP should be well controlled in order to stabilize CBF and prevent cerebral hypo perfusion and ischaemia Nevertheless, the acceptable BP levels after stroke are still not known [66, 67].

After stroke there is insufficient blood oxygenation to the whole or a part of the brain as a result of disturbed circulation. In such situations, the brain will extract more oxygen from the blood to preserve a relatively constant cerebral metabolic rate of oxygen (CMRO2). Oxygen extraction fraction (OEF) is the ability of the brain to detach oxygen from oxyhaemoglobin to satisfy the high metabolic demands. Measuring the increase in OEF is important in the prognosis of stroke [65]. Yamauchi et al (1999) used PET to estimate OEF in stroke patients. The absolute value of OEF was examined in addition to the asymmetry of OEF. They recognized “increased-OEF” as a strong predictor of 5-y recurrent stroke. Their data suggests that the

absolute values of increased OEF are independent predictors of future stroke [5].

Calibrated BOLD MRI is a non invasive technique that can measure the OEF of cerebral tissue [68]. There are several applications of fMRI in the diagnosis and follow-up of stroke patients. In addition to the estimation of diagnostic parameters such as OEF, functional MRI can be used to diagnose the likely source of stroke by measuring the territorial cerebrovascular metrics [69].

1.5 Measuring dynamic cerebral autoregulation

The dynamic CA is estimated by measuring the continuous CBF before and after an induced arterial BP disturbance [9]. There are a number of observable parameters that are used in CA metrics, such as cerebral blood flow (CBF), blood volume (CBV), and cerebral blood flow velocity (CBFV). As described previously, dCA metrics are usually measured in response to a haemodynamic-perturbing stimulus. The haemodynamic response function to a stimulus occurs within a fraction of a second [70]. Therefore, measuring dCA changes requires high temporal resolution techniques. Furthermore, recent literature shows regional variation in dCA metrics. Horsfield et al (2013) estimated dCA metrics using a 1.5T MR scanner for ten healthy volunteers. Thigh-cuff release was used to induce dynamic BP changes and autoregulatory index was used to estimate CA changes. They observed different dCA efficiencies in GM, WM and cerebellum [22]. It is necessary to establish diagnostic tools that provide sufficient spatial and temporal resolution to estimate dCA metrics.

Usually, the dynamic cerebral autoregulation (dCA) metrics are estimated using parameters extracted from the time or frequency domain. The physiological determinants of dCA metrics are strong indicators of the non-stationary nature of dCA [9, 71]. Therefore, developing techniques that allow multiple physiological interpretations of measured parameters are necessary to allow the application of dCA measurement in health and pathological states.

Several diagnostic tools are used to quantify cerebrovascular reactivity metrics such as, positron emission tomography (PET), functional near-

infrared spectroscopy (fNIRS), trans-cranial Doppler (TCD) and functional magnetic resonance imaging (fMRI). The availability and feasibility of some of these techniques has hindered their application. TCD and MRI are the most frequently used techniques in clinical and research settings.

The MRI technique is a characteristically fast and non invasive method that allows visualisation of tissue boundaries as well as functional quantification of neuronal activities. Today, functional neuroimaging allows for the quantification of parameters such as CBF and CBV within milliseconds. With advanced imaging techniques such as endogenous contrast arterial spin labelling (ASL) MRI, it is possible to quantify the flow of blood through cerebral vessels [72]. Blood oxygen level dependent (BOLD) MRI can indirectly measure modulations induced pharmacologically or physiologically in the blood flow or volume through calibrated methods [8, 73]. Phase contrast (PC) MRI is another contrast-free angiographic technique that allows vessel specific quantifications of CBV and CBF. Time resolved three dimensional (4D flow) MRI allows 3D visualization of neurovascular anatomy and flow direction with full volumetric coverage in an easy 3D acquisition [74]. Observing cerebral blood flow and volume changes requires fast techniques, in order that the image acquisition has the same frequency as the fast cerebral haemodynamic changes.

Measuring dCA not only requires a fast physiological acquisition tool but also a repeatable BP-fluctuation method. Cerebrovascular reactivity responses can be induced pharmacologically or non-pharmacologically. Pharmacological interventions are indicated in studies that measure steady state changes of CA [75]. Several non invasive interventions have been used

to induce fast changes in the systemic blood and estimate corresponding CBF changes, as described in the first chapter of this thesis.

1.6 Functional magnetic resonance imaging

The concept of a close temporal relation between the haemodynamic response and cerebral neural activation is not new. For more than a century, scientists have observed the relationship between the haemodynamic response and neural activation [76]. Ogawa et al were the first to observe an MRI signal decrease from deoxygenated blood in a T2* weighted image, at the beginning of the nineties of the last century [77]. The functional MRI (fMRI) signal change depends on the level of paramagnetic deoxyhaemoglobin in the blood. The paramagnetic nature of deoxyhaemoglobin produces different magnetic susceptibility in between the blood vessel and the surrounding tissue [8]. Because of the different magnetic properties of oxyhaemoglobin and deoxyhaemoglobin, they give different signals on MRI. The former is diamagnetic and gives an opposite magnetic field, but the latter has a non-zero magnetic moment that gives weak attraction to a magnetic field.

The haemodynamic response occurs after short neural activation that produces a specific BOLD signal. Haemodynamic response function has been examined by several research studies. Generally, it is distributed over three preliminary key features: first the initial dip, then the positive overshoot and finally the post-stimulus undershoot [78].

There are different views about the detection of the initial dip at different field strengths, as it has been observed that even at high field strength it cannot always be detected [79]. 5-6 seconds after a neurovascular event the oxygenation level will reach its maximum level, at which the BOLD signal effect will be acquired. Following this, the BOLD signal dips down to more

than its original baseline; this is called the "post-stimulus undershoot". The mechanism behind the post-stimulus undershoot is controversial. It might be explained by the large amount of deoxyhaemoglobin that persists in the blood because of the delay in CBV recovery that follows the CBF changes [80]. However, it could also be explained in the light of the hypothesis that supports coupled CBF and CBV, but considers the $CMRO_2$ as a distinct parameter [81, 82].

The increase in blood flow following neural stimulus and the associated increase in cerebral metabolic rate of oxygen $CMRO_2$ are the basics for observed BOLD signal amplitude response [83]. However, the baseline physiological state is also a strong determinant of the BOLD signal amplitude response. The baseline physiological state is determined as the total deoxyhaemoglobin present in a voxel, which is a function of several parameters such as hematocrit, OEF and CBV [84]. As long as these baseline parameters are unknown, the BOLD signal cannot be considered as a quantitative measure of cerebral haemodynamic response [83]. Researchers have sought to measure baseline physiological variables using the calibrated BOLD method [85]. The key component of the calibrated BOLD method is accurate modelling of the BOLD signal amplitude depending on the underlying physiological changes [86]. Although the BOLD signal is a qualitative method, the calibrated BOLD experiment offers the potential to use the BOLD signal as a quantitative probe of brain physiology.

1.6.1 Calibrated BOLD and hypercapnia method

The theory behind calibrated BOLD is an exact mathematical expression of BOLD signal amplitude in relation to the underlying physiological changes [83]. Fully oxygenated blood has approximately a 40% oxygen exchange rate at the capillary bed transit time [87]. This results in a certain amount of deoxyhaemoglobin in venous capillary vessels. [88]. A classical positive BOLD signal occurs when there is a decrease in the level of deoxyhaemoglobin, which leads to a signal increase [89]. The CBV contributes to this by changing the total amount of deoxyhaemoglobin available in a voxel [90].

Previously Davis et al (1998) represented the BOLD signal as [91]:

$$\delta S = M[1 - f æ \left(\frac{r}{f}\right)]ß$$

In which, δS= BOLD signal change percentage, *f*=CBF, *r*=$CMRO_2$ ratio (activation/baseline), and *æ* and *β* are the model parameters

The local deoxyhaemoglobin level directly affects the BOLD signal amplitude, at a constant rate of CMRO2. Thus the signal amplitude is affected by the physiological parameters that affect the local deoxyhaemoglobin level [85].

The above equation is a specific approach; Blockley et al (2011) have used a more general approach:

$$\Delta S = Bh(f, r)$$

Δ S= BOLD signal change percentage

B=calibration parameter

H (f, r) =function, describes changes in CBF and $CMRO_2$ of the BOLD changes.

In this model, which includes different blood compartments such as arterial, capillary, venous and extravascular compartments, they assumed that the new calibration method is unrestrained by the respiratory challenge, in the case that hypercapnia calibration is considered as a consistent method [83].

Switching between hypercapnic and normocapnic intervals leads to changes in the CBF and hence can achieve changes in the deoxyhaemoglobin level in the brain. Since the BOLD signal depends on the level of oxy/deoxyhaemoglobin in the blood, physiological events that alter the blood oxygenation level can non-invasively be detected as BOLD amplitude change in gradient echo proton images [83].

Hypercapnia causes a gradual accumulation of CO2, which is a potent vasodilator. Vasodilatation can be pharmacologically induced by drugs such as acetazolamide or it can be induced by increasing the amount of CO_2 inhaled using breath holding methods [92].

In this thesis respiratory challenge was used to induce transient hypercapnic response changes in the brain. It has already been validated that short periods of breath holding as well as changes in the rate and depth of respiration induce a sufficient hypercapnic response, and the effects of the hypercapnia on cerebral circulation could be estimated by measuring the corresponding BOLD signal change to respiratory challenges [93, 94].

1.6.2 Phase contrast magnetic resonance angiography (PC MRI)

Flow-sensitized 3D phase contrast magnetic resonance imaging (4D PC MRI), also known as time resolved 3D magnetic resonance angiography (MRA) has been introduced recently. Magnetic resonance angiography can assess haemodynamic changes in normal or diseased cerebral vasculature [5-7]. The role of PC MRI in the diagnosis and characterization of cardiovascular diseases has been established [95, 96]. The flow measures obtained with 4D PC MRI correlate well with the measures obtained with reference modalities such as TCD, TCCD at specific cerebral vessels [74]. To date, TCD has been the standard modality for measuring flow velocity in the cerebral blood vessels. However, the lack of angle correction for measured velocities and the limited spatial coverage are drawbacks of this method. 4D PC MRI allows multidirectional velocity sensitization, vessel diameter measurement, as well as very high temporal information coupled with the cardiac cycle. In the following paragraph, the physics behind phase contrast imaging is discussed briefly.

The transverse component of spin magnetization acquires a motion induced phase shift. Thus, transverse magnetization should be induced first by the radiofrequency pulse before adding the flow sensitizing gradients [97]. Two main types of images are acquired in phase contrast imaging: a magnitude (modulus) and a phase (velocity) image. The magnitude image resembles a classic bright-blood image and contains anatomical information. In the phase image the grey value represents the velocity information in that voxel, where the black indicates flow direction towards the viewer and the white represents flow away from the viewer [95]. Velocity encoding detects the highest and lowest velocity encoded by the sequence and it is given in units

of centimetre/second (i.e. velocity encoding=100cm/s describes a phase sensitizing experiment with a measurable range of velocities ±100 cm/s) [97].

2D phase contrast MRI with partial spatial coverage and unidirectional velocity encoding provides haemodynamic information about cerebral vessels. A combination of 2D phase contrast and a breath-hold test has previously been used to estimate the dynamics of CA [98]. The results support capability of 2D PC MRI to measure the cerebrovascular responses to transient hyperaemic responses for short breath-holds of 30 seconds.

1.7 Non invasive methods to induce blood pressure fluctuations

1.7.1 Sudden release of inflated thigh-cuff

Thigh-cuff release was first introduced by Aaslid et al (1982) to induce sudden drops in the systemic BP [6]. To study dCA, a step response change should be induced in the CPP to allow for observing the CBF changes before and after that. Concurrent measures of CBF and ABP from TCD and Finometer respectively have been used as a standard method to derive dCA metrics [17, 22, 99].

Maintaining inflated bilateral thigh-cuffs (20 mmHg above the systolic BP of the subject) for two or three minutes is used to induce a step change in ABP [6, 22]. The sudden release of the thigh cuffs induces a rapid BP drop in less than a second [100]. This step response prompts corresponding changes in the CBF that can be used to plot an autoregulatory response index over several measures [34]. Measuring the CBF rate of regulation (RoR) in response to step-wise changes in BP is a completely non invasive and non-pharmacological method that can provide physiological information on autoregulatory gain and cerebral vasomotor state [6].

The sudden release of thigh-cuffs could have important clinical application for evaluating the effect of anaesthetic agents in clinical care unit patients [31, 101]. Furthermore, it has been applied in patient groups such as those with orthostatic hypotension [102], trauma [103], and carotid artery stenosis [104].

To evaluate the repeatability and robustness of the method, it is necessary to systematically evaluate it by comparing the results in between different

groups of subjects and also with other non invasive modalities that have been used to induce a step-wise BP decrease. This will be discussed systematically in chapter 2.

1.7.2 Respiratory challenges

Respiratory challenges have been used by many researchers to activate dynamic cerebral autoregulation [18, 93, 94, 105]. Different respiratory challenges introduced to induce hypercapnic response include breath-hold and cued deep breathing. The physiological aspects associated with both methods include hypertension, bradycardia, CO2 retention and oxygen conservation [106]. Respiratory challenges have been used in patients and healthy subjects of different age groups to estimate dCA measures [93, 94, 98, 107].

Breath holding starts with the voluntary inhibition of respiratory muscular activity, and is maintained by controlled closure of the glottis [108]. Changes in the rate or depth of respiration, known as cued deep breathing (CDB), can also induce a hypercapnic response [109]. CDB consists of a rhythm of self-paced breathing interleaved with a set of repeated deep inhalations and exhalations [93]. Recent studies have shown that even subtle variations in the rhythm of respiration can induce a BOLD signal change [110].

Despite the motor activations associated with breath-hold performance, there are many other mechanisms associated with breath holding. Hypercapnia and the vasodilatory effects of CO2 on cerebral vessels is the main mechanism described. The chest movement associated with the

respiratory challenge itself can induce magnetic field changes and lead to image distortions [111].

Another physiological alteration associated with breath holding is systemic arterial blood pressure changes. This can be derived from the sympathetic activation as well as the volumetric changes in the circulation associated with the changes in thoracic cavity pressure [112]. These changes do not occur immediately and they prompt fluctuations in the rate of cerebral blood flow and oxygenation, during which the dCA mechanism is activated to compensate for the transient changes and maintain constant blood flow in the brain.

Less attention has been paid to the ventilatory effort occurring at the beginning of a breath hold. An inspiratory breath-hold (iBH) is different from a non-inspiratory breath-hold (BH). Transient sub-atmospheric pressure generated at the beginning of an iBH may affect the physiological parameters associated with the breath-hold performance [108]. Since the dCA measurements depend on the fluctuation rates of cardiovascular parameters, especially BP, it is important to standardize the respiratory interventions that induce concomitant BP changes.

The repeatability of respiratory challenges for different groups and settings as well as the role of the method in estimating dCA metrics is evaluated systematically in the following chapter.

1.8 Conclusion

As described previously, measuring CA metrics is indicated in the prognosis of several cerebrovascular diseases. However, the standard diagnostic tool should be optimized first to examine CA in healthy brain. The physiological parameters of CA metrics are complicated even in a standard context. With the wide range of diagnostic tools and interventions available, it is fundamental to develop a single diagnostic tool that can be applied in healthy and patient populations.

Developing a physiological diagnostic tool to measure CA metrics requires answering a few fundamental questions. For example, what is the most consistent method used to quantify CA metrics? And what is the most robust method to induce BP fluctuation?

The following chapter includes a systematic review of the literature to evaluate the main techniques and interventions that have been used to measure CA metrics in the last ten years.

Chapter 2

2 Systematic Review of Literature

2.1 Introduction

In the previous chapter the significance of CA metrics in the prognosis and follow-up of various cerebrovascular diseases was discussed. "Pressure autoregulation" is the common approach used to test cerebral autoregulation in relation to changes in the mean arterial blood pressure. Different diagnostic methods have been used to assess dCA metrics. This review systematically inspects non invasive studies that have examined cerebral autoregulation in the last ten years (2003-2013), addressing the following questions:

1) What is the best non invasive physiological method to measure CA?

2) How consistent are the methods that have been applied as diagnostic tools to measure CA?

Evaluating the consistency and repeatability of dCA diagnostic methods requires the precise synthesis of some other physiological aspects, such as:

- The main anatomical regions of interest evaluated so far in the literature, and the limitations of wider coverage of specific diagnostic tools.

- The interventions used to stimulate blood pressure (BP), and their influence on the CA measurement efficiency.
- The autoregulation indices that have been used to quantify dynamic response changes.
- The general and specific limitations in measuring CA
- The future direction with regard to developing a simple consistent physiological diagnostic tool to assess CA.

2.2 Methods

The study was conducted according to "preferred reporting Items for Systematic Reviews and Meta-Analyses: The PRISMA Statement" [15]. The literature search was executed by searching the database of the National Center of Biotechnology Information (PubMed-NCBI) and the National Library of Medicine's Medline (Ovid) database, using the following key words:

- "Cerebral autoregulation" and
- "Arterial blood pressure fluctuations"
- OR "arterial blood pressure"
- OR "cerebrovascular reserve" OR "CVR"
- OR "cerebral blood flow" OR "CBF"
- OR "cerebral blood volume" OR "CBV"
- OR "BOLD MRI" OR "blood-oxygen level dependent magnetic resonance imaging"
- OR "ASL MRI" OR "arterial spin labelling magnetic resonance imaging"
- OR "TCD" OR "trans-cranial Doppler "
- OR "HRF" OR "hemodynamic response function"
- OR "neurovascular coupling"
- OR "cerebral metabolism"
- OR "IHGT" OR "hand grip test"
- OR "breath hold test"
- OR "Hypercapnia" OR "hypocapnia" OR "hypoxia" OR "hyperoxia"
- OR "hand Grip" OR "hand grip test" OR "isometric hand grip test" OR "IHGT" OR "HG" OR "HGT".

The search was restricted to papers published between 2003 and 2013 because of the time limitation of the study. Furthermore, the search criterion was restricted to the last ten years in order to include the latest technical advances and analysis methods. All of the papers included were published in English and they included only in-vivo adult human brains. It is known that the pathophysiological mechanism of flow autoregulation is different in

neonates [113]. Therefore neonate studies were excluded from this synthesis.

Studies that estimated the mechanisms of flow regulation in animals were excluded from this review because the main aim is to evaluate simple non invasive techniques that have been used to assess dCA metrics in human, which are clinically valid and accessible.

Estimating the dynamics of CA is usually performed through CA indices that calculate the function of CBFV response according to the ABP changes. This kind of investigation requires continuous CBFV measures. Trans-cranial Doppler and functional MRI are both non invasive techniques that can provide continuous haemodynamic metrics over several minutes. This review includes only CA studies that used TCR and fMRI to quantify the haemodynamic metrics. Studies that used techniques such as PET or fNIRS were excluded from this review to facilitate the comparison of autoregulation indices. Furthermore, TCD and fMRI techniques are less invasive and more commonly used in clinical settings.

After being reviewed for their population characteristics and diagnostic methods, the eligible studies were assembled in a spreadsheet format for analysis. The features recorded included population demographics, methods of measurement, type of intervention, recorded physiological measures, imaging and/or ultrasound characteristics, statistics performed, and methods of analysis (autoregulation indices). The percentage or numerical records of arterial blood pressure change could not be obtained from the majority of the studies, which was a reason for excluding them.

2.3 Results

The first database search resulted in a large number of studies (more than 900,000). The search was then restricted to include studies from 2003-2013; this resulted in about 400,000 studies. The following parameters (infants, animal studies, non-clinical, and non-English published studies) were used to filter the search down to 375 studies (Figure 3). These were scanned for the titles and 202 studies were excluded for being totally irrelevant, within which there were 16 animal studies and one neonate study that had not been identified during the first line filtering. From the remaining 173 studies, a further 102 papers were excluded, as 45 studies included invasive methods and intraoperative patients, and 57 studies included other acquisition methods such as PET, angiography and fNIRS.

In total, 71 papers were reviewed, of which 37 studies (including review papers) were excluded because the methodology was irrelevant to the current study.

Finally, 34 studies were selected to be involved in the synthesis (Figure 3). 19 of them used functional magnetic resonance imaging fMRI and the rest used Trans-cranial Doppler (TCD). Within the MRI studies, three studies included patients with Moyamoya disease, internal carotid artery ICA stenosis and subarachnoid hemorrhage (SAH). The rest of the studies used TCD to quantify cerebral blood flow velocity (CBFV). Four of the TCD studies were performed with patients, such as those with hypertension, obstructive sleep apnea (OSA), sub-arachnoid haemorrhage (SAH) and patients undergoing carotid artery angioplasty (CAA).

In total, 544 subjects participated in the reviewed studies, 317 healthy volunteers and 174 patients. The recorded features were different for the two methods; accordingly two separate spreadsheets were used, one for the fMRI studies and one for the TCD studies (Appendix 1). The MRI studies database included 26 columns and the TCD database included 19 columns. Because of the long columns and to show the data in more coherent way, separate tables were generated for the healthy control studies and the patient data (Appendix 1).

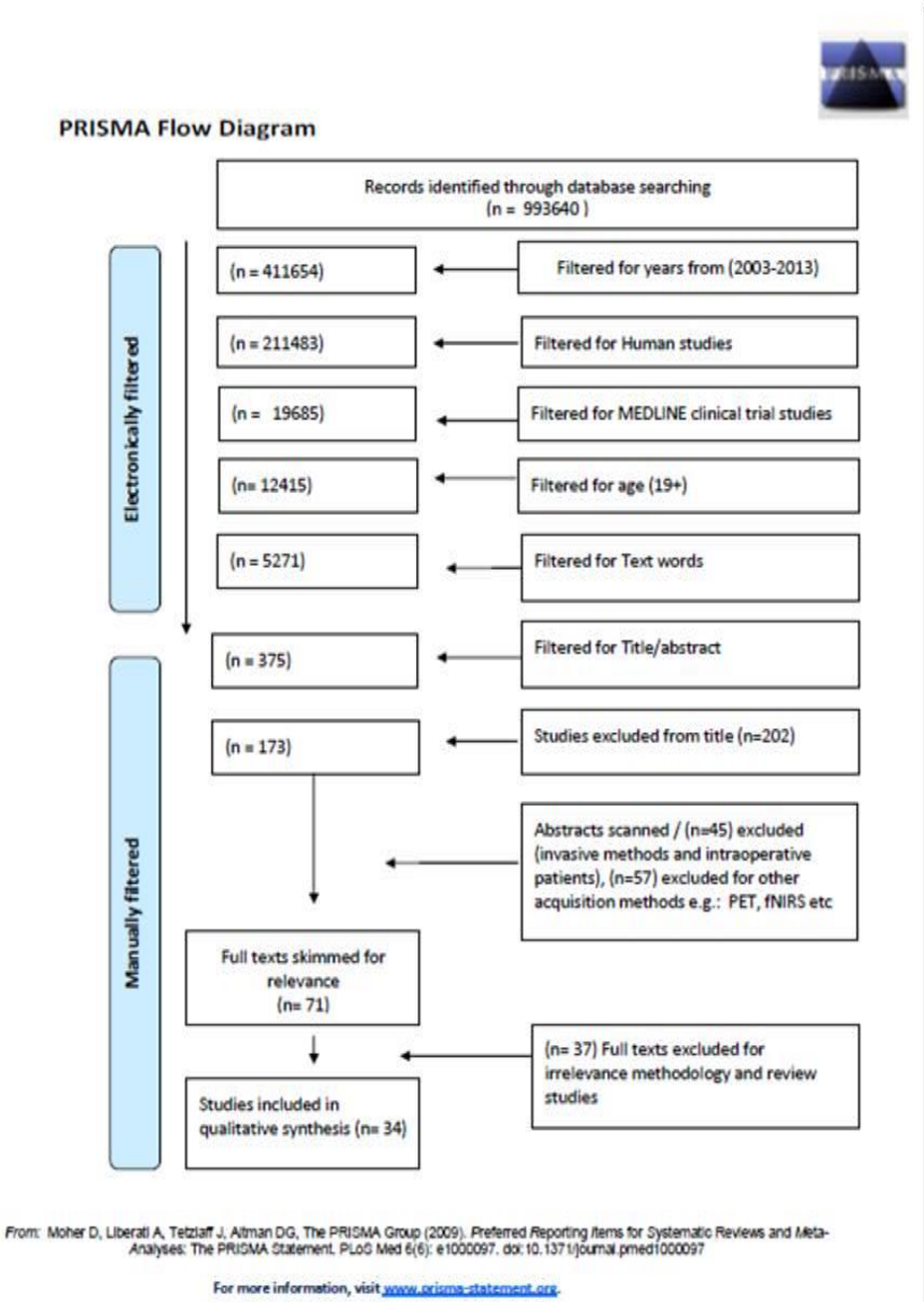

Figure 3 Chart of search results (PRISMA statement)

2.4 Methods to quantify CA metrics

2.4.1 Magnetic resonance imaging (MRI) studies

Functional MRI is a fast non invasive technique that has sufficient spatial and temporal resolution to allow for measuring CA metrics [114]. 19 of the reviewed studies used different MRI sequences at two different field strengths, 3T (13 studies) and 1.5T (6 studies). Different sequences were used to quantify the haemodynamic metrics such as BOLD, ASL, T2*, and PC MRI. Five studies estimated the percentage signal change (PSC) from the magnitude of the BOLD images, to anticipate the underlying vascular response [18, 28, 93, 114, 115].

Within these studies different physiological stimulations were used to induce dynamic changes in cerebral blood flow. The diagram in Figure 4 shows the BP-intervention method for each group of studies with the references stated in numbers.

Magon et al (2009) compared different breath-hold periods to induce dCA changes. Their results show that PSC and volume changes are highly dependent on the duration of BH. In their experiment higher signal changes were observed for the 21-second BH duration compared to the 9-second and 15-second BH durations [114]. These results concur with the results of Murphy et al's (2011) study, in which a 20-second BH was used to induce a cerebrovascular response to hypercapnia. They suggested that considering the individual end tidal CO_2 (ETCO2) responses to BH in the analysis would increase the accuracy of the measured vascular responses, and

consequently more statistically active voxels would be achieved in the group level analysis [18]. These two studies [18, 114] investigated the effects of breath-hold duration on the PSC of the BOLD magnitude. Meanwhile, Thomason et al (2008) established a method to test the effects of inspiration depth on the underlying BOLD signal by giving visual feedback to the individuals during the breath hold task. Different responses were observed in the BOLD signal amplitude changes according to the depth of inspiration. This indicates the effects of the depth of inspiration on the cerebrovascular response [115].

Blood oxygen level dependent (BOLD) signal change is a sensitive tool for mapping the cerebrovascular response to hypo and hypercapnia. However, qualitative interpretation of the BOLD amplitude is complex, because it depends on more than one hemodynamic parameter such as CBF, CBV, hematocrit and CMRO2.

Quantitative CBF maps can be obtained using ASL functional magnetic resonance imaging. Arterial spin labeling fMRI uses magnetically labelled water protons as an endogenous tracer. Four studies included in this review used ASL derived quantitative flow maps to estimate dCA metrics [8, 19, 116, 117].

Noth et al (2008) determined CBF maps with pulsed ASL in 19 healthy subjects under baseline, hypoxia and hypercapnia conditions. There was a statistically significant ($5.8 \pm 0.9\%$) increase in GM-CBF per 1 mmHg increase in partial pressure of CO2. Maps of CVR showed high intra-subject variability to hypoxia but less variability to hypercapnia [19]

Bulte et al (2007) used pulsed ASL interleaved with Gradient Echo echo-planner imaging (EPI) BOLD to estimate CBV changes. They used epochs of hyperoxia as an

endogenous contrast media. The results showed regional heterogeneity in the CBV response (Global CBV 3.77± 1.05%, GM 3.93±0.90%, WM 2.52±0.78% ml/100 gm.) [117]. The complete non-invasiveness of ASL makes it very suitable for perfusion studies of healthy volunteers and patient groups requiring repetitive follow-ups. The only draw back of ASL is the low signal to noise ratio (SNR), which makes averaging necessary, and thus good cooperation from subjects is essential. Further, ASL has limited temporal resolution that may restrict the application of this method to estimate dCA metrics.

Two of the studies used absolute CBF and CBV values obtained by means of phase contrast magnetic resonance angiography PC MRI [74, 98]. This is a contrast free technique that allows non invasive volumetric measures in the brain. De Boorder et al (2012) combined a BH test with 2D PC MRI, while Meckles et al (2004) observed the spontaneous oscillations in the systolic-diastolic phases of the cardiac cycle. The former study validated the BH test as an applicable non invasive method for stimulating physiological changes in the cerebral circulation, which is concurrent with five other studies that used the same physiological stimulation but different sequences [15, 18, 94, 98, 114, 115]. The latter study compared intracranial velocity measures from 4D PC MRI with TCD, TCCD and 2D PC MRI [74, 98]. In their results, the CBFV measures from 4D PC MRI were consistent with other reference modalities, foremost with TCD. There was mild vessel diameter-dependent under- or over-estimation of velocities in smaller (MCA) and larger sized arteries (BA and ICA), respectively. This might be an effect of spatiotemporal averaging [74].

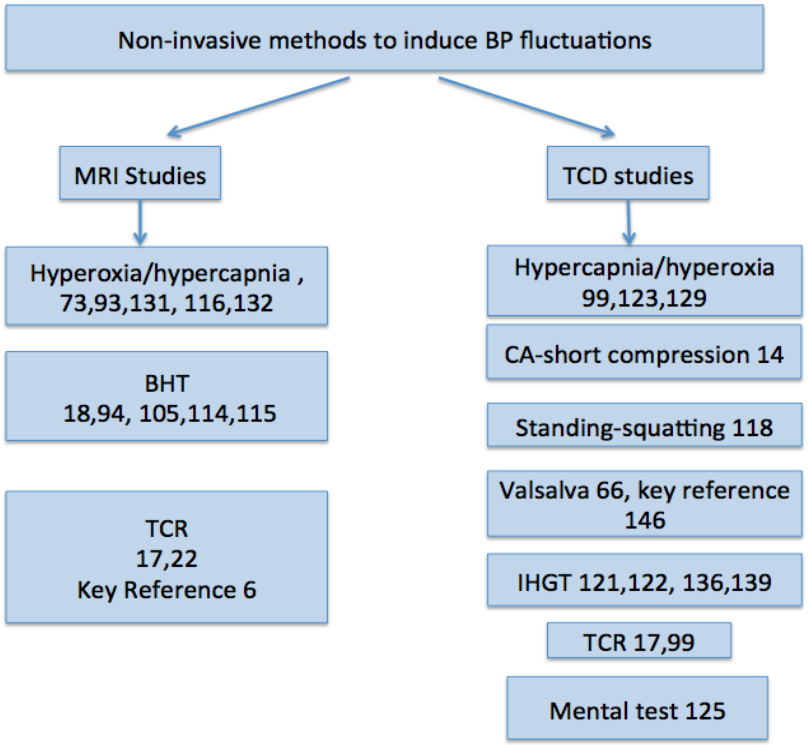

Figure 4Methods to simulate dynamic cerebral auto regulation

TCD=Trans-cranial Doppler ultrasound, MRI=magnetic resonance imaging, TCR=thigh cuff release, IHGT=isometric hand grip, GB=ganglionic blockade, BHT=breath hold test. References stated in numbers

2.4.2 Trans-cranial Doppler ultrasound studies (TCD)

Intra cranial cerebral blood flow velocity (CBFV) measurement obtained by TCD is a validated surrogate for CBF to estimate the dynamics of dCA [6]. Usually a 2MHz trans-cranial Doppler probe is used to illuminate the cerebral arteries through anatomical windows (Appendix 1). 15 studies included in this synthesis used TCD to measure the CBFV of major cerebral arteries (MCA, ACA, ICA, VA and BA). Quantitative comparison of the absolute CBFV values was not applicable because of the different interventions and excessive heterogeneous read-outs.

The flexibility in the hemodynamic perturbation methods is an advantage of TCD over MRI studies. Different physiological interventions were used to stimulate ABP. Blood pressure stimulations such as carotid artery short compression, and standing-squatting test are not applicable in the MR scanner [14, 118]. Despite the applicability of the isometric hand grip test (IHGT) as a validated ABP stimulator [119, 120], no studies could be retrieved from the database that had used this method to measure cerebral autoregulation in an MRI scanner. However, four TCD studies obtained comparative results using IHGT as an ABP stimulator [37, 121, 122] (Figure 4)

Thirteen out of fifteen studies measured CBFV only in the middle cerebral artery (MCA). Willie et al (2012) quantified and compared the CBFV in the posterior cerebral artery (PCA), vertebral artery (VA), ICA, and MCA. They observed different vessel responses to hypercapnia. The measured response was higher for the VA and ICA than the other vessels (50% and 25%, respectively) [123]. These results indicate vessel diameter dependence of the CA response.

Hartwich et al (2010) obtained measures from the left anterior cerebral artery (ACA) in response to IHGT using TCD. They also measured the pial-artery pulsation and sub arachnoid space width (SAS) using near-infrared trans illumination/backscattering Sounding (NIR-T/BSS). IHGT induced a significant increase in Pial-artery resistance, a simultaneous decrease in the SAS width, but no change in the CBFV [121].

Ikemura et al (2012), in addition to the TCD measures of MCA blood flow velocity, quantified the superior temporal retinal arteries (STRA), inferior temporal retinal artery (ITRA), and retinal choroidal vasculature (RCV) using laser speckle flowmetry. They used IHGT and the cold pressor test (CPT) to stimulate dynamic autoregulation. Their results show an increase in the RCV blood flow velocity, more than other arteries, which indicates poor autoregulation performance in the mentioned vasculature [122].

Several methods have been used to estimate the dynamics of cerebral autoregulation from CBFV measures of TCD. One of these is cerebrovascular conductance (CVC), which represents the ratio of the mean blood flow velocity to the mean arterial blood pressure (CVC=MCBFV/MABP) [37, 118, 121-124]. Another method is transfer function analysis (TFA) using ABP and CBFV as the input and output values, respectively [111, 125]. An autoregulatory index (ARI) scaling from 0-9 (0= absence of CA -9=best CA) was used to model the hemodynamic changes in three studies [9, 10, 22]. Panerai et al (2013) observed a highly significant inter-hemisphere correlation for continuous ARI. These TCD measures from different vessels classify the method as a sensitive tool to model the vascular reactivity response. Measuring the flow velocity in different vessels could be used to estimate dCA metrics in different cerebral territories.

2.5 Cerebral autoregulation indices

Routine evaluation of CA in clinical practice requires objective and reliable indices that can provide a continuous measure of cerebrovascular reactivity or other indices of CBF in the presence of fluctuation in the mean ABP or CPP. Autoregulation indices quantify the relationship between the corresponding CBF and BP. Different indices have been used in clinical and research settings (Table 1). Some of these methods approach the BP-CBF relationship as if it were linear. It should be noted that more complex mathematical models have been developed that allow for non-linear dynamics [126-129] Table 1 summarizes the list of indices used to estimate dynamics of cerebral autoregulation.

Linear system analysis facilitates the examination of the transfer function between MABP and CBFV changes as a measure of autoregulation. It is calculated as the function of gain, phase and coherence between these two variables using Welch's method. The impulse response function is calculated as the inverse Fourier transformation of the transfer function. This enables the estimation of transient changes in CBFV during BP fluctuations [130]. The transfer function of autoregulation indices can quantify the extent to which the BP-input signal is reflected in the CBFV-output signal.

The autoregulatory index reflects the changes in CVR per second in relation to the changes in ABP. The actual CBFV curve is compared to a computer based model CBFV curve, which assumes that the CBFV passively follows the course of ABP. For example, if the actual CBFV curve from the given test fits this computer model curve, the ARI will be 0. A scale from 0 (no autoregulation) to 9 (perfect autoregulation) is used to model the autoregulation function. An ARI of 0 indicates that CBFV is passively follows

BP changes, and an ARI grade 9 indicates that CBFV recovers much faster than BP [34]. The autoregulation index can grade the autoregulation by estimating the impulse response function after transient impulse-like BP changes [125].

Principal dynamic modelling (PDM) obtains reliable dynamic non-linear models of the causal relationship between two input signals; MABP and ETCO2 time series and the output signal of the mean CBFV [127]. This model is a variant of the Volterra based approach for modelling a non-linear relationship between two signals [128]. Principal dynamic modelling allows estimation of dynamic changes from short data-records and also facilitates a physiological interpretation of the obtained model. The 2^{nd} order Volterra, function between two inputs, represents the qualitative pattern by which the two inputs interact in order to influence the output. There have been indications that the dynamic characteristics of the autoregulation process might vary over time due to neural and metabolic factors [125]. Time-varying modelling of autoregulation allows quantitative understanding of the time varying characteristics of dynamic cerebral autoregulation, especially the temporal variation in the linear dynamics of CBF and CO2 vasomotor reactivity [126].

Rate of regulation (RoR) is defined as normalised changes in the cerebrovascular reactivity index (ΔCVR) according to BP changes in a particular time. The recovery time of CBFV after a BP event (decrease or increase) is taken as an estimated parameter for the dCA efficiency [6]. This rate shows how the functional response changes over time.

$$\mathrm{RoR} = \frac{\Delta \mathrm{CVR}/\Delta \mathrm{T}}{\Delta \mathrm{MAP}}$$

Linear systems can be described in the time or frequency domain [127]. The frequency domain type of analysis describes the relationship between CBFV and BP with respect to frequency [130]. The rate of regulation describes the analysis of the CBFV-BP

relationship with respect to time. The signal value is known at various discrete time points and the time domain graph shows how this signal changes over time. This type of analysis is used in the current study to estimate the rate of BOLD signal recovery after a fast BP-decrease induced by the sudden release of inflated thigh-cuffs.

Autoregulation Indices	Abbreviation	Reference study	Unit/Value	Definition
Transfer function analysis	TFA	[1-7] [8] Key reference {Panerai, 1998} [32]	mmHg- CBFV per second	Input-ABP Output-CBFV
Autoregulatory-Index	ARI	[9-13]	0-9	9 models for CA 0 =absent regulation 9 =perfect regulation
Principal-Dynamic Models	PDM	[14-16]	mmHg-CBFV per second	Two inputs (ABP and PECO2) Single output CBFV
Cerebrovascular conductance index	CVCi	[17-21]	mmHg/ cm /sec	*CI=mean CBFVMABP*
Rate of regulation	RoR	[19,66] Key References {Aaslid, 1989} [6] {Dawson, 1999} [148]	mmHg- CBFV/sec	RoR=ΔCVR/ΔTΔMAP

Table 1 Summary of the autoregulation indices used to estimate dCA

CBFV cerebral blood flow velocity, CVR cerebrovascular reactivity, ABP arterial blood pressure, MAP mean arterial blood pressure, PECO2, partial pressure of CO2

2.6 Discussion

Despite the wide range of non invasive physiological diagnostic tools developed to assess CA, the definition of a gold-standard method to measure CA is still missing. By a gold-standard method we mean a method that provides satisfactory temporal and spatial resolution in addition to ease of access. The gold standard method should be able to be used in research and on a daily clinical basis in both healthy and patient populations.

It might not be possible to provide all of the standard properties in a single tool, but approaching a balance in the accessibility and accuracy of the diagnostic tool is the main aim. The aim of this study was to explore possible bases and directions for developing a simple diagnostic tool to quantify cerebral autoregulation.

2.6.1 Non invasive physiological method to measure CA

Answering such a question regarding the best method to measure CA might be beyond the limits of this review. But it is possible to discuss the existing literature in the light of the available methods, keeping in mind a few crucial fundaments, such as the effectiveness of the method, and its safety, availability and applicability in patient populations. Thus far in the literature, TCD is the most commonly used technique to measure CA, because of the availability and portable nature of the device, which allows bedside examination. One of the main possible limitations of TCD is spatial resolution. The anatomical windows restrict the vessel illumination of some major cerebral arteries. However, with the recent advances in the fMRI, it is possible to obtain separate CBF and CBV measures with high spatial and temporal resolution. These individual measures obtained from fMRI classify it as a

reliable diagnostic tool to estimate CA. Beat-to-beat measurement of dCA metric is clinically valuable in patients with autonomic failure and cerebrovascular diseases [74]. Cardiac gated 2D phase contrast MR angiography is currently the only promising technique that can obtain beat-to-beat cerebral flow volumetric measures [98].

A combination of a simple physiological ABP stimulation with fMRI measures is necessary in both research and clinical settings. Yet, optimization of this physiological method should be through quantitative and qualitative description. Continuous ABP measures within the MRI scanner would provide better interpretation of the physiological aspects of CA metrics.

2.6.2 Consistency of CA metrics

The consistency within the field of measuring CA is complex, because of lack of a standardized method. Very few studies can be compared because the studies available are using different methods to estimate dCA metrics. In order to examine the consistency of the studies, two types of comparison will be deliberated: first, an intra-method comparison (MRI and MRI, or TCD and TCD); and second, an inter-method comparison (MRI and TCD).

Within the fMRI studies that used BOLD signal amplitude to assess dCA, different methods were used to induce dynamic changes such as hypercapnia [93, 117, 131, 132], BH [133], and TCR [22]. Despite different physiological interventions, six of the MRI studies obtained comparable values for the percentage BOLD signal change, and the results were consistent for regional GM and WM measures (Appendix 1-Tables 21, 22, and 23) [22, 93, 117, 131-133]. Three studies indicated regional differences in the cerebrovascular response within the cerebral cortex [22, 93, 117]. It is important to notice

that the strategy and methodologies applied were not the same across all studies.

The reliability within the TCD studies can be observed by comparing the absolute CBFV measures. Most of the studies obtained a relatively consistent ratio of CBFV-variability despite the diverse ABP fluctuating interventions [9, 10, 99, 111, 123, 134]. Four studies obtained none or little change in CVCi using a handgrip and the cold pressor test (CPT) to stimulate dynamic changes [37, 121, 122, 135].

2.6.3 Regional heterogeneity

The anatomical coverage depends mainly on the method of measurement. Most of the TCD studies focused on MCA measures because of the reliable accessibility through the temporal window. However, some studies acquired repeatable measures from different cerebral vessels using TCD. Wszedybyl et al (2012) calibrated blood flow measures from the ACA using TCD [136].Willie et al (2012) used near-concurrent vascular ultrasound measures of flow through the ICA and VA, and blood velocities in the PCA and MCA [123]. Their results showed larger reactivity in VA compared to other vessels in response to hypocapnia, but similar reactivity for hypercapnia in all vessels. Meanwhile, the MCA and PCA velocity measures showed lower estimates than the ICA and VA. Their findings suggest the underestimation of TCD measures in smaller diameter arteries, which is concurrent with the results from the study by Meckel et al (2012) [74]. Furthermore, their results of regional heterogeneity of blood flow regulation in the brainstem and cortex support the results of Horsfield et al (2013) [22], who showed regional CVR heterogeneity in an fMRI study.

The main debate on regional coverage can be addressed in the MRI studies. There are some consistent recorded regional heterogeneities of cerebrovascular response in between grey matter (GM) and white matter (WM), and also in between cerebellum and cerebral cortex [22, 93, 117, 132] (Appendix 1-Tables 21, 22, and 23). The general agreement, over the recorded larger signal drop being more in GM than in WM, is sensible because of the higher metabolic demand of GM. Nevertheless, in Bright et al (2009), different regions within cortical GM were compared for the BOLD signal intensity. The bilateral medial cortex reached a maximum signal intensity a few seconds earlier than the rest of the cortical GM [93]. Kassner et al (2010) compared "within-day" and "between-day" CVR reproducibility and noticed excellent "within-day" CVR reproducibility in both GM and WM (ICC=0.92 and ICC=0.88 respectively), but excellent "between-day" reproducibility only in WM (ICC=0.66) [132]. Although these results might need further validation, they show the regional sensitivity of BOLD signal response to hypercapnia.

In terms of regional heterogeneity of dCA metrics, there are few consistent results across TCD and MRI studies [22, 93, 117, 123]. The results of these studies show faster recovery in WM than GM, which may be related to the vascular density and vasodilatation. Furthermore, Bright el al's (2009) study showed consistent regional heterogeneity in the BOLD signal response timing to cued deep breathing and a periodic breath-hold test. The BOLD signal amplitude in parts of the basal ganglia, particularly the putamen and bilateral areas of the medial cortex, reached their maximum signal intensity change several seconds faster than GM [93]. Willie et al (2012) used CBFV measures from TCD to estimate the cerebral vaso reactivity in different vessels. The vertebral artery showed more reactivity to hypocapnia than ICA, MCA and PCA, while reactivity to hypercapnia was similar in all major arteries [123].

In order to outline a stepwise intra-method and inter-method comparison a meta-analysis is more reliable; this is not feasible and therefore not included in this review. However, synthesis of the data in terms of average means, ranges and confidence intervals is not applicable because of the excessive heterogeneous data, the different interventions and/or different read-outs.

2.6.4 Interventions to fluctuate blood pressure

Estimating the cerebrovascular reactivity response to rapid arterial blood pressure fluctuations is a convenient method for measuring CA metrics. High variability of MABP results in better estimation of the dCA measures [99]. A range of methods that fluctuate the systemic blood pressure can induce the dynamic response changes of autoregulation. But the safety and availability of these methods are restricted by many factors, such as the method of measurement and the subject's compliance. Autoregulation performance is activated by a decrease or increase in the arterial blood pressure. However, the effectiveness of the decreased or increased BP on the cerebral blood flow regulation might be different. This is not addressed in the literature to the best of the author's knowledge.

Another way to induce dynamic CA is by changing the partial pressures of respiratory gases. Several studies included in this review have used hyperoxia or hypercapnia to stimulate dynamic changes in the cerebral vasculature [18, 73, 93, 94, 98, 99, 114, 115, 117, 123, 131, 132, 134, 137-139]. Different respiratory challenges were used to induce changes in the ETO2 and ETCO2, such as a gas mixture with a high CO_2 concentration (4-8%), short periods of high O2 delivery (100%), and breath holding techniques (Figure 4). The respiratory challenge studies could be considered as relatively robust non invasive methods for inducing dynamic changes.

Hypercapnia can induce a sufficient BOLD signal change and this can be acquired in a short period of time [94]. The spatial extent of the vasomotor response (VMR) to respiratory challenges can be improved by expressing the BOLD response as a percentage signal change using ETCO2 as a

regression value [18, 98]. Nevertheless, fast reproducible vasomotor response measures can also be obtained using a combination of PC MRI and breath-hold (BH) challenge [98]. There are few factors that affect BH test results. These can be classified as follows: first, technical factors such as the depth of respiration, the duration of BH and the phase of respiratory breath-hold (expiratory or inspiratory); and second, physiological factors such as the baseline CBF and regional heterogeneity. The physiological aspects of the dynamic changes in response to hypercapnia are different from those of arterial blood pressure changes. Hence, comparing the effects of these two physiological triggers might enable a better understanding of the dCA performance.

The next most frequently used method is thigh cuff release (TCR). Four studies used this method (Figure 4). TCR is considered as a slightly uncomfortable experience for the subjects, but out of the 62 subjects who underwent this method to stimulate dynamic cerebral autoregulation (dCA), only one subject withdrew due to pain intolerance. The CBFV results obtained under the TCR influence are relatively consistent in all of the studies [17, 22, 99, 134]. Furthermore, Katsogridakis et al (2012) tried to increase the specificity and sensitivity of dCA measures by adding TCR to the hypercapnia method. In their results, combining the two methods improved the sensitivity and specificity of CA impairment diagnosis. Area under the curve (AUC) increased from 0.746 to 0.859 ($p=0.031$) [99].

Another method is the isometric handgrip test (IHGT). Although sufficient blood pressure change is obtained from IHGT [119, 120] and it is possible to use this in the MRI scanner, no studies that have used this method to stimulate dynamic cerebral autoregulation changes in the scanner could be retrieved from the database. On the other hand, four TCD studies used IHGT to stimulate MABP to measure the MCA velocity response changes (MCAv).

Three of these combined IHGT with the cold pressor test (CPT) [37, 122, 135]. Vianna et al (2012) have observed a mild decrease in the cerebrovascular conductance index (CVCi) response to CPT, the rate of reduction was decreased by adding IHGT to the method [140]. Wszedybyl-Winklewska et al (2012) used only IHGT to stimulate blood pressure and obtained a significant increase in the pial artery resistance, with a simultaneous decrease in the width of sub arachnoid space (SAS)[121]. IHGT might give sufficient perturbation in the systemic circulation to allow dynamic cerebral autoregulation activation.

Although a combination of methods may give higher perturbation in the systemic circulation combining different methods should be performed carefully as pathways through which the dynamic changes are induced might be conflicted. The cerebral vascular adaptation that takes place in response could be altered or even blunted.

2.6.5 Limitations

Measuring the dynamics of CA relies on the method of blood pressure fluctuation and the CBFV acquisition technique. Despite advances, the gold standard of assessment remains elusive and clinical practice is limited. In general, one of the challenges in measuring CA is the temporal pattern of the measurement method. Deoxyhaemoglobin accumulates over time in the cerebral circulation. It might interfere with the direction of the principal approach and disperse the absolute values. It is not possible to control the critical variables through a pre-defined time interval. At the same time, the cerebrovascular response is not instantaneous. The hemodynamic response function follows a stimulus by a few seconds. Therefore the stimulus interval should be considered carefully when attempting to induce dynamic changes. Cerebral autoregulation is frequency dependent; accordingly, the applied methods should assume the non-linear nature of autoregulation when trying to quantify the dynamic changes.

MRI studies are limited by technical factors such as the signal to noise ratio (SNR), the resolution and spatial coverage. The physiological noise, which is corrected in most of the fMRI studies, could be used to obtain peat-to-beat dCA measures.

The main limitation of TCD measures is spatial resolution, which is restricted by anatomical windows. The tortuous arteries and angulations can be another restriction in velocity based TCD measures.

Identifying the best method to measure dCA metrics requires a meta-analysis study, to evaluate the measurement methods quantitatively as well as qualitatively. However, a quantitative analysis of the available

measurement techniques is not possible at this stage for the following reasons. First, meta-analysis calculates and compares the weighted average of common measures that are shared between studies. It is obvious from the studies included in this review that CA metrics are affected by inter- and intra-subject variability. Second, there is a lack of standardized measurement methods. Finally, the non-stationary nature of CA restricts the reliability of a longitudinal follow-up for the measured indices.

2.7 Conclusions and future directions

The methodologies and applications of dCA assessment have been reviewed according to their reproducibility and consistency. Autoregulation is time and frequency dependent rather than a concrete value. There is very limited consistency within and between methods. Even so, few studies with consistent changes in CBF and CBV changes were identified. Regional heterogeneity between GM and WM and also the cortical and sub-cortical regions was consistent in a few studies regardless of the different acquisition methods applied.

A standard physiological tool to measure autoregulation parameters is still under development. The majority of studies that have evaluated CA are proof of the concept while what is necessary is the development of standards for physiological interventions, haemodynamic sensitive imaging, and analysis methods. A comparison of standardized methods would give more rigorous results. The development of fMRI studies with different analysis methods provided a better understanding of the physiological parameters of autoregulation. Arterial blood pressure variation provides a strong element for mapping the dCA pressure response. Studies that compare the methods of ABP perturbation are necessary in the field. The potential of MRI as a physiological diagnostic tool for CA may be improved by the application of a higher field of strength (7T), reliance on a more consistent physiological ABP fluctuation method, and the ongoing improvement of analysis methods.

Chapter 3

3 Obtaining beat-to-beat Arterial Blood Pressure Measurements using Non invasive methods

3.1 Background

To study dynamic cerebral autoregulation, a step response change should be induced in the arterial BP to allow recording of the corresponding CBF changes [9]. Another method to induce a cerebrovascular response change as an index of CA is hypercapnia or hypocapnia. Changing the end tidal CO2 (ETCO2) concentration has been used in several studies to induce dynamic responses [93, 94, 98, 109, 110]. Different respiratory challenges have been used for this purpose such as breath-hold and increasing the inhaled CO2 concentration (5%). Respiratory challenges are also associated with BP changes (The mechanism behind this process is discussed in Chapter one).

Previous studies have successfully estimated CA changes using instantaneous recordings of CBFV and ABP step changes from TCD and Finapres (Finometer), respectively [6, 17, 22, 34]. The Finometer system is approved as a reliable non invasive ABP monitoring device. The reliability of Finapres ABP recordings has been examined previously by comparing the results with invasive arterial blood pressure measurements [141]. Nonetheless, in the current study, the CA assessment was to be undertaken using fMRI, an Finapres is not compatible with the magnetic field. Instead, the Caretaker device was used from the Biopac® system, which is an MR compatible plethysmographic device that can be used to monitor beat-to-beat ABP measurements [142].

Several non invasive interventions were used to induce step changes in ABP. The reliability and consistency of these methods are controversial. The selection of the non invasive stimulus type depends on the patient group and also the compatibility with the CBF acquisition device. This thesis examines two main types of non invasive autoregulatory-stimuli to be used in healthy volunteers. These include: thigh-cuff release (TCR), and respiratory challenges. The respiratory challenges consist of three different tests: deep-inspiratory breath-hold (iBH), non-inspiratory breath-hold (BH) and cued deep breathing (CDB). The physiological background of each method is discussed in Chapter 1. These methods were examined outside the scanner first to evaluate the feasibility and repeatability of each experiment. Before assessing each method for robustness and consistency, it was necessary to assess the feasibility of the recording device outside the scanner, to be used later as a reliable ABP acquisition tool in the scanner. For that reason we acquired instantaneous ABP recordings during TCR and BH using both devices, the Caretaker and Finometer. The BP response to the CDB test was recorded using only the Finometer because during the data acquisition time the Caretaker system was not available due to some technical issues. Figure 5 shows a graphic summary for the pilot studies and the measurement devices used in this chapter.

During the study to develop non invasive BP measurement methods, another two methods were used in five healthy subjects to induce BP fluctuation, IHGT and leg elevation. Blood pressure fluctuation could not be obtained from either of these two methods; therefore they were excluded from the method development studies (Data is not shown).

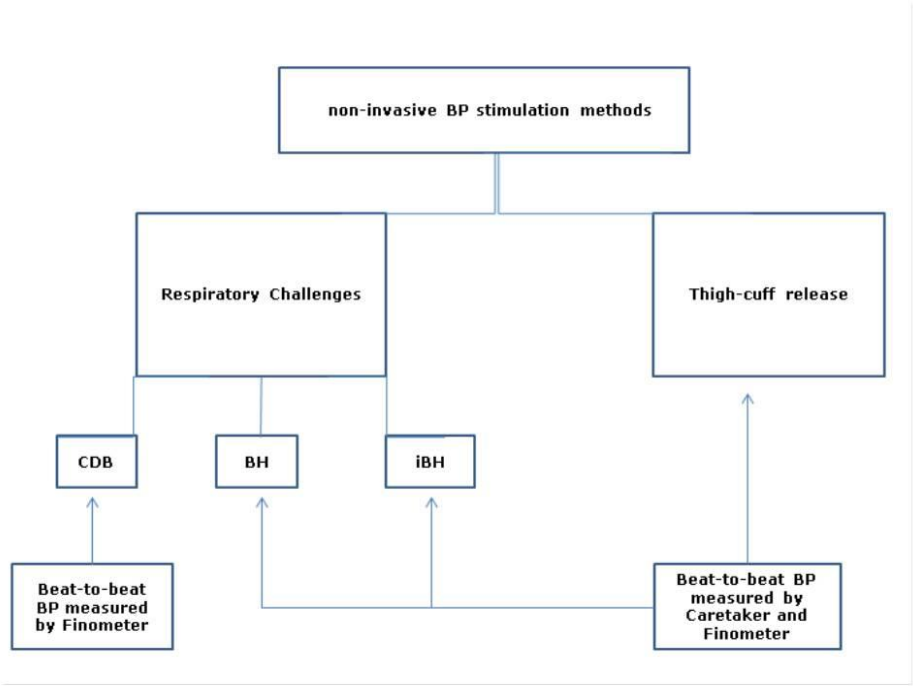

Figure 5 Summary of non invasive BP fluctuation methods

Diagram shows a summary of the measurement devices used outside the scanner. CDB cued deep breath, iBH deep-inspiratory breath-hold test, BH non-inspiratory breath-hold test, BP blood pressure

3.2 Plethysmographic arterial blood pressure recording devices

3.2.1 MR compatible arterial blood pressure monitoring device (NIBP-MRI/Caretaker; Biopac®)

The Caretaker system (Empirical technologies Corporation, Charlottesville, VA) estimates arterial blood pressure on the finger (Figure 6) by analysing the amplitudinal and temporal behaviour of the component pulses that constitute the peripheral arterial pulse [142]. The Caretaker effectively records the arterial blood pressure through reconstructing the estimated peripheral arterial pressure. It is MR compatible, which allows for obtaining the continuous arterial blood pressure estimation at any field strength (http://www.biopac.com/Noninvasive-Blood-Pressure-MRI).

The sampling rate depends on the heart rate (HR). Like other plethysmographic devices, the Caretaker records the BP value at the beginning of each cardiac cycle (heart beat). This might be a limitation for large sample size studies, particularly for populations with a very wide range of variable heart rates.

Tracking and quantifying the arterial component pulses is a challenging task and the algorithms that perform this task are still being refined. Under optimum conditions the acquisition process still experiences intermittent drop-outs [143].

3.2.2 Non invasive Continuous Arterial Blood Pressure Monitoring Device from (Finometer ®)

By clamping an artery, the Trans mural pressure (the pressure difference across arterial wall) is set to zero. When the artery is fixed at its unstressed and non-zero diameter, the intra and extra- arterial pressure are parallel; this is referred to as the "Penaz method" [144]. The Finometer uses the Penaz method to indirectly measure arterial pressure from the finger [145]. It is a reliable alternative to invasive arterial pressure monitoring (Figure 7) [146]. The beat-to-beat ABP measures from the Finometer and the CBF measures from the TCD have been used to estimate CA metrics [17].

The accuracy of the device has been evaluated for clinical and experimental settings [147, 148]. In addition to BP, it measures several other physiological entities such as cardiac output (CO), stroke volume (SV), and heart rate (HR). The BP recordings focus on the absolute measurement of the systolic and diastolic measures and their variability [147].

The recorded data is susceptible to technical and physiological artefacts. The physiological confounds are mainly due to changing posture, sneezing, coughing and other normal physical reflexes [147, 148]. The servo-control system that inflates the finger cuffs maintains sufficient pressure in the cuffs according to the blood volume available in the peripheral artery. This is controlled by a physical algorithm [145]. The physical auto-calibration allows long term recordings of BP. It corrects for changes in the stress and tone of smooth muscles in the arterial wall that occur during recording. The main limitation of using the Finometer in this experiment was the non-MR compatibility of the device.

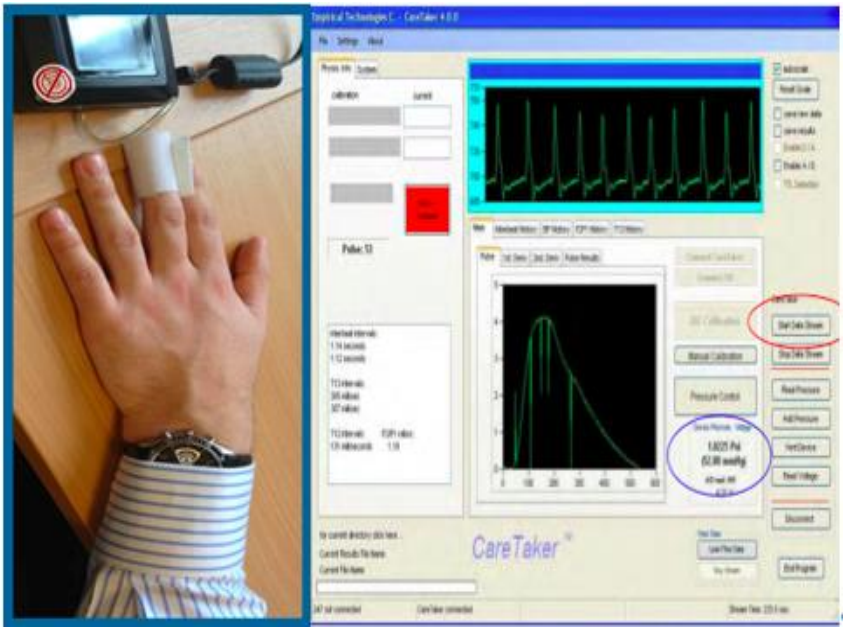

Figure 6 Caretaker finger cuff, port and graphical user interface GUI

Figure 7 Finometer finger cuff and device

3.2.3 Technical issues

At the beginning of this study the Caretaker device was suffering from severe technical issues. The BP measurement was crucial for the dCA metrics. Therefore, at the beginning of this pilot study the BP measures were obtained manually at an interval of 1 minute using a (OMRON HEM-790IT) sphygmomanometer (data not shown). The Caretaker device had been returned to the manufacturer because of some technical issues. The main issue was a rupture in the one-way control valve that controls the coupling pressure between the NIBP port and the finger cuff. Maintaining the coupling pressure at 40-50 mmHg is necessary in order to receive a good signal from the device. Another BP recording problem was the GUI control system, which suffered from frequent drop-outs during the BP recordings. Even though the software was updated to the latest version, this problem still occurred sometimes. As I noticed that the drop-outs often occurred when the saving results function was activated before the calibration process, the BP data recorded by the Caretaker were shared with the Biopac system support team to check the quality of the data. Another problem associated with the Caretaker BP recording was the long connecting tube that controls the finger cuffs from the control room to the scanner that has lead to loosening of the cuff pressure and required multiple calibrations within a scanning session.

3.3 Monitoring beat-to-beat arterial blood pressure measures

3.3.1 Methods and materials

Five healthy adult subjects were recruited for the cued deep breath (CDB) study (22-31 years; 2 females). Another three healthy volunteers (22-31; 1 male) were recruited for the TCR and BH test. Table 2 summarizes the number of healthy volunteers recruited for each protocol. The thigh-cuff release and breath-hold test were performed during the same session with the same volunteers. The BH test was implemented first, followed by the TCR challenge; ten minutes rest was allowed between the protocols. This study was conducted according to the approved ethics of Nottingham ethics committee for developing novel MRI techniques (appendix 2).

The subjects were positioned comfortably on a medical couch. Instantaneous BP recordings from both devices were acquired at a sampling rate of 100Hz. Each device cuff was attached to the middle finger of the contralateral hand (Figure 6 and 7). For all of the pilot studies outside the scanner, the author performed the application of the devices, the subject preparation, the data acquisition, the study observation, and the data analysis.

The Finometer device was calibrated automatically at the beginning of each experiment and after changing posture or replacing the finger-cuffs. The starting and stopping points for each experiment were marked manually for both devices, which led to a gap of a few seconds. To compensate for the timing latency, the Caretaker device was always marked before the Finometer, because the latter is provided with a single key marking function that may limit the time gap to one second or less. The recorded BP data was

marked for the time of each stimulus (BH or TCR). This helped to separate the artefactual pressure curves from the stimuli induced BP fluctuations.

The blood pressure was manually calibrated for the Caretaker system. After establishing Bluetooth communication between the power supply and the GUI control system, the brachial artery blood pressure was used as a reference for calibration. This was measured using a (OMRON HEM-790IT) sphygmomanometer.

The Caretaker data was observed and collected using graphical user interface (GUI) control software (vs. 4.1.0 - 4/20/2012) (Figure 6). This allows for controlling and maintaining the pressure in the sensor pad through a single pathway valve system.

During the TCR test, large inflatable cuffs (Model C22, Hokanson Inc., USA) were wrapped around each thigh. The inflation of the thigh-cuffs was started after securing a sufficient recording signal from both devices. The thigh-cuffs were inflated to at least 20 mmHg above the systolic BP and this was maintained for three minutes. A one-minute recovery period was recorded after the sudden release of the thigh-cuffs. A custom-made wooden footrest was used to support the leg against the deflation manoeuvre, this was provided by a study collaborator (Mark Horsfield) from the University of Leicester. The footrest allows subjects to brace their feet at a comfortable knee flexion angle and also prevents motion artefact during deflation. At the end of the experiment, all of the volunteers were asked to give feedback about the TCR experiment and rate any discomfort or pain they had experienced during the cuff inflation and/or deflation.

During the breath hold test the instructions for breath hold and release were delivered using the subject's visual inspection of a sequential power point presentation on a 15.6'' HP laptop. A four-minute recording was obtained

for each protocol, in which three 20s breath holds were performed with 30s rest in between. The instruction was given at the beginning of each iBH, to take the deepest inspiration and then hold the breath. For the BH test, the cessation of breath was performed at any phase of the respiratory cycle that corresponds to the timing of breath hold without any effort to change the phase of respiration. To confirm a consistent breath hold test, the cessation of breathing was observed carefully by the author throughout the experiment. This was further verified by comparing the HR disparity during the apnoeic phases.

The transfer function between the CDB test and BP was estimated by having the subject perform a series of 2 second deep inhalations and 2 second exhalations interleaved with 60 seconds of normal breathing. The cued deep breaths were repeated six times in one recording session; the overall recording time was seven minutes (Figure 8). The beat-to-beat systolic/diastolic compartments of BP were measured using the Finometer device.

Blood pressure fluctuating method	Number of healthy volunteers participated in each method			
	Caretaker BP measurement	Finometer BP measurement	MRI (BOLD) sequence	MR-angiography (4D PC) sequence
TCR	Φ 3	Φ 3	æ 6 (1* excluded)	Non
iBH	Φ 3	Φ 3	æ6 (2**excluded)	Ψ 2
BH	Φ 3	Φ 3	Non	Ψ 2
CDB	◊ 5	◊ 5	Non	Non

Table2 Summary of the volunteers who participated in each protocol. TCR, Thigh-cuff release, iBH, deep-inspiratory breath-hold test. BH, non-inspiratory breath-hold test. CDB, cued deep-breathing. BOLD, Blood oxygen level dependent MRI, 4D PC, Time resolved Phase-contrast MR angiography.

Matching symbols signified by the number of volunteers represent identical subjects.

* Results for one TCR were excluded because of a severe motion artefact present in both scans.

** Results of two iBH were excluded because different scanning parameters were used (Time of repetition of 500 ms and 1000 ms)

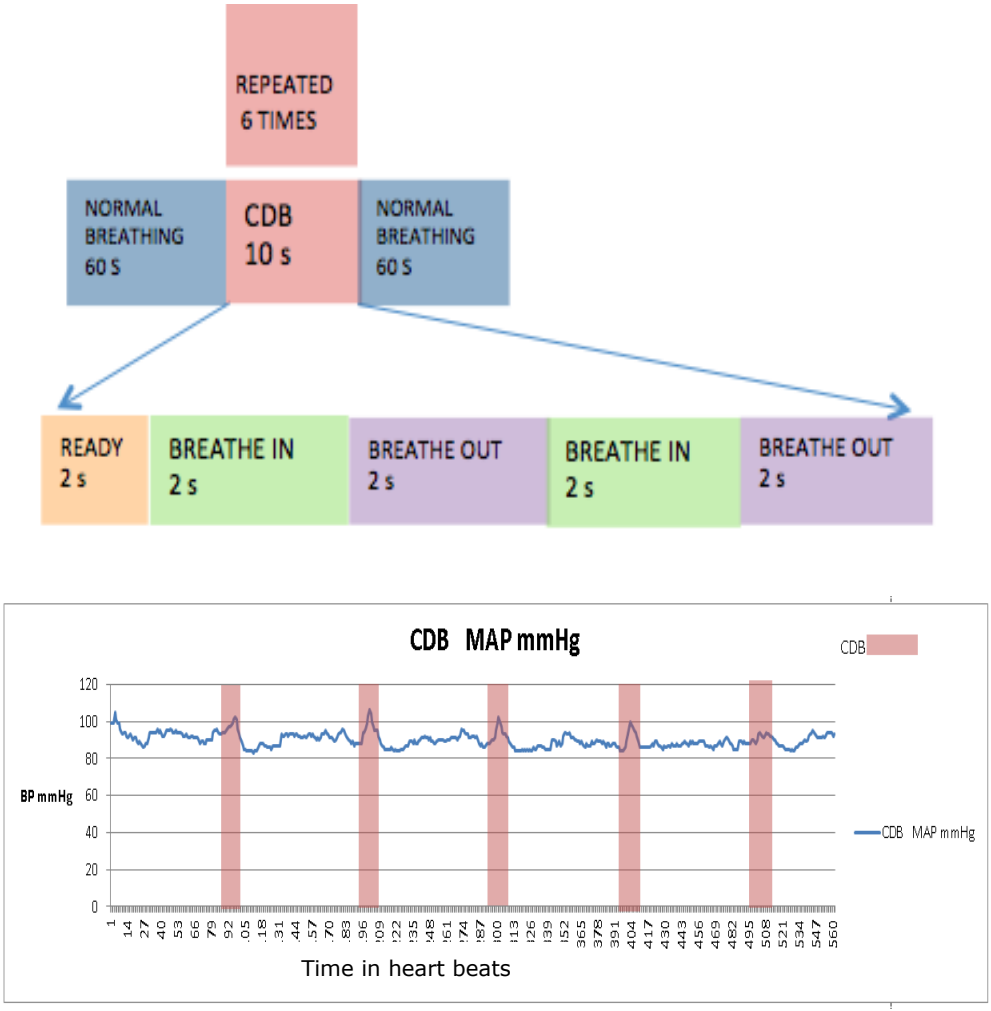

Figure 8:Schematic representation of cued deep breathing test (CDB) and observed BP response.

The top panel shows the sequential presentation of respiratory performances during CDB.
The lower panel shows the average recorded MAP during CDB (averaged for five subjects)

3.3.2 Data Analysis

The Finometer data was transferred to digital format using (Beat scope 1.1a) software (www.adinstruments.com/products/beatscope). The functional marks that defined the starting and stopping points were selected and then exported after reformatting the (beat) files to text files. The data were saved in Excel spread sheets for further processing.

The caretaker data were saved in ASCII format. The data were transferred to text files to be processed later into Excel format. During the data acquisition the Caretaker device recorded the following parameters inter-beat interval, systole, diastole, cardiac output (CO), and heart rate (HR), as well as the parameters that the algorithm calculates. The selected time points (markings) throughout the experiment (time of inflation and deflation) were applied to the recorded BP measures (Appendix 3 contains the output file formats and relevant information). The acquired data were filtered manually using Microsoft Excel to remove any zero readings and drifts. This was performed by applying a filter to remove any zero values from the data. The mean arterial blood pressure (MAP), which is the average blood pressure during one complete cardiac cycle, was calculated from the systolic and diastolic compartments of arterial blood pressure. This was compared to the brachial artery MAP measurements acquired at the beginning and end of the experiment to estimate the reliability of the quantitative readings from the Caretaker.

The MAP was calculated using this formula

$$\text{MAP (mmHg)} = \frac{2 \times Diasotle(mmHg) + Systole(mmHg)}{3}$$

Equation 1: In which MAP is the mean arterial BP, Systole is systolic part of BP in mmHg and Diastole is diastolic part of BP in mmHg [149]

The sampling rate for all devices that operate using the Penaz method or arterial clamping depends on the heart rate. In other words, a BP reading is recorded at the beginning of each cardiac cycle from both devices. Therefore, it was possible to compare the data between the devices.

The time point at which the minimum BP drop occurred after each stimulus was visually identified. The MAP for each subject and each method at the baseline was calculated according to equation 1. By definition, the recovery of BP is equal to the baseline BP before the stimulation, and this was standardized to detect the recovery BP for all of the BP fluctuating methods. The average MAP for three subjects was compared to show the step changes measured with each device for the TCR, BH and iBH methods. The descriptive statistics were performed using a statistics package for the social sciences (SPSS v.22). An unpaired student t test was used to compare the means.

3.3.3 Thigh-cuff release method

- **Results**

  During the pre-MRI TCR protocol, all of the subjects (n=3) showed a distinct BP drop after the thigh cuff-deflation. All of the subjects tolerated the test and their rating for the discomfort level was minor to moderate. The MAP for the three cases measured with the Caretaker and Finometer were relatively close and comparable to the brachial artery MAP measures measured with the arm-cuff sphygmomanometer (Table 3). Table 4 summarizes the results averaged over the three TCR tests. The BP drop after TCR was deeper for the Caretaker measurements than for the Finometer (Caretaker 58±8 mmHg, Finometer 70±1 mmHg; mean±SD). The percentage BP decrease after thigh-cuff deflation was (29±1.3%) and (20±0.5%) for the Caretaker and Finometer, respectively. However the two-tailed t-test was not statistically significant for the two values (P=0.3). Both devices were able to represent the fast BP–drop after the deflation and the post-stimulus recovery (Figure 9). The average recovery time for the BP to re-align to the baseline after the drop was (12-25) and (15-22) heart beats for the Caretaker and Finometer, respectively.

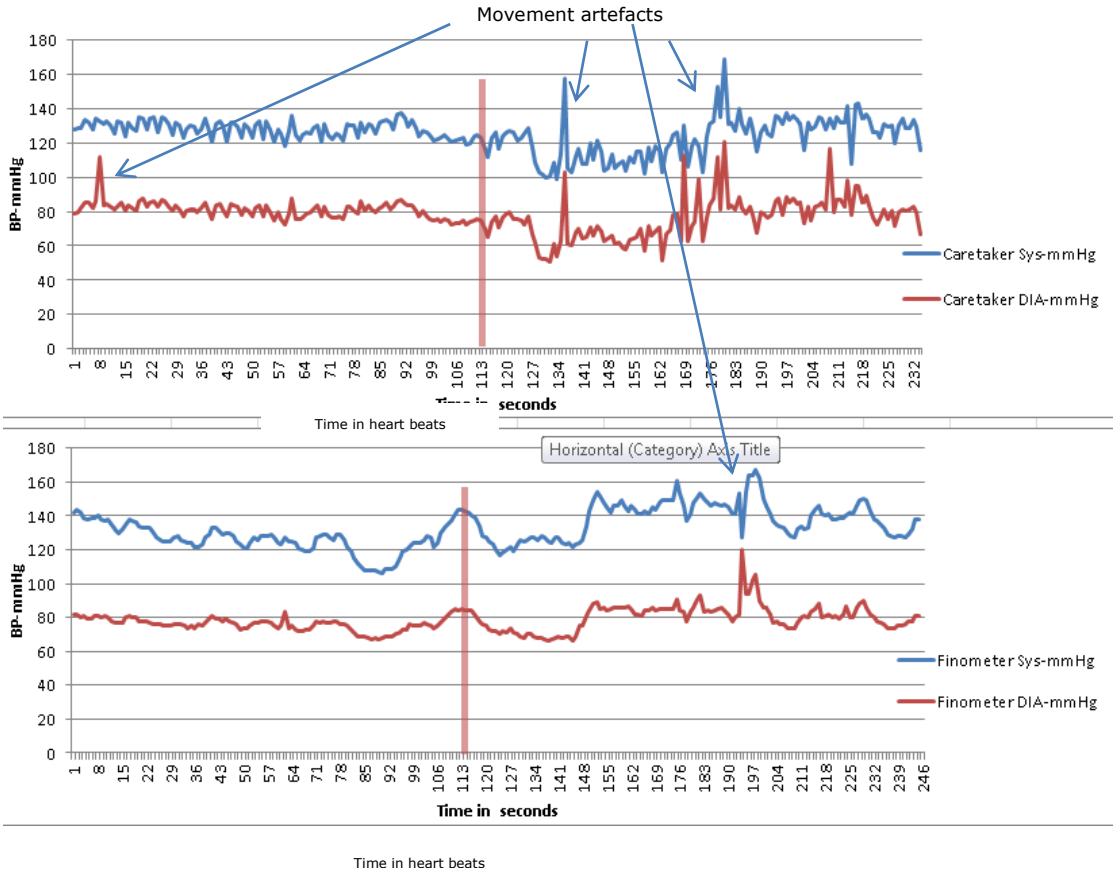

Figure 9: Blood pressure (BP) response curve to thigh-cuff release (TCR) method

(32 years; male subject) shows the systolic (Sys) and diastolic (DIA) arterial BP measures recorded simultaneously, measured by the Caretaker (top panel) and the Finometer (lower panel). The pink bar indicates the time of thigh-cuff release.

Subjects	Brachial-artery	Caretaker	Finometer
TCR1	92 mmHg	89 mmHg	89 mmHg
TCR2	96 mmHg	99 mmHg	90 mmHg
TCR3	90 mmHg	93 mmHg	92 mmHg
(mean±SD)	(92±3)mmHg	(93±5)mmHg	(90±1)mmHg

Table 3: Mean arterial blood pressure measures (MAP) at the baseline from the three devices (Omron-HEM, Caretaker, and Finometer)

MAP (mmHg)	Caretaker (mean±SD)	Finometer (mean±SD)
Baseline BP	(88-95)	(88-91)
BP at the time of deflation	(87-98)	(84-95)
minimum BP after deflation	(55-66) (~30%)decrease	(69-72) (~20%)decrease
baseline BP after deflation	(84-98)	(89-91)

Table 4 MAP measures from the Caretaker and Finometer devices at different time points after cuff-deflation

- **Discussion**

This experiment shows that the Caretaker and Finometer can both track BP changes over very short periods of time (<second). The MAP acquired at different time points after the release of the thigh-cuff was repeatable across the devices and subjects. The Caretaker derived MAP measures were slightly higher than the Finometer MAP measures (1-3 mmHg). This might be due to the over-sensitivity of the Caretaker device to movement artefacts and changes of posture (Figure 9). Furthermore, the Caretaker finger cuffs are single layered; therefore they should be applied with caution to avoid extra tight application, which can lead to higher readings. On the other hand, the Finometer finger cuffs are double layered and less vulnerable to false readings. This can be seen in our data, where the MAP measures show less variability in the Finometer recordings than in the Caretaker readings (Figure 9).

The Caretaker Device does not require frequent re-calibration as long as there are no changes in the subject's posture and the position of the cuff. The algorithm has to detect and analyse each heartbeat. Therefore the Caretaker data is more prone to physiological noise interference, such as coughing and sneezing. Even normal tone speaking affects the results of the ABP measures. The main cause of a poor signal from the Caretaker is inadequate coupling pressure between the device and the finger-cuffs (≥50 ≤ 40). Poorly perfused and cold fingers are other sources of artefact.

The Caretaker device recorded deeper BP-drops in response to a sudden release of the thigh-cuffs compared to the Finometer but the difference was not statistically significant ($p = 0.3$).

The Caretaker and the Finometer were both able to track BP changes over short periods of time. The MAP readings were reliable in comparison to the

brachial artery acquired MAP. The results of this experiment show reliable BP quantifications by the Caretaker device. However, the long connecting tube that connects the finger-cuff to the acquisition port in the MRI control room may affect the consistency of Caretaker measures inside the scanner.

A pilot study would be necessary before using it for haemodynamically unstable patients in the scanner. The sudden release of the thigh-cuffs induces a fast BP drop with corresponding CBFV changes in the brain that can be used to measure dCA metrics in healthy subjects. This study included only a healthy population with normal range BP. Evaluating the reliability of the dCA diagnostic tool requires examination at high blood pressure levels and in patient populations [12].

In conclusion, the results of this experiment suggest the feasibility of an MRI compatible NIBP- Caretaker device to track induced BP changes inside the scanner.

3.3.4 Inspiratory and non-inspiratory BH

- **Results**

  For the three healthy volunteers, a total of nine iBH and eight BH were obtained (the BP recordings of one BH test were excluded because of severe movement artefact). An iBH of 20 seconds resulted in a transient increase in BP followed by a step-response decrease, while the BH resulted in a gradual increase in BP without any considerable decrease at the end of the breath-hold (Figure 10). The different BP-response curves to inspiratory and non-inspiratory breath-hold were detected after initial observation of a single subject. This was the main reason for comparing the deep inspiratory with the non-inspiratory breath-hold tests in this pilot study. There was a significant difference between the BP response to the iBH and BH (P=0.0015). The BP drop was (17±3%; mean±SD) from the baseline for the iBH. The BP increase was (20±0.5%) for the iBH and (20±1%) for the BH. Tables 5 and 6 show the results of the BP fluctuation for both the iBH and BH. The difference between the BP-increases for the iBH and BH were statistically not significant (P = 0.3). The BP increase from the baseline was ~20% for both the iBH and BH. The BP response curves to the BH and iBH were consistent across repeats of the same experiment.

Subjects	MAP mmHg	%BP-drop	%BP-increase
iBH1	82	14%	21%
iBH2	78	17%	21%
iBH3	99	21%	20%
Means	86±11 (m±SD)	17±3 %	20±5%

Table 5: mean arterial blood pressure (MAP) responses to 20-second deep-inspiratory breath-hold (iBH)

Subjects	MAP mmHg	%BP-increase
BH1	89	20%
BH2	105	19%
BH3	78	21%
Means	90±13 (m±SD)	20±1%

Table 6: mean arterial blood pressure (MAP) responses to 20-second non-inspiratory breath-hold (BH)

A

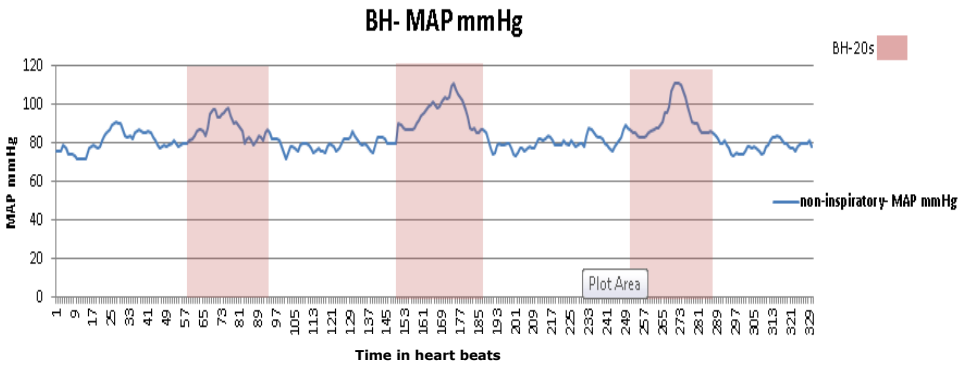

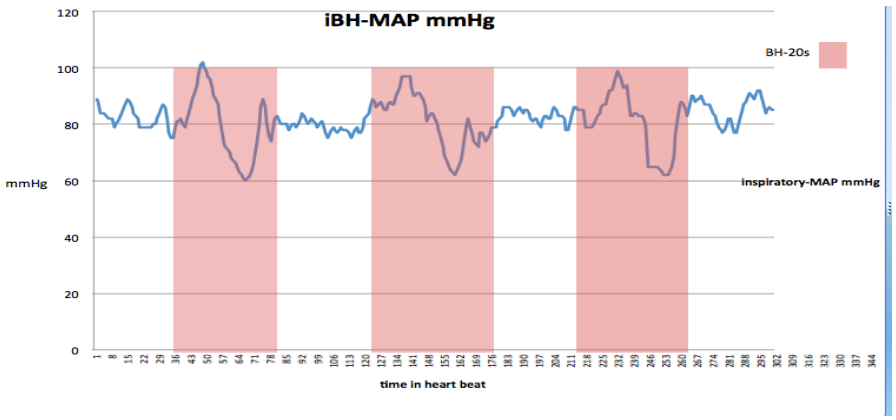

B

Figure 10 Mean arterial blood pressure (MAP) from Caretaker device

(31 years, male). A: during non-inspiratory breath-hold test B: during deep-inspiratory breath-hold test. The three BP effects were averaged for each experiment. The data is shown in Tables 5 and 6.

- **Discussion**

The transient cessation of breathing resulted in a BP change in both the iBH and BH tests. In all of the subjects the iBH resulted in a BP increase followed by a step response decrease, while the BH resulted in a gradual increase in BP. The BP increase was similar for both methods ~20%. The BP increase was in line with other study findings [105].

The iBH method results in a biphasic BP response, whereas the BH method results in a monophasic BP increase (Figure 10). This kind of fluctuation in BP response to the iBH method develops a sufficient gradient in the BP change from the minimum to the maximum BP levels, which could improve the stimulation of dCA changes.

The difference in the BP response curve for the iBH and BH resembles the negative pressure that occurs in the thoracic cavity at the beginning of deep inspiration. This derives a transient pressure drop in the arterial tree. Maintaining BH for 20 seconds is associated with a sympathetic activation, which is derived from both the fear of suffocation and the efforts made to maintain a closed glottis against the urge for respiration [109]. This might be the cause of the BP increase associated with breath-holding technique.

Breath-hold is a non invasive method that results in adequate BP fluctuation to induce dCA changes. The iBH and BH give different BP fluctuation curves. The BP-drop associated with iBH may improve the dCA activation in brain. The BP-curve response to iBH is more similar to the valsalva effect that has been used previously to induce dCA changes [150]. Monitoring the respiratory volumes with a Capnograph would be necessary to give a better insight into the associated ETCO2 changes. This is because ETCO2 is an indicator of the CO2 level in the blood, which is a potent vasodilator that affects haemodynamic metrics.

In conclusion, the BP change associated with iBH can induce sufficient BP fluctuation to improve the corresponding BOLD signal changes. This method will be taken forward by applying it in healthy volunteers to induce dCA in the scanner.

3.3.5 Cued Deep Breaths

- **Results**

  Cued rhythmic deep inspirations induced a BP increase that is visually apparent in Figure 8. Table 7 shows the results of the BP records for the five healthy volunteers. The average BP increase in response to CDB for the five subjects was (10±5%; mean±SD). The average baseline BP for the five cases was (84±2; mean±SD). The difference between the baseline and the CDB BP-peaks was statistically significant (p=0.01). The average MAP during the recovery period between the repeated CDB was (81±5; mean±SD).

Subjects	Baseline-MAP (mmHg)	Recovery-MAP (mmHg)	Peak-MAP (mmHg)	% change
CDB1	81	76	93	12
CDB2	87	88	106	19
CDB3	86	83	96	10
CDB4	83	78	87	4
CDB5	85	82	91	6
(mean±SD)	84±2	81±5	94±7	10±5%

Table 7: summary of mean arterial blood pressure (MAP) measures after cued deep breath test (CDB).

Baseline is the MAP before the CDB performance, Recovery-MAP is the MAP after CDB performance, Peak is MAP during CDB. Percentage change is calculated from the baseline before CDB.

- **Discussion**

  Cued deep breathing induced a MAP change that was recorded using a Finometer beat-to-beat BP measurement. The CDB induced BP changes in all of the subjects (n=5). The average response was (10±5%; mean±SD), which is less than the BH-induced BP changes (~20%). Although the average BP response to CDB was less than for BH, the associated ETCO2 change was enough to induce a BOLD signal change [93].

  The CDB induced transient hypocapnia that prompted a dCA reactivity response. Previously it has been shown that the depth of inspiration affects the BOLD response to BH [115]. This might also be a fundamental factor in the variability in the rate of BP response to CDB. In this study, the rate of BP response was variable from one subject to another (6-19%). Yet, the shape of the BP-peak responses was similar for recurrent CDB episodes (Figure 8).

  CDB could be a good alternative for situations where BH and other long-term respiratory modification are not applicable to induce dCA changes. This study could be further ascertained with respiratory volume measurements to determine the possible merit of the methods described.

3.4 Conclusions

The sudden release of inflated thigh-cuffs and respiratory challenges were used to induced BP changes in all of the subjects. The shape and amplitude of the induced BP modification was different across the methods. Table 8 summarizes and compares the induced MAP changes for all of the methods. The inspiratory breath-hold test induced biphasic and the most robust MAP fluctuating response and hence it was selected for the fMRI respiratory challenge study.

Both devices could track fast BP changes. The quantitative measures from the Caretaker and Finometer results were parallel. This indicates the feasibility of using the Caretaker as a reliable continuous BP monitoring device for the fMRI experiments.

Based on the findings of these pilot studies, the TCR and iBH methods will be used in the MRI scanner to induce BP fluctuation in healthy volunteers to stimulate a CA response in the brain.

Methods	% BP change	BP response pattern
TCR	(29±1%)↓	↓
iBH	(17±3%)↓. (20±5%)↑	↓ ↑
BH	(20±1)↑	↑
CDB	(10±5%)↑	↑

Table 8: Summarizing the percentage BP change-responses to non invasive arterial blood pressure fluctuating methods.

TCR thigh cuff release, iBH deep inspiratory breath-hold, BH non-inspiratory breath-hold, CDB cued deep breath. ↑ BP increase, ↓ BP decrease

Chapter 4

4 Using Physiological MRI to Estimate dCA Metrics

4.1 Introduction

The objectives of this chapter are: to examine the feasibility of estimating dCA metrics at 3T MRI scanner, using this in combination with two non invasive BP fluctuation methods that have been selected based on the pilot tests detailed in the previous chapter; and, to obtain beat-to-beat arterial blood pressure measures from the scanner for these two methods.

The dynamics of the BOLD signal amplitude are dependent on changes in CBF, CBV and CMRO2 [6], as described in Chapter one. Furthermore, changes in these parameters induce corresponding changes in the BOLD signal amplitude. Rapid changes in systemic BP induce instantaneous CBF changes in the brain. Measuring the amplitude of such concurrent changes in the CBF and BP allows for estimation of the CA metrics.

The sudden release of inflated thigh cuffs has been used to induce dynamic changes in the systemic BP [12]. The BP drop in response to the TCR method was examined in the previous chapter for healthy subjects outside the scanner, and a (29%) change in the MAP was obtained. Measuring the beat-to-beat arterial pressure in response to the TCR inside the scanner provides a better understanding of the corresponding BOLD signal changes. This was examined in this chapter by concurrent measurement of the BP and BOLD signal amplitude at 3T MRI scanner.

Breath-hold is another method that induces a BOLD signal change [83]. The average MAP change in response to a 20 second breath-hold was about (20%). The transient hypercapnia associated with breath-hold results in a gradual increase in CO2 concentration [83]. In addition to the vasodilatory effect of increased CO2, the breath-hold method is also associated with systemic BP changes. Blood pressure change stimulates the autoregulation process of the brain in order to maintain a relatively constant CBF despite the increase or decrease in BP. The shape of the BP response curve was examined for different respiratory challenges in the previous chapter. The deep-inspiratory breath-hold (iBH) induced a biphasic BP response, which is more similar to the valsalva effect. This kind of BP step response could improve the dCA metrics [150].

In this chapter, the dynamics of iBH BP correspondence in relation to the resultant BOLD signal change are examined. The methods, subject demographics, data acquisition and analysis methods are discussed first. After that, the specific results for each method are described. Finally, there is a general discussion and the limitations of the methods and applications are explained.

4.2 Methods and materials

Six healthy volunteers with a mean age of 28±7 (age range 23-42 years, 2 females) were recruited. Each subject was scanned for two protocols, TCR and iBH, in the same scanning session (Table 2). The results for one subject for the TCR method were excluded because of a severe motion artefact in both scans (details of detection for a severe motion artefact are described in the data analysis session). The results of the iBH for two subjects were not included in the group analysis because of different acquisition parameters (Time of repetition TR, 500 ms and 1000 ms vs. standard 2000 ms) (Appendix 4). This study has been approved by the Nottingham Ethics committee for the development and optimization of novel MRI techniques (B12012012A).

All of the volunteers signed a MRI safety questionnaire and informed consent form (a copy of both can be found in Appendix 2). The subjects were asked to refrain from consuming caffeine and alcohol for at least 12 hours before scanning. They were screened before the start of the experiment by the author for any respiratory disease that may affect or limit their performance in the respiratory challenge. Ten minutes rest was allowed after arriving at the MRI control room to allow the subjects' BP to settle down.

The brachial artery BP was measured using a (OMRON HEM-790IT) sphygmomanometer. The subjects were positioned comfortably in the scanner. All of the physiological recordings were acquired using respiratory bellows and a vector cardiogram by GE healthcare. The Caretaker finger cuff was attached to the middle finger between the proximal and distal inter phalangeal joints. The pulse oximeter finger pad was attached to the index finger of the contralateral hand. The respiratory band was wrapped around the chest just below the xyphoid process of the sternum at a full inspiratory

phase to allow for flexible expansion during the respiratory challenge. The instructions for the breath holding stimuli were presented on a projector screen and PowerPoint presentation. The subjects viewed the screen through a mirror attached to the RF coil placed approximately 10 cm away from their face. For subjects with low visual acuity, MRI compatible correction glasses matching the degree and type of their visual impairment were provided. These special glasses are MRI compatible and designed to diminish the interference with the magnetic field. All of the settings and subject preparations were performed by the author and supervised by a specially trained MR scanner technician.

A soft cushion pad was used to support the knee joint at a flexion angle of about 40° to add extra comfort and prevent movement during the scanning. For the TCR protocol this was replaced by the custom-made leg support, which is described in Chapter 3, to prevent movement during the thigh-cuff deflation maneuver.

The author stood beyond the 300 Gaussian-line in the scanner to inflate and deflate the thigh-cuffs during the scanning session for the TCR protocol. Soundproof insulating headsets were applied to cancel out the noise form the scanner. The thigh-cuffs were inflated to 20 mmHg above the systolic BP level. The BOLD sequence acquisition was started immediately after the barometric pressure reader reached 20 mmHg above the systolic blood pressure. This was observed carefully and kept constant across all of the scanning sessions.

4.3 Data Acquisition

All of the MRI data were acquired at 3T GE scanner (General electric, MR750 3.0 T) and 32-channel head coil. After localizer and ASSET calibration, an anatomical axial FSPGR BRAVO sequence was acquired with the following parameters (TE 3.18 ms, TR 8.172 ms, Flip angle 12, acquisition matrix 256×256, slice thickness 1mm, and FOV 240×240 mm). For the physiological MRI a T2* w, 2D GE EPI sequence was acquired with these scanning parameters (TR 2000ms, TE 35ms, Flip angle 77, FOV 240 ×240, Slice thickness 3.6mm). Overall 120 volumes were acquired during a four-minute acquisition time. The time of repetition (TR) for the BOLD sequence was selected as 2000 ms to avoid short TRs that might interfere with the variability in the heart rate when inducing the BP changes. TR 2000ms was selected subsequent to a few pilot scans at different TRs (500ms and 1000 ms). Reliable BOLD signal response results were achieved at 2000ms TR (Appendix 4).

The BOLD sequence was repeated five times. The first time was a resting state BOLD with eyes closed. This was acquired to provide the baseline BOLD signal without any stimuli or event. The next two scans were an iBH fMRI paradigm, which was repeated twice for additional quality assessment and accuracy. During the iBH fMRI paradigm, the subjects were asked to take a deep breath and hold their breath for 20 seconds followed by 60 seconds of normal-breathing recovery time. The deep inspiration was based on the subject's own capacity to take the deepest gasp that they were able to maintain. Figure 11 shows the schematic presentation of the iBH protocol. The subjects underwent another two scans with the same BOLD sequence parameters for the TCR protocol.

The overall scanning time for both the iBH and TCR protocols was 30 minutes without the anatomical scan and 35 minutes with the anatomical scan. However, one hour scanning time was allowed because the BP measurements as well as the TCR and iBH task preparations took extra time. Following the acquisition of the images, the data were written to an optical disc (CD or DVD) to be securely transferred and stored on the internal server of the Radiological Sciences department for further analysis.

All of the study participants were anonymized with regard to all identifiable details.

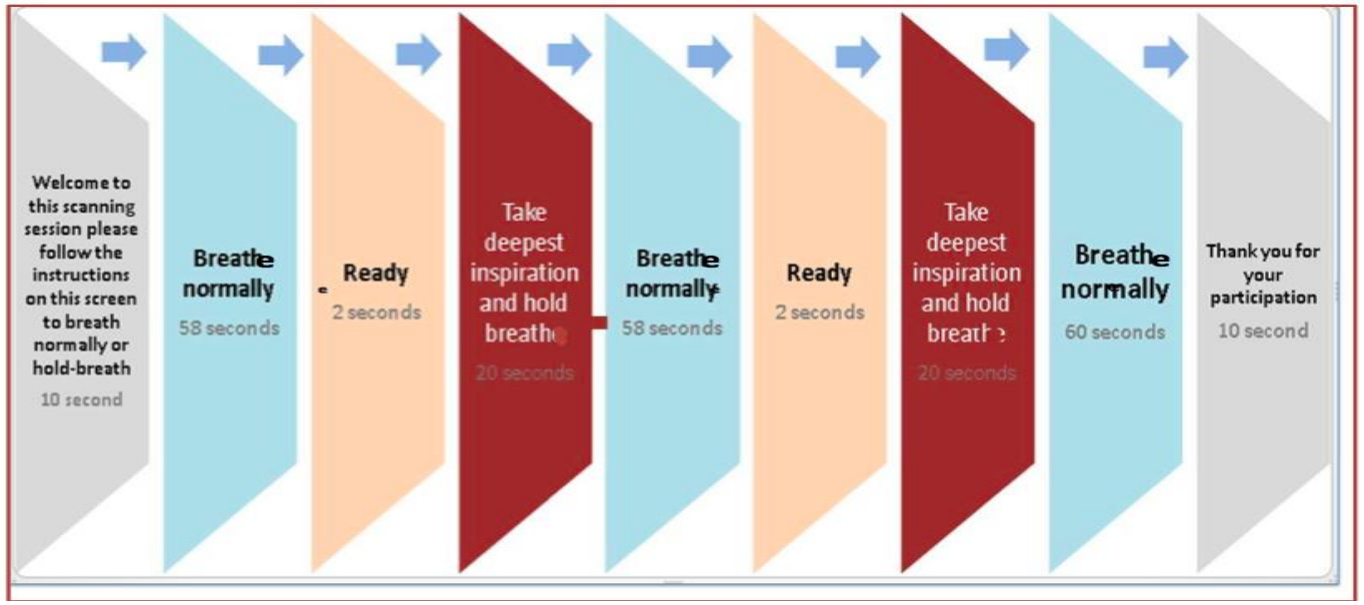

Figure 11 :Sequential representation (from left to right) of iBH protocol instruction slides

Used in the scanner to direct the iBH paradigm

4.4 Data analysis

4.4.1 Pre-processing

The raw data were transferred from DICOM to NIFTI format images in preparation for the analysis; this was performed using a (dtoa) command line on the in-house software of the Radiological Sciences department. The data analysis was performed using an FMRI Expert Analysis Tool (FEAT FSL) (v6.00;http://fsl.fmrib.ox.ac.uk/fsl/fslwiki/FSL). The functional images acquired were volume registered, time shifted, motion corrected, and brain extracted. The functional images were co-registered to a standard MNI brain (MNI152, non-linearly derived, McConnell, Brain Imaging, Montreal Neurological Institute, Montreal, Canada). The total acquired volumes were time-shifted to a common temporal origin. FEAT FSL performs this automatically when the temporal derivative function key is on. The motion correction was performed to calculate for any translational or rotational gross head motion using a 6-parameter rigid-body registration. This is performed through realigning the images by minimizing the sum of the square of the residual signals. Images with severe motion related artefacts were excluded from further analysis (Motion larger than a voxel is defined as a severe motion correlated artefact). This is estimated from the MCFLIRT motion correction output parameter, which defines the absolute and relative corrected motion in millimetres [151]. Non-brain matter was removed from all volumes using the FSL automated Brain Extraction Tool [152].

4.4.2 Regional time series extraction

The functional images were segmented according to the tissue specific differences of dCA identified in the literature; accordingly the whole cortical grey matter (GM), and the white matter (WM) time series were extracted [22]. There is a strong relation between the cortical watershed areas and severe haemodynamic impairment in the brain. Furthermore, the haemodynamic nature of the watershed areas may be important in the diagnosis of the origin of thromboembolic stroke [69]. Therefore, additional regional analysis was performed to show the magnitude of signal intensity of the watershed areas in relation to the non invasive BP stimulation methods (TCR and iBH). The time series for the three watershed areas were extracted separately (two cortical border zones and internal border zone). Figure 12 shows the ROI used to extract the watershed areas signal intensity maps. The reactivity maps of the total co-registered volumes (120 volumes) were averaged for each subject and each stimulus. Furthermore, the whole brain reactivity maps in relation to each watershed area were interpreted on a voxel-wise basis.

The regional segmentation was performed manually using the interactive FSL view toolbox (v4.0.1 http://www.fmrib.ox.ac.uk/fsl/fslview).

1. Tissue specific CA metrics

   For the GM time series extraction, the signal were selected from WM, cerebrovascular fluid (CSF), and subcortical regions as an ROI first and then masked out from the whole cortical GM manually. This sub-step in the analysis helped in acquiring regionally segmented functional images for future re-analysis, such as comparing regional modifications in dCA metrics. The region specific time series for the BOLD signal change was extracted using the FSL MEANTS command line [153]. The Harvard-Oxford anatomical

atlas available in the FSL view toolbox was used as the standard atlas for regional identification.

2. Regional watershed and CA

   For the watershed areas segmentation, a cluster of voxels available in each watershed area was manually selected as an ROI, based on the predefined watershed areas and the Harvard-Oxford anatomical atlas available in FSL (Figure 12) (so marked as WS1, WS2, and WS3 for the anterior cortical, internal border zone and posterior cortical border zones respectively). The time series of the BOLD signal was extracted from each ROI separately using the FSL MEANTS command line. These three regions (WS1, WS2, and WS3) were used as explanatory variables for FEAT FSL stats. The statistical F test tool function was used to threshold the effects of each contrast against zero base. The three regions were entered into the F-test as a function of [1,0,0], [0,1,0] [0,0,1] for the WS1, WS2 and WS3 areas respectively. This kind of modeling allows the complete fit to be tested against zero without having to define the relative weights of the basis function.

3. Average whole brain dCA map

   Because of the lack of standardized input and difficulties in formatting individual BP regressors (due to the variable timing), group averaging was not attempted. Therefore, only illustrative images for single subjects are provided without group registration.

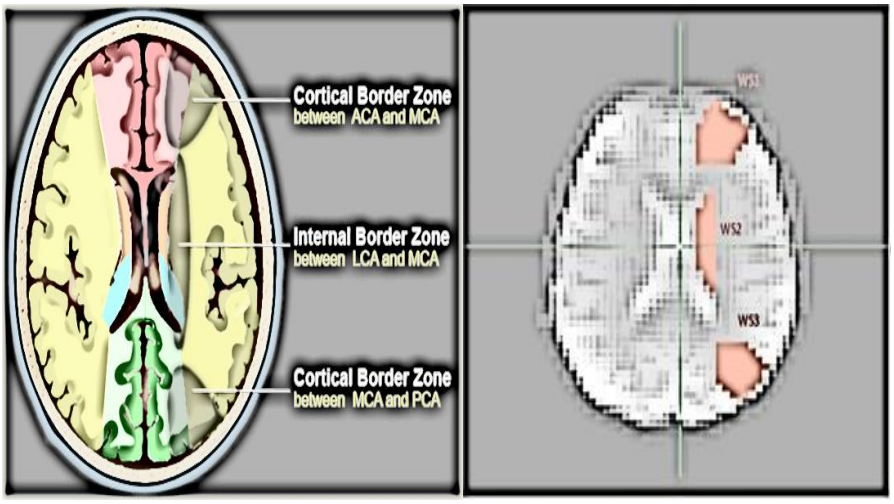

Figure 12: Watershed areas segmentation

The left image explains the three watershed areas (http://www.radiologyassistant.nl). The right image is the ROI selected using the FSL view tools box (v4.0.1 http://www.fmrib.ox.ac.uk/fsl/fslview) (23 year male. iBH protocol, BOLD image). The image shows an axial slice with the three watershed areas selected in red (WS1, WS2, WS3). The ROI was selected in three consecutive slices for each watershed area. A single watershed area was selected exclusively for each functional MR image. The three ROI are shown in a single axial slice image for explanatory purposes.

4.4.3 Non invasive interventions to induce BP fluctuations

4.4.3.1 Thigh-cuff release challenge

During the TCR protocol the time points at which the sudden deflation occurred were standardized across all of the scans and subjects. The time of deflation and the minimum signal intensity after the thigh-cuff release were visually detected (Figure 13). The baseline BP before the deflation was calculated by averaging over the three minutes of recorded base line BP data. This average was used to estimate the post TCR recovery of the BP. The relation between the first and second TCR tests for each subject was examined to determine intra-subject repeatability. This intra-subject comparison was also performed for the iBH test. A paired student T test was used to compare the intra-subject results. The statistical tests were performed using the Statistical Package for the Social Sciences (IBM SPSS v. 21).

4.4.3.2 Breath-hold challenge

The depth and duration of breath-hold affect the magnitude and dynamics of the BOLD signal response [114, 154], and thus may impact the estimated CA. The associated hypo/hypercapnia with respiratory challenges need to be accounted for when estimating the dCA metrics, because the ETCO2 level is affecting the cerebral haemodynamics as well as BOLD signal amplitude. When modelling respiratory challenges, either the recorded ETCO2 values (Capnograph measures) or the duration of the breath-hold are accounted for as the main confound of interest to estimate the corresponding CA changes [18, 93]. Invasive ETCO2 estimation using mass spectrometry is the ideal method to obtain the actual ETCO2 changes during breath-hold. However, the invasive ETCO2 measuring technique was not applicable in this study as our methods involved only non invasive techniques to estimate CA metrics. ETCO2 changes induced by 20-second breath holds were simulated in similar studies in the literature and modelled as linear ramps increasing gradually with a final amplitude of 1 [94]. This is a suboptimal way of representing ETCO2 changes but it is an acceptable practical alternative to avoid invasive measures. Figure 14 shows the illustrative curve used to simulate the expected ETCO2 changes during the iBH. The real-time recorded BP changes associated with the breath-hold challenge were used as the main regressor. However, the ETCO2 fluctuation is one of the most important physiological parameters associated with breath-hold challenge. Therefore it is necessary to include it in the modelling of the breath-hold challenge. Thus, in this study, three dependent variables are incorporated with the corresponding BOLD signal changes: the expected ETCO2 changes (Figure 14), the duration of the breath-hold, and the real-time recorded BP fluctuations, to better fit to the BOLD response.

Furthermore, each of these confounds is incorporated into the corresponding BOLD changes separately to examine the effect of each entity. Figure 14 shows the schematic explanation for the BH modelling.

Gradual accumulation of CO2 causes a transient BOLD signal increase because of the vasodilatory effects. However, the associated hypercapnia and hypertension may act synergistically to change the BOLD signal amplitude.

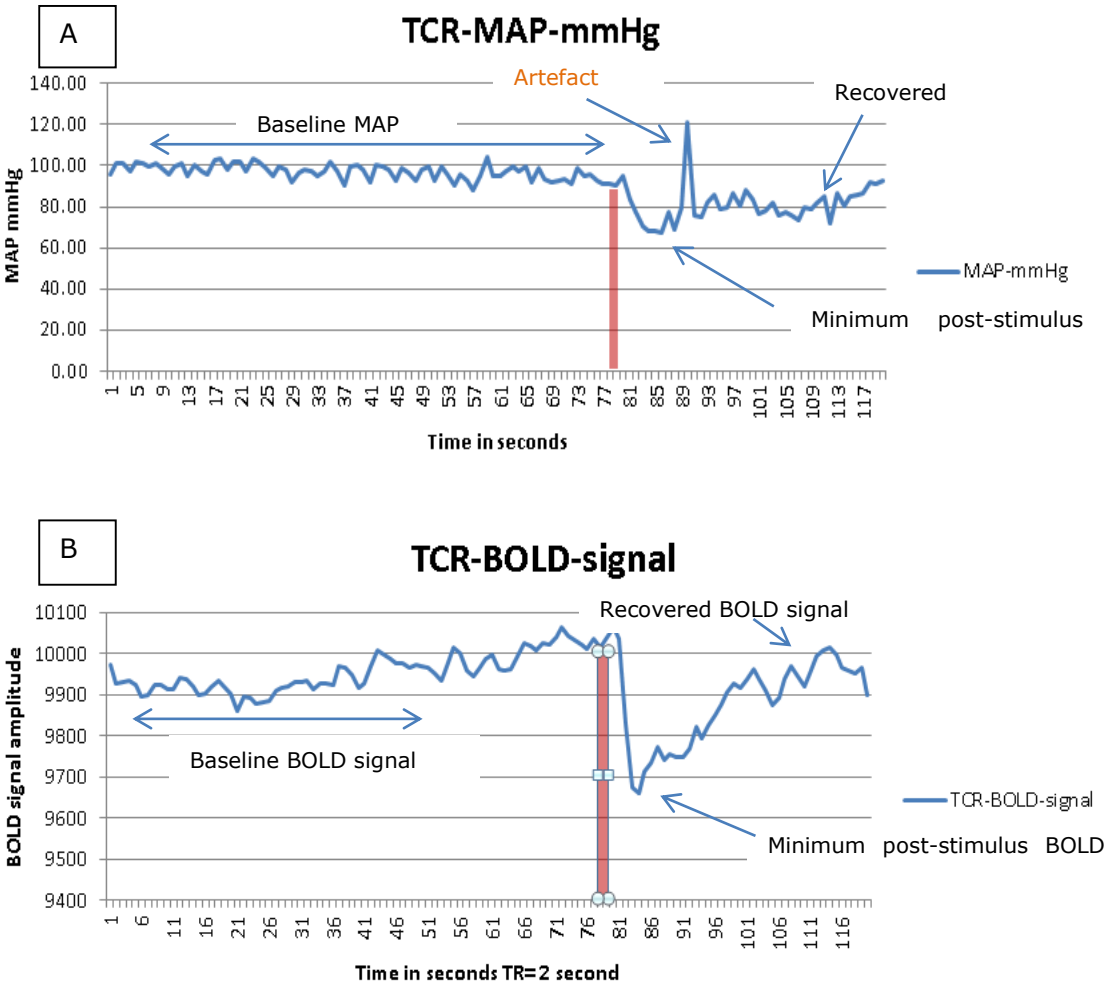

Figure 13: Thigh-cuff release test (TCR) in the scanner

A: Time series of mean arterial blood pressure (MAP) changes in response to TCR, acquired by the Caretaker device within the MR scanner (23 years male subject).
B: Corresponding BOLD signal amplitude change (sequence parameters, TR 2000ms, TE 35ms, Flip angle 77, FOV 240 ×240, Slice thickness 3.6mm).
The pink bar represents the time of the sudden release of the thigh-cuffs

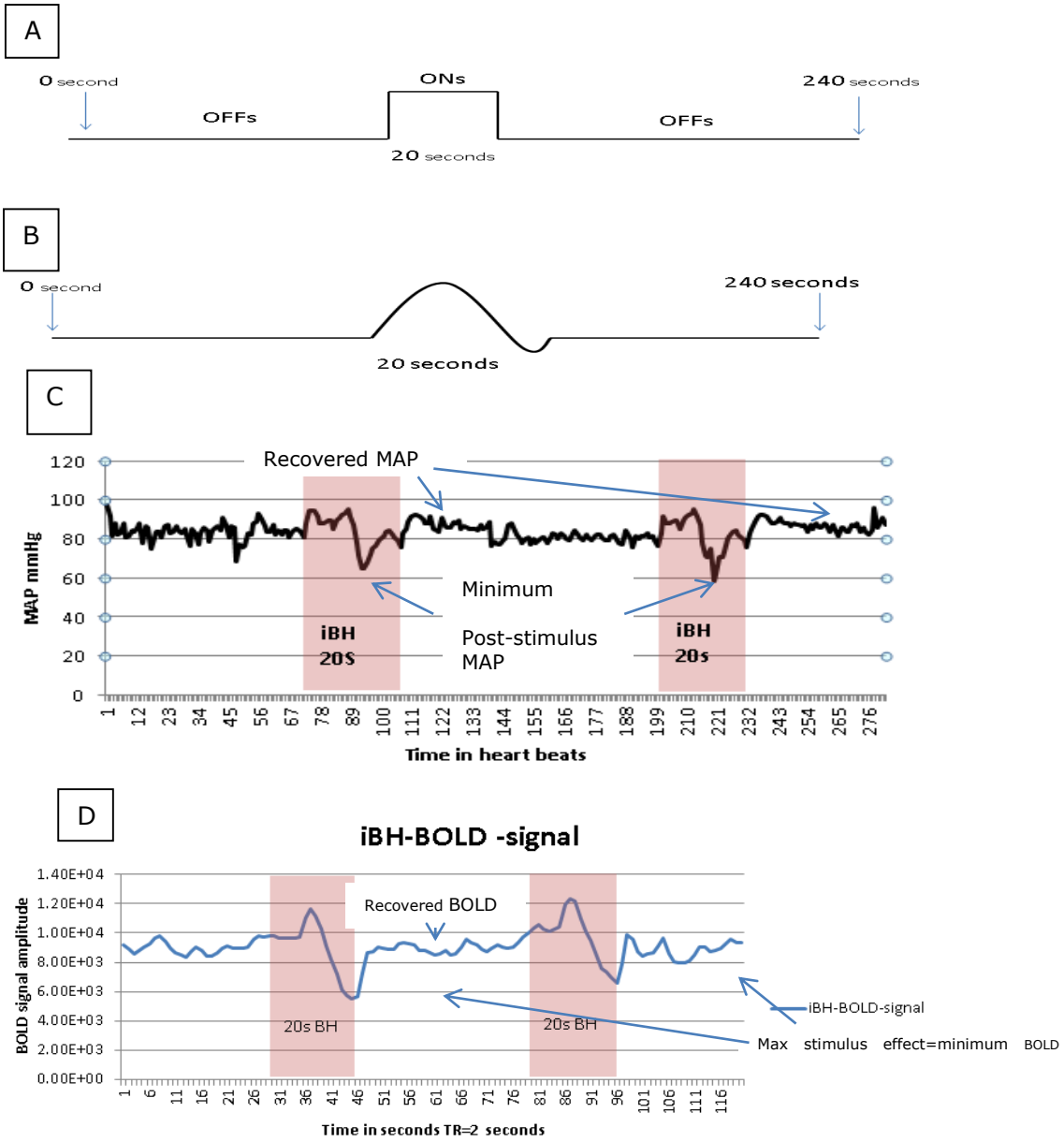

Figure 14: Breath-hold test (modeling different variables)

iBH modelling parameters used as confounds to the BOLD signal response. A: representation model for the duration of BH, entered as a block design function to FSL FEAT full model setup. B: representation of the expected ETCO2 changes in response to 20-second breath-hold, used as confound of interest to model the BOLD iBH paradigm. Adapted from similar study by Bright et al [94]. C: Real time beat-to beat arterial blood pressure from the Caretaker plethysmograph (single subject, 23 years male). The real time acquired MAP was used as a confound of interest to model the BOLD signal amplitude response to iBH. D: BOLD signal amplitude in response to 20s BH for the same subject (sequence parameters, TR 2000ms, TE 35ms, Flip angle 77, FOV 240 ×240, Slice thickness 3.6mm)

- **Derived haemodynamic metrics**

  The transfer function gain, phase and coherence between changes in arterial pressure and CBFV could estimate the transient changes in CBFV during rapid BP changes [130]. The response impulse function is calculated as inverse Fourier transform of the transfer function between CBFV and BP. These metrics cannot be directly applied on BOLD fMRI data.

  The signal amplitude of the BOLD fMRI depends on several underlying cerebrovascular parameters, most importantly CBF and CBV. Calculating the response function between the BP and the corresponding BOLD signal is important when estimating the dCA metrics [15]. The rate of recovery of BP and the BOLD signal were calculated from concurrent time points. The three time points were: when the BP stimulus started, when the maximum effect occurred, and when recovery to the baseline was visually identified (Figure 13 and 14). The respective three time points were determined on BOLD time series.

  The sampling rate of the plethysmographic BP measurement devices depends on the heart rate, and thus a BP reading was recorded at the beginning of each cardiac cycle. In other words, the time interval between the recorded BP values varied according to the heart rate at the given time. This is a major restriction for intra-subject and inter-subject averaging.

  Usually a resampling at a common sampling rate for all sets of data would be the optimum solution for such variables. However, resampling negatively affects experiments that are strictly dependent on the quantitative change that happens in a relatively short period of time (20 seconds in our example). Therefore, the times at which the BP events occurred were

selected and accordingly the BP time point of maximum effect was visually identified and matched to the corresponding BOLD signal.

The rate of change after stimulus was calculated for each BP event and the corresponding BOLD signal changes across subjects. The rate of change (Δ) for the BOLD signal was calculated by subtracting the percentage of the post-stimulus minimum BOLD signal from the recovered signal (=baseline BOLD) divided by the baseline BOLD signal amplitude to represent the step change.

$$R - rec(BOLD) = \frac{\Delta BOLD\ n}{\boldsymbol{\Delta T}\ (\boldsymbol{Seconds})}$$

$$\Delta BOLDn = \frac{S\ recov - S\ min}{\boldsymbol{S\ recov}}$$

$$\Delta Time\ = T\ recov - T\ min$$

S$_{recov}$= BOLD signal amplitude at baseline

S $_{min}$ = minimum post-stimulus BOLD signal amplitude

T$_{recov}$= time at which the BOLD signal recovered to baseline

T$_{min}$= time at which the BOLD signal reached the minimum post-stimulus amplitude

The same equation was used to calculate the rate of change in MAP.

$$R - rec\ (MAP) = \frac{\Delta MAPn\ (mmHg)}{\Delta Time\ (seconds)}$$

$$\Delta MAPn = \frac{\boldsymbol{MAP}\ recov\ - \boldsymbol{MAP}\ \min\ (mmHg)}{MAP\ recov}$$

$$\Delta Time = \boldsymbol{T}\ recov - \boldsymbol{T}\ \min\ (in\ seconds)$$

MAP $_{recov}$= Mean arterial blood pressure at the baseline.

MAP $_{min}$= minimum post-stimulus mean arterial blood pressure

T$_{recov}$= time at which the MAP returned to the baseline

T$_{min}$= time at which MAP reached the minimum post-stimulus value.

Usually, for larger sample studies (n≥ 10), an autoregulatory index (ARI) is generated by fitting the ten possible CBF response template curves, scaling in between 0-9 (0 is absence of autoregulation and 9 is best observed autoregulation) [22]. Nevertheless, the autoregulation can also be represented by modelling the dynamic relationship between the CBF and BP [32]. The CBFV measures from the TCD have been considered as a valid surrogate marker of CBF [7]. Furthermore, Aaslid et al (1989) estimated CA metrics using CBFV and MAP measured by TCD and Servo-cuff system respectively [6]. They estimated the rate of regulation after thigh-cuff release in 10 healthy volunteers. The rate of regulation RoR after the fast blood pressure drop was calculated as the (ΔCVR/ΔT), which defines the rate at which cerebrovascular reactivity (CVR) changes. This rate depends on ΔMAP, and full haemodynamic recovery will occur if the ΔCVR and ΔMAP are equal. Hence the estimated RoR was defined as:

$$\mathrm{RoR} = \frac{\Delta \mathrm{CVR}/\Delta \mathrm{T}}{\Delta \mathrm{MAP}} \times 10^3 [6]$$

Considering the BOLD signal amplitude response as an indirect indicator of CBF change, a BOLD based CA metric could be estimated using a similar model using the transients of the BOLD signal amplitude and the MAP step changes induced by the TCR and iBH methods.

4.5 Results

4.5.1 Thigh –cuff release

The results of the MAP responses to the TCR method are comparable to the previous results obtained outside the scanner (Figure 9 & 13). Figure 13 shows the BP and corresponding BOLD signal amplitude change in response to the TCR protocol. The sudden release of the inflated thigh-cuffs induced simultaneous changes in the MAP and BOLD signal amplitude in five out of six subjects. The results of the first and second TCR were compared for each subject and there was no significant difference (P=0.72). The percentage change response across all accepted scans was (22-31 %) for MAP and (1.55-3.63 %) for the corresponding BOLD signal amplitude change. The rate of regulation (RoR) was (10.27±5; GM, 6.93±4.8; WM, 11±5.5; WS, mean±SD) (Table 9). The average time for recovery from the maximum stimulus effect to the baseline was (15±6 s; mean±SD) for the BOLD signal and (20±9 s; mean±SD) seconds for the MAP. Thus, the BOLD signal showed a 25% faster response compared to the MAP. Table 9 summarizes the calculated CA parameters for all of the subjects.

For the regional analysis, the time interval from the maximum stimulus effect to recovery was (11±0.5 s; mean±SD), (14±1 s; mean±SD), (16±3 s; mean±SD) for the WS1, WS2 and WS3 respectively. For the (22-31%)

change in the MAP the corresponding percentage BOLD change was (1.98-1.99%), (2.11-3.63%), (2.1-2.55 %) for the WS1, WS2 and WS3 areas respectively.

The group averaging for the reactivity maps is not illustrated because the averaging across the subjects resulted in an instant error of function, for the same reasons described in the methods.

Subjects	Parameters	GM-BOLD	WM-BOLD	WS-BOLD	MAP mmHg
TCR1	Δ paramters	0.04	0.02	0.04	0.29
	RoR	12.26	6.90	12.41	
	Precentage changes	2.70	1.89	2.77	26
TCR2	Δ parameters	0.03	0.02	0.05	0.39
	RoR	6.23	3.66	9.16	
	Precentage changes	2.49	2.30	2.33	31
TCR3	Δ parameters	0.05	0.05	0.05	0.7
	RoR	13.72	14.29	15.43	
	Precentage changes	3.16	3.11	3.50	30
TCR4	Δ parameters	0.02	0.01	0.02	0.53
	RoR	2.70	1.75	2.56	
	Precentage changes	1.87	1.55	1.98	27
TCR5	Δ parameters	0.04	0.02	0.04	0.31
	RoR	16.45	8.06	16.13	
	Precentage changes	3.50	3.12	3.63	22
Averages	Δ parameters (mean±SD)	(0.03±0.01)	(0.02±0.01)	(0.03±0.01)	(0.45±0.17)
	RoR (mean±SD)	(10.27±5)	(6.93±4.8)	(11±5.5)	
	% changes (mean±SD)	(2.72±0.6)%	(2.39±0.7)%	(2.84±0.7)	(27±3)%

Table 9: Estimated CA parameters for five accepted TCR measures

CA parameters for grey matter GM, white matter WM, and averaged watershed areas WS. Individual TCR measures are averaged over two scans for each individual. The intra-individual means were calculated by averaging the numerical values rather than the curve response. Averaging across curve responses may attenuate the effects of the coupled BOLD signal and BP changes because of the time latency.
RoR, Rate of regulation. Δ parameters are for the regional Blood Oxygen Level Dependent BOLD signal changes (ΔBOLD), and mean arterial blood pressure changes (ΔMAP)

4.5.2 Inspiratory breath-hold method iBH

The results of the MAP responses to the iBH test confirm the results obtained for the iBH test outside the scanner. The inspiratory breath holds of 20 seconds induced sufficient changes in the MAP and BOLD signal amplitude. The averaged percentage change from the baseline was a (19-23%) decrease for the MAP and a (1.95-3.14%) for the BOLD signal amplitude. The results of the repeated iBH tests for each subject were not significantly different (P= 0.3). The rate of change was (0.61±0.15) for the MAP and (0.03±0.01; GM, 0.02±0.01; WM, 0.04±0.01 WS, mean±SD) for the BOLD signal amplitude. The rate of regulation (RoR) was (5.06±1.5;GM, 3.5±1.17;WM, 6±1.7; WS; mean±SD). Table 10 summarizes the estimated parameters for all of the subjects. The time interval from the maximum stimulus effect to the recovery point was (15.5±5s GM, 14±3 s WM, 17±2s WS; mean±SD) for the BOLD signal, and (24.7±11, mean±SD) seconds for the MAP.

The reactivity analysis for the BP change and ETCO2 change simulation model resulted in a relatively similar distribution of signal intensity distribution in the brain. Meanwhile, the reactivity maps for the BH period model showed a slightly different distribution and larger signal amplitude. The combined effects of the BP and ETCO2 simulation resulted in a similar distribution as for the separate confounds. Figure 15 shows three reactivity maps generated for the iBH test, using the three different models separately

(BH-period, ETCO2 simulation curve, and real time recorded BP data) and also for the combined effects.

Subjects	Parameters	GM-BOLD	WM-BOLD	WS-BOLD	MAP mmHg
BH1	Δ paramters	0.03	0.03	0.04	0.45
	RoR	3.51	3.04	4.09	
	Precentage changes	2.06	2.18	3.11	22.00
BH2	Δ parameters	0.04	0.03	0.05	0.80
	RoR	5.56	4.17	6.94	
	Precentage changes	2.64	2.70	2.88	23.50
BH3	Δ parameters	0.03	0.02	0.04	0.69
	RoR	4.35	2.17	5.07	
	Precentage changes	3.12	2.50	3.14	21.30
BH4	Δ parameters	0.05	0.04	0.06	0.52
	RoR	6.87	4.81	7.97	
	Precentage changes	2.19	1.94	2.30	19.20
Averages	Δ parameters (mean±SD)	(0.03±0.01)	(0.02±0.08)	(0.04±0.01)	(0.61±0.15)
	RoR (mean±SD)	(5.06±1.5)	(3.5±1.17)	(6±1.7)	
	% changes (mean±SD)	(2.55±0.4)%	(2.33±2.86)%	(2.85±3.4)%	(21.4±2)

Table 10: summary of CA parameters calculated for iBH method

Whole cortical grey matter (GM), white matter (WM), and averaged watershed areas for each individual and the average over four subject measures. The individual measures are averaged over two iBH stimuli each. RoR is the rate of regulation after the stimuli. Max effect ratio is the ratio of maximum step change after the stimulus, and CA is the estimation of cerebral autoregulation

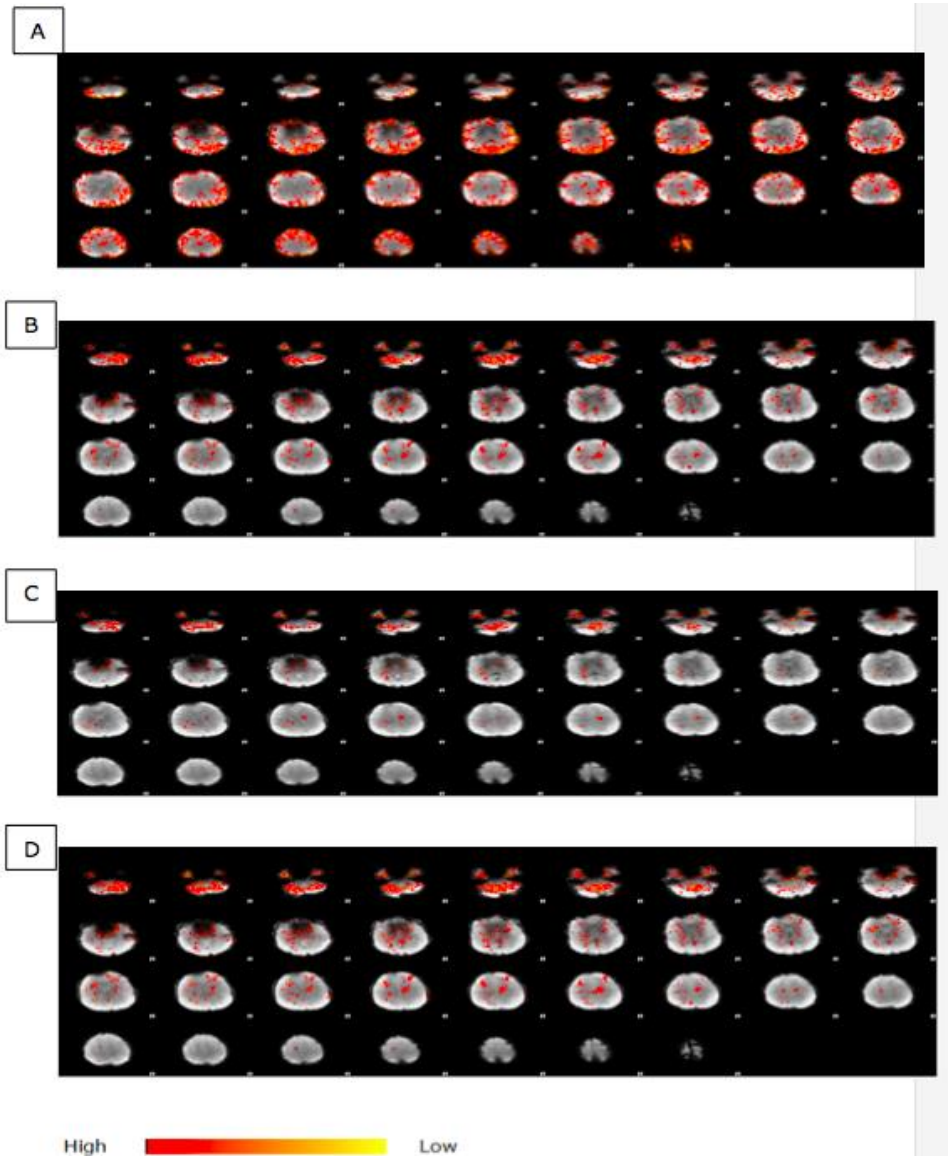

Figure 15 Reactivity analysis of brain, for iBH challenge (23 years, male subject)

This is a contrast map denoting the magnitude of the signal intensity change. Reactivity map of a healthy volunteer showing signal intensity change relative to three different confounds A: BH period used as the regressor of interest B: Simulated ETCO2 curve used as the regressor of interest C: Real-time recorded beat-to-beat MAP used as the confound of interest D: Combination reactivity map (BP, and ET simulation curve).

4.5.3 Statistical analysis

The autoregulation parameters obtained from the BH and TCR in grey matter, white matter and the watershed areas are expressed as mean±SD (Table 9 &10). The differences in the rate of regulation in the BOLD signal for the BH and the TCR methods were compared and analysed using the Student *t test*. In all of the tests, $P \leq 0.05$ was considered statistically significant. The regional RoRs for the WM, GM and WS areas were calculated separately and then the mean RoR of three regions was calculated (Table 9 &10).

The reproducibility of the calculated RoR obtained by the breath-hold and thigh-cuff release challenge was analysed according to the method of Bland and Altman [155].With the difference between the RoR for the BH and TCR challenges, the standard deviation of the difference (SDD) was calculated (Figure 16). The SDD is a measure of the repeatability of the method. The 95% limits of agreement were calculated (i.e., the mean difference±1.96 × SDD). The scattered distribution of the results above and below the mean difference denotes the minimum bias of one approach versus the other. The results of the statistical tests show good agreement between the RoR results obtained with the TCR and iBH methods.

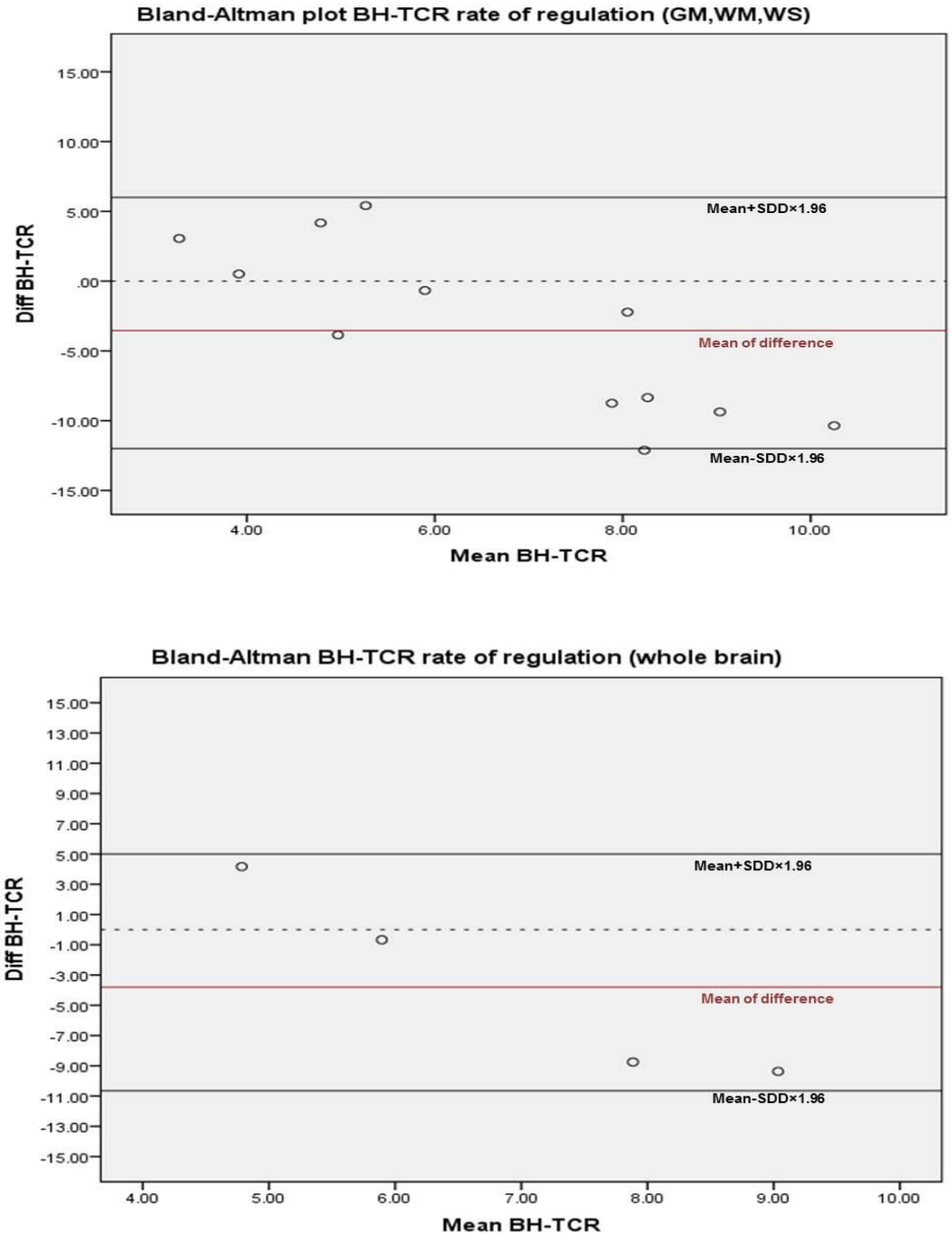

Figure 16 Bland-Altman plots

RoR s compared between the BH and TCR challenges. The top panel includes the region specific RoRs (Grey matter GM, white matter WM, and Watershed areas WS). The bottom panel shows the Bland-Altman plot comparing between the mean BH and TCR challenge for the averaged RoRs for four healthy volunteers.

4.6 Discussion

The sudden release of thigh cuff and the inspiratory breath-hold challenge both induced simultaneous MAP and BOLD signal amplitude changes. The time interval for the BOLD signal amplitude recovery after the event was faster than the MAP recovery for both methods suggesting intact cerebral autoregulation. The MAP change was higher and more prompt in response to the TCR than the iBH method; the difference was not statistically significant (P= 0.72). The resultant percentage BOLD signal change was relatively close for the iBH and TCR (2.5±1%, mean±SD). The BOLD signal response in the whole of the cortical GM and WM tissue was comparable to previous studies (GM 1.81±0.67%, WM 1.18±0.59%, Horsfield et al 2013) and consistent across the TCR and iBH methods (0.5-2.2 %, Emir et al 2008) [22] [15].

Beat-to-beat BP changes associated with TCR have been reported for studies outside the scanner [17]. Furthermore, regional variation in the BOLD response to TCR has previously been detected in a 1.5 T MR scanner [22]. Nevertheless, in this study, the beat-to-beat arterial BP measures acquired within the scanner (at 3T) were used in combination with the BOLD signal amplitude to estimate dCA metrics. This is the first study that could record the real time ABP at 3T scanner for the best of the author's knowledge. Controlling for the beat-to-beat ABP could improve the derived dCA metrics using TCR method. Acquiring concurrent BOLD and ABP changes allows deriving the rate of regulation after the BP disturbance following the sudden release of the thigh cuff. This improves the physiological interpretation of the autoregulation index and may be clinically significant for estimating dCA metrics in haemodynamically unstable patients.

The recorded BP-response to the iBH method in this study and also outside the scanner, in the previous chapter, showed a sufficient BP change to allow dCA activation. This was further confirmed by corresponding BOLD signal changes. A short breath hold of 20 seconds causes transient hypercapnia and a BOLD signal deflection in opposite direction to the expected hypercapnia effect. The respiratory challenge is associated with the gradual accumulation of CO2 in brain. CO2 is a potent vasodilator that increases the CBF in the brain [15]. The relationship between ETCO2 and blood flow is a linear relationship with CBF almost doubling as PaCO2 increases from 40-100 mmHg. Buxton et al (2010) demonstrated a linear association between CBF increase and the corresponding BOLD signal change, as represented in Figure 17 [156]. In our experiments, the BOLD signal response to a 20-second iBH resulted in a gradual increase in signal, which is in line with the accumulated CO2 effect. This was followed by a larger decrease in signal intensity, which may be caused by the BP drop (Figure 14).

Recent studies have shown that even subtle variations in the rhythm of respiration that occurs at rest can induce a BOLD signal change [110]. The amplitude of BOLD signal change in response to different breath-hold periods (9 s, 11 s, and 20 s) has been examined previously [94]. Two confound variables have been used to model the breath-hold response effect; the breath-hold period and the measured ETCO2 change. However, another physiological alteration associated with breath holding is systemic arterial blood pressure changes. To the best of the author's knowledge, no studies that have examined CA in response to respiratory challenge have accounted for the associated BP changes (Figure 13 and 14). The BP drop in response to the Valsalva manoeuvre has been used to estimate dCA metrics [150]. In this study, the iBH resulted in a relatively similar response curve to the Valsalva manoeuvre (Figure 14). The transient BP increase at the beginning

of the iBH might be caused by the transient sympathetic activation associated with the voluntary act of breath holding, which tends to increase the BOLD signal amplitude.

The CBF decreases in response to induced fast BP drops; this could lead to transient neuronal hypoxia, which activates the regulatory modulators. The regulatory modulators decrease the vascular smooth muscle tone to allow vasodilatation [157]. There is a time delay from the onset of excreting regulatory modulators until the effects are fully developed on vascular smooth muscle tone, which may lead to an overshoot in CBF response [6].

Dynamic CA metrics estimated from MAP and CBFV recordings from TCD and TCR have been shown to detect pathological changes in CA, but the wider clinical application is hindered by the limited spatial resolution of TCD [17]. Detecting the regional variations in CA may be important in the follow-up and prognosis of neurodegenerative diseases, as well as tumor and stroke [69]. In this study, GM tissue showed faster recovery than WM after a BP event; this is physiologically predictable because of the higher metabolic rate of GM compared to WM [158]. The rates of regulation for the GM and WS areas were relatively similar (Tables 9 & 10). The multiple source vascular supply of the watershed area classifies the region as less haemodynamically active in response to fast BP changes, and thus less reactivity response is expected. However, the GM and WS areas showed close RoR in this study. This is probably because this experiment studied only healthy volunteers with intact dCA. Furthermore, the specificity and sensitivity of the software used to segment and extract the regional BOLD signal amplitude may have affected the results.

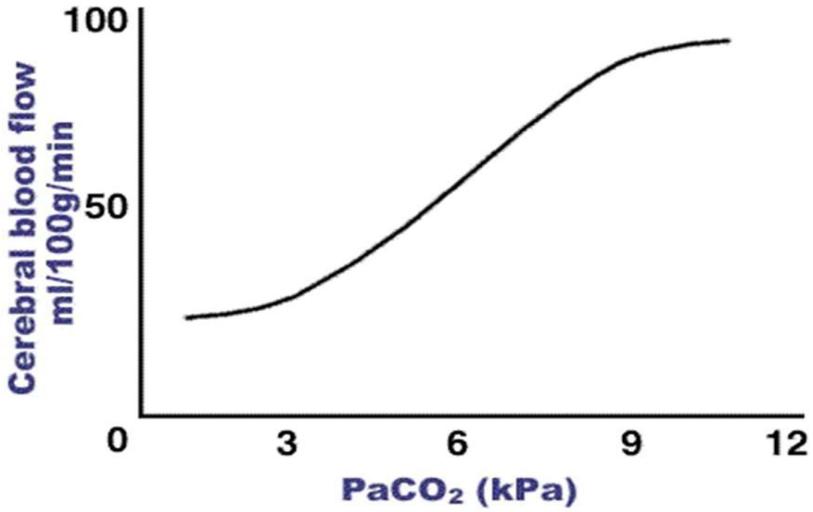

Figure 17 Graphical representation of the relationship between CBF and PaCO2 [131].

4.7 Limitations

There were two main types of limitations in this study: CA related and technical related limitations. The CA related limitations were similar to the published studies on CA that are discussed in Chapter two. These are mainly related to the non-stationary nature of CA, multi variable reliance (CBF, CBV, and CMRO2), as well as the temporal and spatial resolution of the applied techniques.

This study included only healthy adult volunteers. Developing a diagnostic technique for such a dynamic process should include comparisons with patient group implementations. Another source of bias in this study is the small sample size; this was due to the restricted timescale of the study. In order to take the results of this study forward, the sample size should be increased and patient groups such as hypertensive cases should be added. Increasing the number of participants may also improve the method of intra- and inter-comparisons due to the non-stationary nature of CA.

Technical restrictions included sequence related and non-sequence related limitations. Despite the high spatial and temporal resolution of BOLD MRI, it is highly dependent on several other factors that are directly related to the cerebral haemodynamic parameters, such as hematocrit, CBF, CBV and CMRO2 [68]. Furthermore, the BOLD signal, similar to any fMRI data, has two main kinds of noise: thermal noise and physiological noise. The new high-field MRI systems could improve the apparatus sensitivity and stability, which are responsible for the thermal noise [159]. Noises of a physiological origin can be diminished by selecting a low flip angle in BOLD MRI [160]. In our experiments, the flip angle was selected according to the Ernst equation [161].

The motion artefact associated with the TCR and iBH methods was another scanning related limitation. Despite maintaining a 40° knee flexion angle during the scanning and adding motion correction into the analysis, there were some instant motion artefacts that led to the rejection of some scans.

Other technical issues were related to the BP measurement method. The Caretaker system was very sensitive to external noises. The long connecting tube that connects the outer port to the finger-cuff in the scanner affected the coupling pressure and led to some repeated drop-outs during the data acquisition.

Furthermore, the cold temperature that helps to maintain the working environment for the magnet affected the volunteers' body temperature. Maintaining a warm periphery is important to allow enough vascular-bed circulation while acquiring BP measures using the Caretaker and other finger plethysmographic devices. Portable self-heating hand pads were provided to the volunteers before, but not during scanning. The MRI safety team in the Department of Radiological Sciences examined these pads beforehand; the pads were not qualified as MR compatible. These pads contain a mixture of iron dust, activated charcoal and cellulose, and are capable of maintaining instant heat production (122-130 F) for up to 8 hours.

The Caretaker device was not triggered to the signal from the MR scanner during the BP acquisition process. This led to a gap of a few seconds between the BP and MR signal data. The Caretaker could accept or deliver a trigger signal by pairing it with another device (MP 150, Biopac ®); this was not available during this study.

Another way of identifying the actual time R-R intervals is by registering the beat-to-beat BP measures to the recorded physiological data from the attached cardiac vector. The physiological recordings were collected and

saved on Spike software (Cambridge Electronic Design, CED). However, to compare the R-R intervals and the BP data, it was necessary to transfer the analog data from Spike to digital format. Unfortunately this was not possible during the time of this study because the corresponding person from CED was on leave at the time.

Another limitation was the lack of ETCO2. The breath-hold method was performed without ETCO2 recordings because an MRI compatible Capnograph was not available in the department. An MRI compatible Spirometer is an alternative method. However, the sampling rate for the Datex spirometer (Datex Ohmeda anesthesia machine, GE healthcare) to record the ETCO2 value is every five minutes and this was not compatible with our experiment. The lack of ETCO2 measures may be a major restriction for studies that include the rate and depth of continuous breathing. Our study included a 20-second breath-hold during which the Capnograph could not estimate the ETCO2 measures. An alternative method that can be applied to deal with this issue is explained in detail in the data analysis section. Temporal resolution could be another limitation of this study, providing higher temporal resolution sequence may allow disentangle BP-induced transient change from more prolonged hypercapnia effects, particularly if the associated ETCO2 metrics could be acquired on continuous basis. We are aware of dCA studies that have incorporated ETCO2 measures into CBF measures to calculate the transfer function between both variables using the principal dynamic modeling technique [126]. This will be considered in our future studies.

Conclusion

In conclusion, we have shown that the iBH and TCR methods can both induce a BOLD signal change in response to the induced MAP changes at 3T MRI scanner. The measured beat-to-beat BP data was in line with the corresponding BOLD signal changes. The signal amplitude recovered back to the baseline after the BP-event faster than the MAP. Connecting the Caretaker device to the MR scanner signal can improve the temporal registering between the MAP and the corresponding BOLD signal. Using a concurrent BOLD signal and BP data to calculate the rate of regulation after BP stimulus could better evaluate the reliability of estimating dCA metrics using physiological fMRI. The TCR method could be more reliable to be applied to induce dynamic changes in less competent subjects and unconscious patients. The iBH method is more subjective and requires more cooperation therefore it might be not reliable for critically ill patients.

Chapter 5

5 Time Resolved Phase Contrast Angiography (4D PC MRI) and Breath-Hold method

5.1 Background

The iBH method used to induce dynamic changes in the previous chapter resulted in a (11-20%) change in MAP and a (0.5-1.8%) corresponding BOLD signal change. With that in mind, it is important to note that the BOLD signal change is sensitive to several underlying parameters, and even subtle variations in the depth and rhythm of respiration at rest can induce a BOLD signal change [109, 110]. Furthermore, the BOLD signal amplitude response depends on several parameters in addition to the CBF, such as the baseline CBV, the haematocrit and the metabolic rate [83].

In the previous chapter, an inspiratory breath holding challenge was used to induce transient hypercapnic responses followed by a transient BP drop and the rate of response of the delayed percentage BOLD signal amplitude reduction was used to estimate dCA metrics. However, quantifying the absolute CBF and CBV change to a breath-hold test would give a better insight into the physiological aspects of this method. Hereafter, we have used the multidirectional high temporal capability of 4D PC MRI to preliminarily measure the vessel specific haemodynamic response to a respiratory challenge test, in two healthy volunteers. The aim of the study

was to show the feasibility of 3D magnetic angiography in detecting and quantifying the transient haemodynamic responses. Two types of breath-hold method, iBH and BH, were used to induce dynamic change response quantification by 4D PC MRI to allow a quantitative comparison between the two methods. As stated in Chapter three, they resulted in different MAP response curves outside the scanner.

5.2 Methods and Materials

Two healthy volunteers (23 and 24 years old; males) were recruited for this feasibility study. The details of the ethics approval, subject preparation and BP acquisition are explained in the methods section in the previous chapter.

5.3 Data acquisition

The scanning was performed in a 3T GE 750 Discovery scanner. A time of flight (TOF) image was acquired before the phase contrast to show the anatomy of the cerebral vessels and localise the slice position. Following that, a 4D PC MRI sequence acquired for the Circle of Willis at the base of the skull to measure the flow and velocity through three major arteries: the BA, and the left and right ICA. The sequence parameters for 4D PC MRI were (RT 4.627, ET 1.908, Spatial Res 1.562, Flip Angle 15, Scan time ~ 4 minutes, Voxel size: 1.17 X 1.17 X 8mm, Image matrix: 256 X 256, FOV 300 X 300 X 96 mm, 12 Slices over 20 TF X 38 ms = 722 ms, velocity encoding 80 cm/second). The 4D PC MRI sequence is provided by a license agreement with "Dr Marcus Alley, Lucas Medical Centre, Radiological Sciences Labs, University of Stanford, CA, USA". The sequence parameters for the TOF were (RT 23, TE 3 ms, space between slices 0.5, display FOV 156, flip angle 15).

The 4D PC sequence was repeated three times for each subject. The first scan was a baseline scan. The second scan was an iBH test with 20-second iBH intervals at the beginning of each minute throughout the four minutes of scanning (33% breath-holding and 67% normal breathing). The third scan was a non-inspiratory breath hold (BH) with similar settings to the iBH.

5.4 Data Analysis

The acquired data were saved on an internal server to be reconstructed and transferred later to DICOM format. The data reconstruct was performed on a 64-bit Linux system PC. Two programs, (MEDICOR) and (OFFLINE.RECON) were used to develop the DICOM format files with mag, speed and three directions of flow. The dataset was corrected for eddy current induced phase offsets. Gyro tools software (GT-flow, Gyro Tools LLC, Winterthur, Switzerland) (www.gyrotools.com) was used to visualize and interpret the multidirectional phase contrast MRI flow datasets. The net flow and through-plane velocities for the BA, and right and left ICA arteries were plotted, after which the vessel diameters were selected semi-automatically (Figure 18). The vessel diameter selection has automatic and manual options on the GT-flow software. After selecting the diameter of the vessel on the magnitude image the selection is automatically registered to the phase image from which the flow velocity information is plotted.

The flow and velocity data output from the GT-flow is divided over 20 phases for a single cardiac cycle (Figure 18) and (Table 11). Phase contrast MRI acquires flow and velocity data using a time-averaged signal over several cardiac cycles. Hence, the velocity and flow information curves are displayed as a single cardiac cycle containing information about the average flow and velocity for the total cardiac cycles throughout the acquisition time. Table 11 shows the flow velocity and volume measures from the GT-flow for one subject.

A

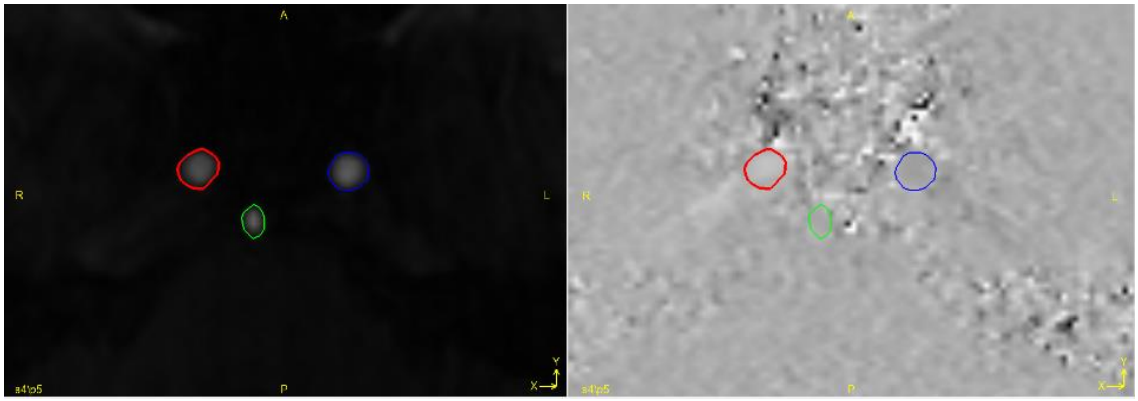

B

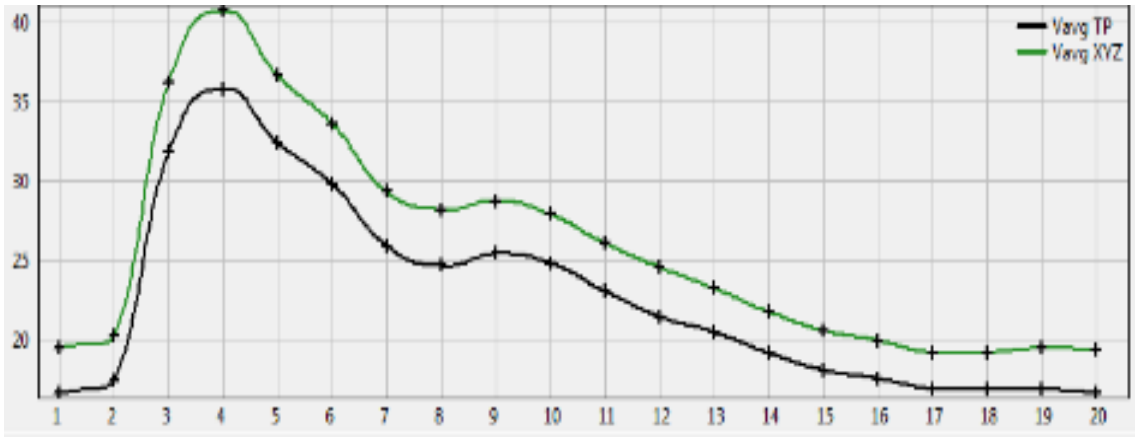

Figure 18: 4D PC MRI data analysis from GT-flow

(23 years old, male, four minute acquisition time)
A: selected arteries (BA, left and right ICA). The right side is a magnitude image (classic blood bright image), mostly for anatomical orientation. The left side is a phase (velocity) image in which the grey value represents the velocity in that voxel (grey denotes flow velocity towards the viewer and white is the flow direction away from the viewer)
B: Average flow velocity through BA. Averaged into one cardiac cycle and sub-divided into 20 phases. The green line (upper-line) represents multi-direction flow velocity and the black line (lower-line) is the through-plane flow velocity.

Phase	Time	Area	Net	Flow	Avg	TPVel
	[ms]	[mm2]	[ml/s]	[cm/s]	[cm/s]	[cm/s]
1	35	12.56389	5.2197	41.54522	22.55859	50.75684
2	107	12.56389	5.20625	41.43818	22.55859	50.61035
3	179	12.56389	4.40354	35.0492	16.40625	43.72559
4	250.99998	12.56389	4.64634	36.98167	21.16699	45.62988
5	323	12.56389	4.49344	35.76472	22.9248	42.91992
6	394.99997	12.56389	4.2556	33.8717	22.26563	40.86914
7	466.99997	12.56389	3.91017	31.1223	17.3584	39.55078
8	538.99994	12.56389	3.70065	29.45463	14.13574	38.74512
9	611	12.56389	3.50599	27.90527	15.82031	34.86328
10	683	12.56389	3.41114	27.15032	16.91895	32.44629
11	754.99994	12.56389	3.36442	26.77847	16.11328	33.10547
12	826.99994	12.56389	3.18887	25.38124	15.9668	31.71387
13	898.99994	12.56389	3.08623	24.5643	14.35547	31.12793
14	971	12.56389	2.99775	23.86005	13.33008	29.44336
15	1042.99988	12.56389	2.80875	22.35577	13.84277	31.4209
16	1114.99988	12.56389	2.77336	22.07407	11.42578	27.75879
17	1187	12.56389	2.70753	21.55011	11.71875	25.63477
18	1259	12.56389	3.20798	25.53335	16.91895	33.54492
19	1331	12.56389	5.96082	47.44403	29.95605	57.12891
20	1402.99988	12.56389	5.17015	41.15084	21.75293	51.26953

Table 11 Example of flow velocity output data from GT-flow software (Basilar artery at baseline) (23 years; male)

Data averaged for total cardiac cycles. The time series is subdivided into 20 phases of single cardiac cycle. Area represents the diameter of the artery. Net is the total volume in millilitres/second. Flow is the blood flow at the selected slice. Avg, is the average of velocity in all directions, TPVel is the through plane velocity. Note that the Flow is given in cm/s from the GT flow.

5.5 Results

The vessel specific flow and velocity information were averaged for two scans and three vessels at the baseline, iBH and BH (Table 12) (Figure 19). The average flow (averaged at intra-subject level, for 4 min acquisition time total cardiac cycles, 2 subjects) at the baseline was lower for BH than iBH conditions (Figure 19). There was no significant change in the flow curve between the different vessels (Figure 20). Furthermore, the cerebral blood flow curve was slightly higher for iBH compared to BH. The 33% breath hold resulted in a corresponding 29% CBF change for the iBH protocol and a 7.5% average change for the BH (Table 12).

The end diastolic velocity (EDV) and peak systolic velocity (PSV) values were acquired at the same slice for each vessel (BA, right and left ICA). Figure 21 summarizes the vessel specific PSV and EDV values acquired at the baseline, iBH and BH. The PSV and EDV values were averaged for both subjects. As shown in Figure 21, the average PSV and EDV are vessel-diameter dependent. The ratio between PSV and EDV for each method (baseline, iBH and BH) was calculated to estimate the variable flow responses of each method.

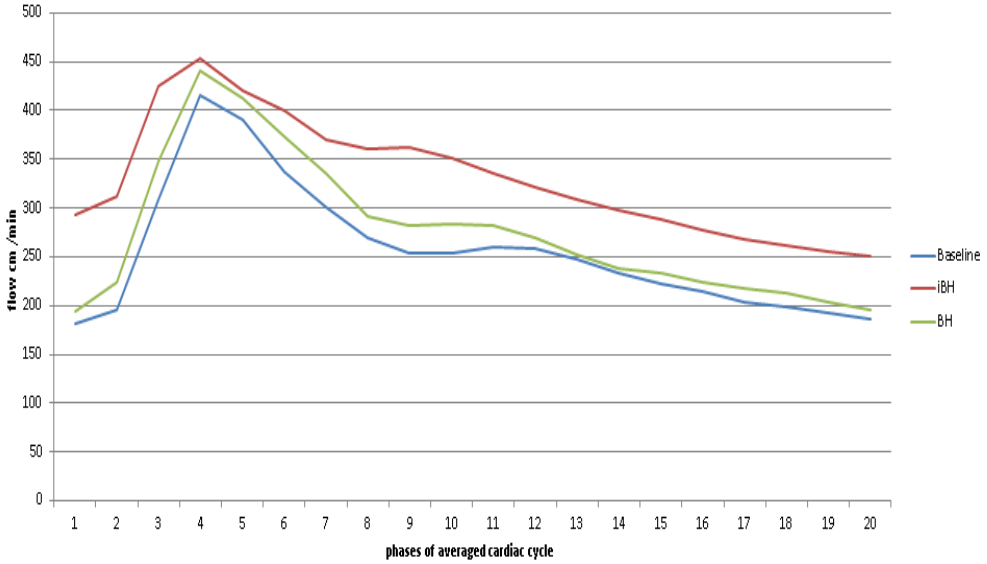

Figure 19: Average flow velocity

(Averaged for two subjects and three main intracranial arteries BA, Rt and Lt ICA), at baseline (blue line), during inspiratory breath-hold (iBH- red line) and non-inspiratory breath hold (BH-green line).

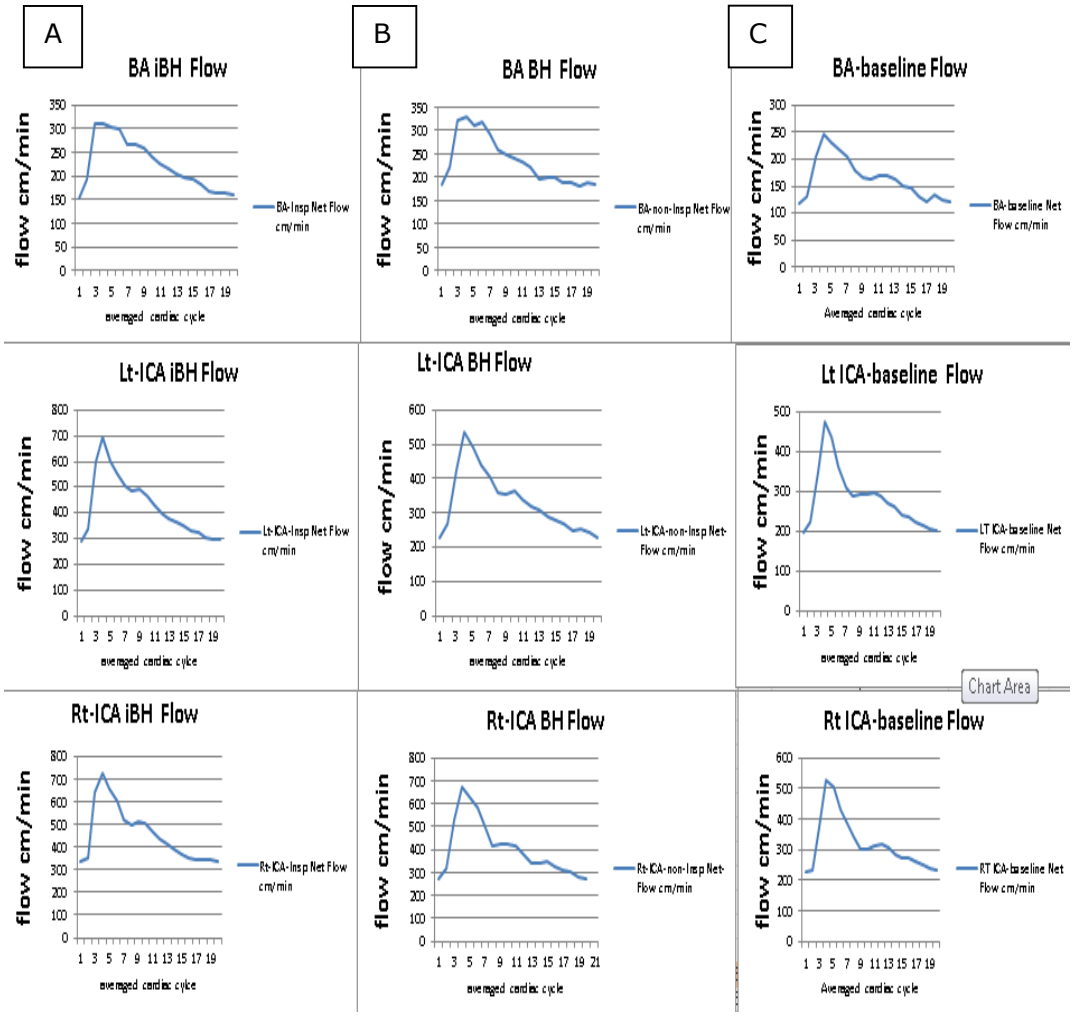

Figure 20 Flow curve through three different arteries

During, A: inspiratory breath-hold (iBH), B: non-inspiratory breath-hold (BH), and D at the baseline. BA basilar artery, LT-ICA left internal carotid artery, RT-ICA right internal carotid artery.

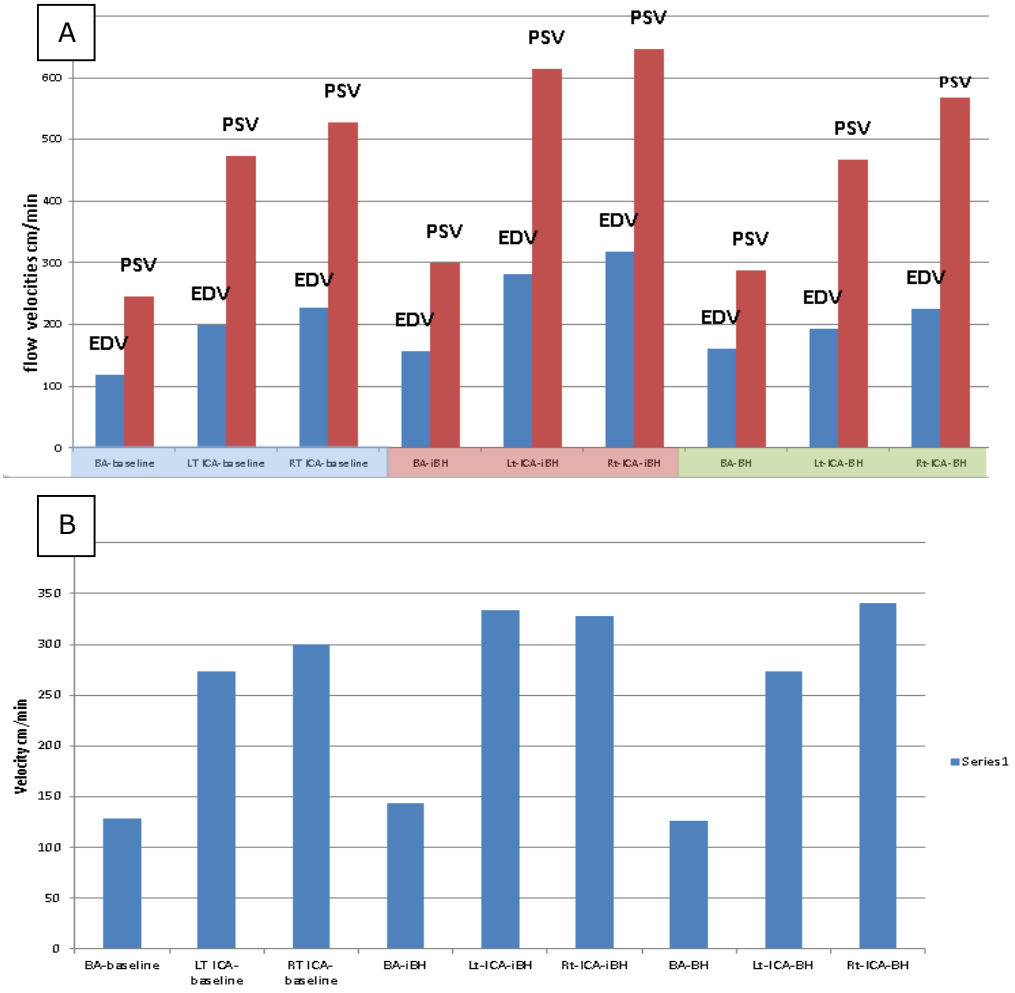

Figure 21: Peak systolic and end diastolic velocities

A, peak systolic velocity (PSV) and end diastolic velocities (EDV) averaged for two subjects at baseline, iBH and BH. (for three major arteries BA, right and left ICA)
B, PSV/EDV ratio for the three arteries at baseline, iBH and BH respectively.

BA Basilar artery, LT-ICA left internal carotid artery, Rt-ICA right internal carotid artery, iBH= inspiratory breath-hold, BH= non-inspiratory breath-hold.

Baseline flow cm/min	iBH flow cm/min	BH flow cm/min
181.412	292.947715	193.629
196.273	312.2775632	224.285
309.5108	425.5821111	347.4152
415.5134	452.5698235	440.6722
390.2252	420.1504188	412.2059
337.1652	399.40952	373.224
300.99	370.1632714	335.5451
268.715	360.2278538	291.9371
253.3792	361.4746417	282.25
254.06	351.1824818	283.3916
259.251	335.60699	281.2385
258.5968	320.5593111	269.4728
247.1162	309.133075	251.5702
232.7044	298.2566571	237.81
222.3494	288.9089167	233.6505
214.5476	277.78708	223.7122
202.7938	267.846	217.0222
199.2822	261.3230333	212.8631
191.7208	255.97855	203.2128
185.8532	250.5607	195.447
256.07296 Average	**330.5972857 Average**	**275.52772 Average**

Table 12 Flow velocity for two subjects at averaged 20 phases of cardiac cycle time points. At baseline, at 33% inspiratory breath-hold (iBH), and at 33% non-inspiratory breath-hold (BH)

5.6 Discussion

The results show an increased flow in response to iBH 29% and BH 7.5%. The difference between the iBH and BH was statistically significant for the averaged twenty phases of the cardiac cycle (P=0.012). There were no recorded changes in the vessel diameter at the baseline, iBH and BH. There was no significant difference for the flow response between the three vessels (P=0.75).

Preliminary results in two subjects show in principle the feasibility of contrast free non invasive time resolved 4D phase contrast MR angiography to quantify the absolute volume flow within specific cerebral vasculature. The beat-to-beat arterial blood pressure was measured continuously within the scanner during the MR angiography acquisition (Figure 22). However, the major limitation of the study was the averaged signal over several cardiac cycles, which led to missing the time-specific flow information within sequential cardiac cycles. Averaging for the total cardiac cycles is essential in 4D MRA technique to provide sufficient SNR and time resolved 3D coverage. Another limitation was the small number of volunteers scanned for this study; this limits the statistical value of comparing the CBF change responses. Only two healthy volunteers were scanned for this feasibility study because of the restricted time of the study. The sequence was lost after a software upgrade of the 3T GE scanner because of the incompatibly with the new software version. Furthermore, this feasibility study was performed to show the possibility of measuring volumetric response changes in the cerebral haemodynamics under the effect of non invasive physiological intervention.

The observed increased flow in both subjects in response to iBH and BH shows the feasibility of this technique for identifying induced changes in the cerebral haemodynamics.

Cardiac gating is a technique that allows for collecting the same data at the same time points in the cardiac cycle for each repetition of the pulse sequence [162]. It has the advantage of monitoring the cardiac cycle prospectively to initiate RF application as well as retrospectively determining the R-R interval within the acquired data. The only drawback is that it has negative effects on time dependent protocols. The averaged signal for total cardiac cycles leads to omission of specific haemodynamic information in particular cardiac cycles. This led to missing the linear relation between the coupled flow response and the acquired beat-beat BP in this experiment. Furthermore, the time point at which the BH was performed was missed after averaging. The breath-hold time points were at the beginning of each minute during the four minutes of the scanning time.

The iBH induced a (1.5-3.2 %) change in the BOLD signal amplitude. As discussed previously, several parameters contribute to developing the BOLD signal amplitude. Furthermore, the baseline cerebral blood volume is an important indicator of the estimated percentage BOLD signal change. This might also be imperative in phase contrast imaging. The convoluted change responses during apnoeic phases and normal breathing in 4D PC MRI might de-emphasize the corresponding changes in flow velocity. Resampling and extracting the flow velocity separately for the apnoeic phase and normal pace breathing might provide a better understanding of the effects of baseline blood volume.

The quantitative reproducibility of 4D PC MRI has been validated in previous studies [74]. The CBF response to transient breath-hold has been quantified

successfully using 2D PC MRI and 30-second BH, and ~64% increase observed in the volume flow of the cerebral vessels on breath holding [105]. This concurs with other study findings that have used acetazolamide to induce flow volume changes (40%-50%) [55, 163, 164]. The data sampling for 2D PC MRI depends on quantifying the haemodynamic difference between two predefined slices in a vessel i.e. the flow velocity is measured at two selected slices within the artery and the haemodynamic change is estimated in relation to the transit time between these slices [98].

The effect of the breath-hold periods was averaged over four breath-holds (20 seconds each) plus the total volume flow during recovery in-between the breath-holds (40 seconds each). In other words, the averaged flow velocity was acquired during 67% normal pace breathing and 33% breath-hold (inspiratory or non-inspiratory). As a consequence, estimating the percentage of the absolute volume flow increase in response to the 20s breath-hold was not applicable at the time. However the 33% breath-hold resulted in a 7.5-29% increase in the total CBF (Figure 19&20). These findings could represent the CA response to transient hyperaemic changes. However, the exact time points of the CBF response change were not acquired because of the averaged signal for the total cardiac cycles.

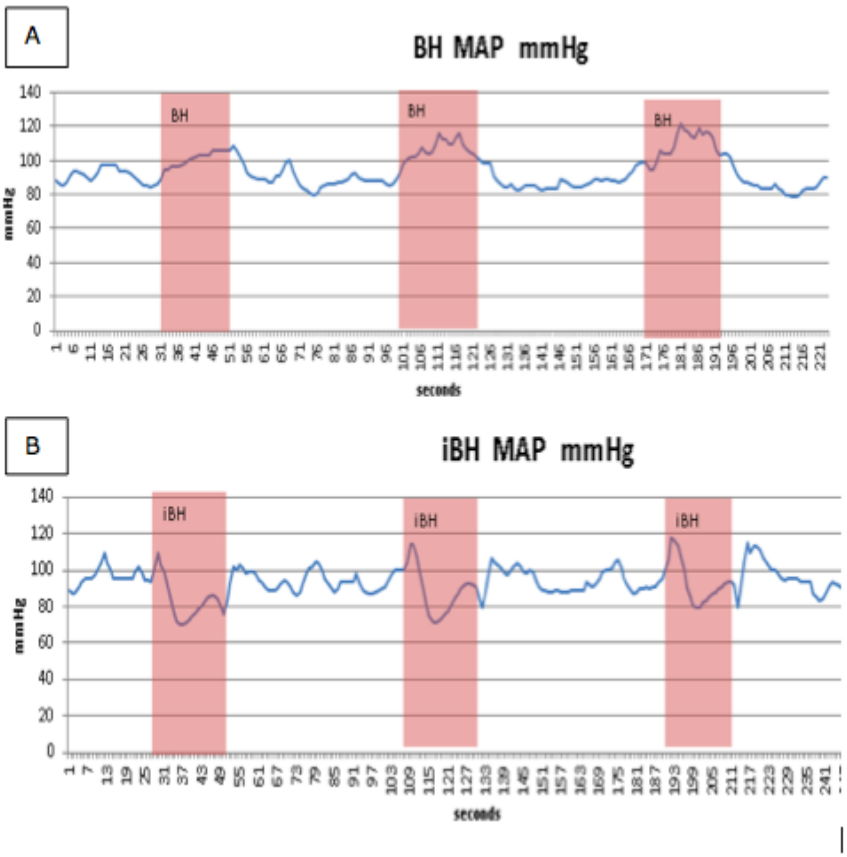

Figure 22 Mean arterial blood pressure (MAP) during BH and iBH protocols

Measured during, A non-inspiratory breath-hold (BH) and B inspiratory breath-hold test (iBH) (23 year old subject; male). Averaging across subjects was not possible because of heart rate variability and different breath-hold response timing.

5.7 Conclusion

The results of this study show that it is possible to measure vessel specific volume flow through cerebral vasculature using time resolved 4D PC MRI at 3T. The volume flow response at the baseline was slightly lower than the iBH and BH response changes. Furthermore, there was a slight difference between the total volume flow of the iBH and BH.

The major limitation of this study was the small sample size as well as the eluded time points at which the volume flow response occurred. Matching the time points of the BH with the consecutive BP data was another limitation of the study. Increasing the sample size and including patient groups will be necessary in future studies to evaluate the effects of a breath-hold test on absolute CBF changes. Using 2D PC MRI with two predefined slice locations may help to match the time interval of the acquired volumetric data.

6 Summary of the work presented in this thesis

This thesis describes the feasibility of using functional MRI to assess dynamic cerebral autoregulation in healthy subjects. Furthermore, this thesis evaluates the common diagnostic methods used to estimate dynamic cerebral autoregulation metrics. In particular, it investigates non invasive approaches to fluctuate arterial blood pressure to allow stimulation of dCA metrics.

The first chapter described the pathophysiology of cerebral haemodynamics and intact autoregulation. It outlined some of the cerebrovascular disorders that are either an outcome or a causal factor of impaired autoregulation. There are two types of autoregulation: static CA, which is cerebrovascular flow adaptation to chronic changes in ABP or CPP; and dynamic CA, which is CBF alternations in response to rapid arterial blood pressure fluctuations. The recent literature has pointed towards a potential benefit of dCA assessment in the diagnosis and follow-up of several critical cerebrovascular disorders such as stroke, traumatic brain injury and dementia. CBFV measures from TCD are used to evaluate dCA metrics in health and disease. The limited spatial resolution of TCD is the only drawback of this technique. The development of fMRI techniques has allowed the assessment of different CBF indices with high temporal resolution as well as anatomical orientation. This has led to the observation of some regional heterogeneity of cerebral autoregulation.

Chapter two systematically reviewed the consistency and reproducibility of non invasive physiological methods used to assess dynamic CA. Measuring dCA metrics depends on several parameters: the CBF quantification tool, the ABP fluctuating method, the analysis methods, and the indices used to represent the autoregulation curve.

The systematic evaluation of 34 studies that used fMRI or TCD to quantify dCA metrics in response to non invasive physiological ABP interventions has revealed

that there is no consistency or standardisation between CA evaluation studies. In the absence of a gold standard it is also not possible to define which method is best. The desired CA evaluation method should be accessible, non invasive and direct to allow its application in daily clinical practice. The quality of CA metrics is related to the CBF quantification technique, the BP fluctuating method and the autoregulation modelling used. The major limitations could be related to the fact that CA is not a concrete value but rather a physiological phenomenon. This makes inter- and intra-individual comparisons of the metrics difficult. Different methods used to induce BP fluctuation and the effects of these methods need to be compared quantitatively and qualitatively.

The third chapter described a pilot study that evaluated and compared the effects of several non invasive physiological interventions to stimulate ABP. Measuring beat-to-beat arterial blood pressure is important in estimating dCA metrics in order to allow better physiological interpretation. To the best of the author's knowledge, no CA study has measured beat-to-beat ABP in a 3T MR scanner. In this pilot study, the MRI compatible Caretaker plethysmographic system was used to estimate continuous ABP from finger pulse pressure. Comparing the BP results with the validated Finometer plethysmographic device validated the results of the Caretaker. Different non invasive interventions were used to stimulate BP. These included thigh-cuff release, inspiratory breath-hold, non-inspiratory breath-hold, and cued deep breathing. The inspiratory breath-hold test resulted in a biphasic BP response change similar to the Valsalva effect. The different BP responses to iBH and BH were preliminary observations of this pilot study. Biphasic BP fluctuation may improve the dynamic CA activation. The TCR method resulted in sharp BP drops of sufficient amplitude. Thus the TCR and iBH methods were selected for use in the MR scanner to induce dynamic flow regulation in the brain.

Chapter four in this thesis investigates the feasibility of estimating dCA metrics using Blood Oxygen Level Dependent BOLD signal fMRI. The beat-to-beat ABP

changes in response to the TCR and iBH tests were obtained at 3T MR scanner. The BOLD signal amplitude depends on the diamagnetic and paramagnetic properties of the oxyhaemoglobin and deoxyhaemoglobin levels in the blood. The signal intensity is mainly affected by the CBF but it is understood that it is also affected by other parameters such as CBV and the metabolic rate. The Time series of BOLD signal amplitude was extracted for different brain regions: GM, WM and the watershed areas (WS). The rate of regulation (RoR) of the BOLD signal amplitude was estimated as an autoregulation index. This is the rate at which the BOLD signal changes according to the underlying BP changes at the given time. The mean arterial blood pressure (MAP) changes in response to the TCR and iBH methods were comparable. The fMRI data indicated the BOLD signal amplitude change in response to the induced fast MAP changes. The GM and WS areas showed similar rates of regulation, and this was nominally higher than the WM RoR in both the TCR and iBH methods.

Chapter five described a preliminary observational study that evaluated the effects of the iBH/BH method on CBF and CBFV. Time resolved 3D Phase Contrast angiography (4D PC MRI) was used to quantify the CBF and CBFV response to iBH in two healthy subjects. The 4D PC MRI data suggested a 29% CBF-increase in response to 33% iBH in a four-minute acquisition time.

The main limitations of this study were the lack of ETCO2 measures and the small number of healthy volunteers recruited because of the restricted time of the study. Other limitations included the technical issues related to the Caretaker device and the beat-to-beat BP resampling, which may have led to blunting the BP-fluctuating curve.

This study demonstrated the feasibility of mapping dCA metrics using functional MRI. Different non invasive physiological methods used to induce BP fluctuations.

Future studies including ETCO2 measures and patient groups may improve the physiological interpretation of dCA metrics.

7 References

1. Powers, W., et al., *Autoregulation of cerebral blood flow surrounding acute (6 to 22 hours) intracerebral hemorrhage.* Neurology, 2001. **57**(1): p. 18-24.
2. Birns, J., et al., *Cerebrovascular reactivity and dynamic autoregulation in ischaemic subcortical white matter disease.* Journal of Neurology, Neurosurgery & Psychiatry, 2009. **80**(10): p. 1093-1098.
3. Detre, J.A. and D.C. Alsop, *Perfusion magnetic resonance imaging with continuous arterial spin labeling: methods and clinical applications in the central nervous system.* European journal of radiology, 1999. **30**(2): p. 115-124.
4. Paulson, O.B., et al., *Cerebral blood flow response to functional activation.* J Cereb Blood Flow Metab, 2010. **30**(1): p. 2-14.
5. Yamauchi, H., et al., *Significance of increased oxygen extraction fraction in five-year prognosis of major cerebral arterial occlusive diseases.* Journal of Nuclear Medicine, 1999. **40**(12): p. 1992-1998.
6. Aaslid, R., et al., *Cerebral autoregulation dynamics in humans.* Stroke, 1989. **20**(1): p. 45-52.
7. Bishop, C., S. Powell, and D. Rutt, *Transcranial Doppler measurement of middle cerebral artery blood flow velocity: a validation study.* Stroke, 1986. **17**(5): p. 913-915.
8. Leontiev, O., D.J. Dubowitz, and R.B. Buxton, *CBF/CMRO2 coupling measured with calibrated BOLD fMRI: Sources of bias.* Neuroimage, 2007. **36**(4): p. 1110-1122.
9. Panerai, R.B., *Nonstationarity of dynamic cerebral autoregulation.* Medical engineering & physics, 2013.
10. Panerai, R., et al., *Continuous estimates of dynamic cerebral autoregulation: influence of non invasive arterial blood pressure measurements.* Physiological measurement, 2008. **29**(4): p. 497.
11. Busija, D.W. and D.D. Heistad, *Factors involved in the physiological regulation of the cerebral circulation*. 1984: Springer.
12. Aaslid, R., T.-M. Markwalder, and H. Nornes, *Noninvasive transcranial Doppler ultrasound recording of flow velocity in basal cerebral arteries.* Journal of neurosurgery, 1982. **57**(6): p. 769-774.
13. Ai, L., et al., *Functional MRI detection of hemodynamic response of repeated median nerve stimulation.* Magn Reson Imaging, 2012.
14. Budohoski, K.P., et al., *Cerebral autoregulation after subarachnoid hemorrhage: comparison of three methods.* Journal of Cerebral Blood Flow and Metabolism, 2013. **33**(3): p. 449-456.
15. Emir, U., C. Ozturk, and A. Akin, *Multimodal investigation of fMRI and fNIRS derived breath hold BOLD signals with an expanded balloon model.* Physiological measurement, 2008. **29**(1): p. 49.
16. Hall, E.L., *Quantitative methods to assess cerebral haemodynamics*. 2012, University of Nottingham.
17. Saeed, N.P., et al., *Measurement of cerebral blood flow responses to the thigh cuff maneuver: a comparison of TCD with a novel MRI method.* Journal of Cerebral Blood Flow & Metabolism, 2010. **31**(5): p. 1302-1310.
18. Murphy, K., A.D. Harris, and R.G. Wise, *Robustly measuring vascular reactivity differences with breath-hold: Normalising stimulus-evoked and resting state BOLD fMRI data.* Neuroimage, 2011. **54**(1): p. 369-379.
19. Nöth, U., et al., *Mapping of the cerebral vascular response to hypoxia and hypercapnia using quantitative perfusion MRI at 3 T.* NMR in Biomedicine, 2008. **21**(5): p. 464-472.
20. Serrador, J.M., et al., *MRI Measures of Middle Cerebral Artery Diameter in Conscious Humans During Simulated Orthostasis.* Stroke, 2000. **31**(7): p. 1672-1678.
21. Harel, N., et al., *Origin of negative blood oxygenation level–dependent fMRI signals.* Journal of Cerebral Blood Flow & Metabolism, 2002. **22**(8): p. 908-917.

22. Horsfield, M.A., et al., *Regional Differences in Dynamic Cerebral Autoregulation in the Healthy Brain Assessed by Magnetic Resonance Imaging.* PloS one, 2013. **8**(4): p. e62588.
23. Zaharchuk, G., *Theoretical basis of hemodynamic MR imaging techniques to measure cerebral blood volume, cerebral blood flow, and permeability.* American Journal of Neuroradiology, 2007. **28**(10): p. 1850-1858.
24. van Beek, A.H.E.A., et al., *Cerebral autoregulation: an overview of current concepts and methodology with special focus on the elderly.* Journal of Cerebral Blood Flow & Metabolism, 2008. **28**(6): p. 1071-1085.
25. FitzGerald, M.J.T., G. Gruener, and E. Mtui. *Clinical neuroanatomy and neuroscience*. 2012; Available from: http://search.ebscohost.com/login.aspx?direct=true&scope=site&db=nlebk&db=nlabk&AN=458797.
26. Hesse, B., et al., *Regulation of cerebral blood flow in patients with autonomic dysfunction and severe postural hypotension.* Clinical physiology and functional imaging, 2002. **22**(4): p. 241-247.
27. Girouard, H. and C. Iadecola, *Neurovascular coupling in the normal brain and in hypertension, stroke, and Alzheimer disease.* Journal of Applied Physiology, 2006. **100**(1): p. 328-335.
28. Goode, S., et al., *Carotid endarterectomy improves cerebrovascular reserve capacity preferentially in patients with preoperative impairment as indicated by asymmetric BOLD response to hypercapnia.* European Journal of Vascular and Endovascular Surgery, 2009. **38**(5): p. 546-551.
29. Gordon, A.L., et al., *Cerebral misery perfusion diagnosed using hypercapnic blood-oxygenation-level-dependent contrast functional magnetic resonance imaging: a case report.* Journal of medical case reports, 2010. **4**(1): p. 1-5.
30. Aoi, M.C., et al., *Impaired Cerebral Autoregulation Is Associated with Brain Atrophy and Worse Functional Status in Chronic Ischemic Stroke.* PloS one, 2012. **7**(10): p. e46794.
31. Strebel, S., et al., *Dynamic and static cerebral autoregulation during isoflurane, desflurane, and propofol anesthesia.* Anesthesiology, 1995. **83**(1): p. 66-76.
32. Panerai, R.B., *Assessment of cerebral pressure autoregulation in humans-a review of measurement methods.* Physiological measurement, 1998. **19**(3): p. 305.
33. Lassen, N.A., *Cerebral blood flow and oxygen consumption in man*. 1959: Am Physiological Soc.
34. Tiecks, F.P., et al., *Comparison of static and dynamic cerebral autoregulation measurements.* Stroke, 1995. **26**(6): p. 1014-1019.
35. Paulson, O., S. Strandgaard, and L. Edvinsson, *Cerebral autoregulation.* Cerebrovascular and brain metabolism reviews, 1989. **2**(2): p. 161-192.
36. Greenfield, J., J.C. Rembert, and G.T. Tindall, *Transient changes in cerebral vascular resistance during the Valsalva maneuver in man.* Stroke, 1984. **15**(1): p. 76-79.
37. Newell, D.W., et al., *Comparison of flow and velocity during dynamic autoregulation testing in humans.* Stroke, 1994. **25**(4): p. 793-797.
38. Edvinsson, L., E.T. MacKenzie, and J. McCulloch, *Cerebral blood flow and metabolism*. Vol. 1185. 1993: Raven Press New York:.
39. Moore, S., et al., *3D models of blood flow in the cerebral vasculature.* Journal of biomechanics, 2006. **39**(8): p. 1454-1463.
40. Alastruey, J., et al., *Modelling the circle of Willis to assess the effects of anatomical variations and occlusions on cerebral flows.* Journal of biomechanics, 2007. **40**(8): p. 1794-1805.
41. Alpers, B.J., R.G. Berry, and R.M. PADDISON, *Anatomical studies of the circle of Willis in normal brain.* Archives of Neurology and Psychiatry, 1959. **81**(4): p. 409.
42. Maaly, M.A. and A.A. Ismail, *Three dimensional magnetic resonance angiography of the circle of Willis: Anatomical variations in general Egyptian population.* The Egyptian Journal of Radiology and Nuclear Medicine, 2011. **42**(3–4): p. 405-412.

43. SHENKIN, H.A., M.H. HARMEL, and S.S. KETY, *Dynamic anatomy of the cerebral circulation.* Archives of Neurology and Psychiatry, 1948. **60**(3): p. 240.
44. Gaillard, P.J., et al., *Establishment and functional characterization of an in vitro model of the blood–brain barrier, comprising a co-culture of brain capillary endothelial cells and astrocytes.* European Journal of Pharmaceutical Sciences, 2001. **12**(3): p. 215-222.
45. Baron, J., et al., *Reversal of focal" misery-perfusion syndrome" by extra-intracranial arterial bypass in hemodynamic cerebral ischemia. A case study with 15O positron emission tomography.* Stroke, 1981. **12**(4): p. 454-459.
46. Leoni, R.F., et al., *Magnetic resonance imaging quantification of regional cerebral blood flow and cerebrovascular reactivity to carbon dioxide in normotensive and hypertensive rats.* Neuroimage, 2011. **58**(1): p. 75-81.
47. Aoi, M.C., et al., *Impaired Cerebral Autoregulation Is Associated with Brain Atrophy and Worse Functional Status in Chronic Ischemic Stroke.* PloS one, 2012. **7**(10): p. e46794.
48. Messerli, F.H., *Definition of hypertension.* Clinician's Manual: Treatment of Hypertension, 2010: p. 1-2.
49. Calhoun, D.A., et al., *AHA Scientific Statement.* Hypertension, 2008. **51**: p. 000-000.
50. Immink, R.V., et al., *Impaired cerebral autoregulation in patients with malignant hypertension.* Circulation, 2004. **110**(15): p. 2241-2245.
51. Brickman, A.M., et al., *Long-term blood pressure fluctuation and cerebrovascular disease in an elderly cohort.* Archives of neurology, 2010. **67**(5): p. 564.
52. Faraci, F.M., G.L. Baumbach, and D.D. Heistad, *Cerebral circulation: humoral regulation and effects of chronic hypertension.* Journal of the American Society of Nephrology, 1990. **1**(1): p. 53-57.
53. Dickinson, C.J., *Why are strokes related to hypertension? Classic studies and hypotheses revisited.* Journal of hypertension, 2001. **19**(9): p. 1515-1521.
54. Detre, J.A., et al., *Noninvasive magnetic resonance imaging evaluation of cerebral blood flow with acetazolamide challenge in patients with cerebrovascular stenosis.* Journal of Magnetic Resonance Imaging, 1999. **10**(5): p. 870-875.
55. Eicke, B., et al., *Influence of acetazolamide and CO2 on extracranial flow volume and intracranial blood flow velocity.* Stroke, 1999. **30**(1): p. 76-80.
56. Pantoni, L. and J.H. Garcia, *Pathogenesis of leukoaraiosis a review.* Stroke, 1997. **28**(3): p. 652-659.
57. Wardlaw, J., et al., *Is breakdown of the blood-brain barrier responsible for lacunar stroke, leukoaraiosis, and dementia?* Stroke, 2003. **34**(3): p. 806-812.
58. Bocti C, S.R., Gao FQ, Sahlas DJ, Behl P, Black SE., *A new visual rating scale to assess strategic white matter hyperintensities within cholinergicpathways in dementia.* Stroke., 2005. **36**(10): p. 2126-31.
59. Birdsill AC, K.R., Jonaitis EM, Johnson SC, Okonkwo OC, Hermann BP, Larue A, Sager MA, Bendlin BB., *Regional white matter hyperintensities: aging, Alzheimer's disease risk, and cognitive function.* Neurobiol Aging., 2014. **35**(4): p. 769-76.
60. Fazekas, F., et al., *White matter signal abnormalities in normal individuals: correlation with carotid ultrasonography, cerebral blood flow measurements, and cerebrovascular risk factors.* Stroke, 1988. **19**(10): p. 1285-1288.
61. Matsushita, K., et al., *Periventricular white matter lucency and cerebral blood flow autoregulation in hypertensive patients.* Hypertension, 1994. **23**(5): p. 565-568.
62. Herholz, K., et al., *Regional cerebral blood flow in patients with leuko-araiosis and atherosclerotic carotid artery disease.* Archives of neurology, 1990. **47**(4): p. 392-396.
63. Isaka, Y., et al., *Decreased cerebrovascular dilatory capacity in subjects with asymptomatic periventricular hyperintensities.* Stroke, 1994. **25**(2): p. 375-381.
64. KAWABATA, K., et al., *A comparative I-123 IMP SPECT study in Binswanger's disease and Alzheimer's disease.* Clinical nuclear medicine, 1993. **18**(4): p. 329-336.

65. Zia, E., et al., *Blood pressure in relation to the incidence of cerebral infarction and intracerebral hemorrhage. Hypertensive hemorrhage: debated nomenclature is still relevant.* Stroke, 2007. **38**(10): p. 2681-5.
66. Dawson, S.L., R.B. Panerai, and J.F. Potter, *Serial changes in static and dynamic cerebral autoregulation after acute ischaemic stroke.* Cerebrovascular diseases, 2003. **16**(1): p. 69-75.
67. Eames, P., et al., *Dynamic cerebral autoregulation and beat to beat blood pressure control are impaired in acute ischaemic stroke.* Journal of Neurology, Neurosurgery & Psychiatry, 2002. **72**(4): p. 467-472.
68. Mandell, D.M., et al., *Mapping Cerebrovascular Reactivity Using Blood Oxygen Level-Dependent MRI in Patients With Arterial Steno-occlusive Disease Comparison With Arterial Spin Labeling MRI.* Stroke, 2008. **39**(7): p. 2021-2028.
69. Momjian-Mayor, I. and J.-C. Baron, *The pathophysiology of watershed infarction in internal carotid artery disease review of cerebral perfusion studies.* Stroke, 2005. **36**(3): p. 567-577.
70. Diamond SG, P.K., Boas DA., *A cerebrovascular response model for functional neuroimaging including dynamic cerebralautoregulation.* Math Biosci., 2009. **220**(2): p. 102-17.
71. Hamner, J.W., J.A. Taylor, and C.O. Tan, *Defining the physiology of cerebral autoregulation.* The FASEB Journal, 2013. **27**: p. 925.11.
72. Borogovac, A. and I. Asllani, *Arterial Spin Labeling (ASL) fMRI: Advantages, Theoretical Constrains and Experimental Challenges in Neurosciences.* International Journal of Biomedical Imaging, 2012. **2012**.
73. Leontiev, O. and R.B. Buxton, *Reproducibility of BOLD, perfusion, and CMRO2 measurements with calibrated-BOLD fMRI.* Neuroimage, 2007. **35**(1): p. 175-184.
74. Meckel, S., et al., *Intracranial artery velocity measurement using 4D PC MRI at 3 T: comparison with transcranial ultrasound techniques and 2D PC MRI.* Neuroradiology, 2012.
75. Zhang, R., et al., *Autonomic neural control of dynamic cerebral autoregulation in humans.* Circulation, 2002. **106**(14): p. 1814-1820.
76. Wilcox, T., et al., *Hemodynamic response to featural changes in the occipital and inferior temporal cortex in infants: a preliminary methodological exploration.* Developmental science, 2008. **11**(3): p. 361-370.
77. Ogawa, S., et al., *Brain magnetic resonance imaging with contrast dependent on blood oxygenation.* Proceedings of the National Academy of Sciences, 1990. **87**(24): p. 9868-9872.
78. Glover, G.H., *Deconvolution of Impulse Response in Event-Related BOLD fMRI< sup> 1</sup>.* Neuroimage, 1999. **9**(4): p. 416-429.
79. Kim, D.S., T.Q. Duong, and S.G. Kim, *High-resolution mapping of iso-orientation columns by fMRI.* nature neuroscience, 2000. **3**(2): p. 164-169.
80. Kim, S.G. and S. Ogawa, *Biophysical and physiological origins of blood oxygenation level-dependent fMRI signals.* Journal of Cerebral Blood Flow & Metabolism, 2012.
81. Thees, S., et al., *Dipole source localization and fMRI of simultaneously recorded data applied to somatosensory categorization.* Neuroimage, 2003. **18**(3): p. 707-719.
82. Yücel, M.A., et al., *The possible role of CO2 in producing a post-stimulus CBF and BOLD undershoot.* Frontiers in neuroenergetics, 2009. **1**.
83. Blockley, N.P., V.E.M. Griffeth, and R.B. Buxton, *A general analysis of calibrated BOLD methodology for measuring CMRO< sub> 2</sub> responses: Comparison of a new approach with existing methods.* Neuroimage, 2011.
84. Fox, P.T. and M.E. Raichle, *Focal physiological uncoupling of cerebral blood flow and oxidative metabolism during somatosensory stimulation in human subjects.* Proceedings of the National Academy of Sciences, 1986. **83**(4): p. 1140-1144.
85. An, H. and W. Lin, *Impact of intravascular signal on quantitative measures of cerebral oxygen extraction and blood volume under normo‐and hypercapnic conditions using an asymmetric spin echo approach.* Magnetic Resonance in Medicine, 2003. **50**(4): p. 708-716.

86. Pike, G.B., *Quantitative functional MRI: concepts, issues and future challenges.* Neuroimage, 2012. **62**(2): p. 1234-1240.
87. Marchal, G., et al., *Regional cerebral oxygen consumption, blood flow, and blood volume in healthy human aging.* Archives of neurology, 1992. **49**(10): p. 1013-1020.
88. Uludağ, K., B. Müller-Bierl, and K. Uğurbil, *An integrative model for neuronal activity-induced signal changes for gradient and spin echo functional imaging.* Neuroimage, 2009. **48**(1): p. 150-165.
89. Buxton, R.B., E.C. Wong, and L.R. Frank, *Dynamics of blood flow and oxygenation changes during brain activation: the balloon model.* Magnetic resonance in medicine, 1998. **39**(6): p. 855-864.
90. Bandettini, P.A., et al., *Time course EPI of human brain function during task activation.* Magnetic Resonance in Medicine, 1992. **25**(2): p. 390-397.
91. Davis, T.L., et al., *Calibrated functional MRI: mapping the dynamics of oxidative metabolism.* Proceedings of the National Academy of Sciences, 1998. **95**(4): p. 1834-1839.
92. Mittal, S., et al., *Susceptibility-weighted imaging: technical aspects and clinical applications, part 2.* American Journal of Neuroradiology, 2009. **30**(2): p. 232-252.
93. Bright, M.G., et al., *Characterization of regional heterogeneity in cerebrovascular reactivity dynamics using novel hypocapnia task and BOLD fMRI.* Neuroimage, 2009. **48**(1): p. 166-175.
94. Bright, M.G. and K. Murphy, *Reliable quantification of BOLD fMRI cerebrovascular reactivity despite poor breath-hold performance.* Neuroimage, 2013.
95. Markl, M., et al., *Time‐resolved three‐dimensional phase‐contrast MRI.* Journal of Magnetic Resonance Imaging, 2003. **17**(4): p. 499-506.
96. Markl, M., et al., *Time-resolved 3-dimensional velocity mapping in the thoracic aorta: visualization of 3-directional blood flow patterns in healthy volunteers and patients.* Journal of computer assisted tomography, 2004. **28**(4): p. 459-468.
97. Lotz, J., et al., *Cardiovascular Flow Measurement with Phase-Contrast MR Imaging: Basic Facts and Implementation 1.* Radiographics, 2002. **22**(3): p. 651-671.
98. de Boorder, M.J., J. Hendrikse, and J. van der Grond, *Phase-Contrast Magnetic Resonance Imaging Measurements of Cerebral Autoregulation With a Breath-Hold Challenge A Feasibility Study.* Stroke, 2004. **35**(6): p. 1350-1354.
99. Katsogridakis, E., et al., *Detection of impaired cerebral autoregulation improves by increasing arterial blood pressure variability.* Journal of Cerebral Blood Flow & Metabolism, 2012.
100. Mahony, P.J., et al., *Assessment of the Thigh Cuff Technique for Measurement of Dynamic Cerebral Autoregulation.* Stroke, 2000. **31**(2): p. 476-480.
101. Summors, A.C., A.K. Gupta, and B.F. Matta, *Dynamic cerebral autoregulation during sevoflurane anesthesia: a comparison with isoflurane.* Anesthesia & Analgesia, 1999. **88**(2): p. 341-345.
102. Lagi, A., et al., *Cerebral autoregulation in orthostatic hypotension. A transcranial Doppler study.* Stroke, 1994. **25**(9): p. 1771-1775.
103. White, R.P. and H.S. Markus, *Impaired dynamic cerebral autoregulation in carotid artery stenosis.* Stroke, 1997. **28**(7): p. 1340-1344.
104. Newell, D., et al., *Evaluation of hemodynamic responses in head injury patients with transcranial Doppler monitoring.* Acta neurochirurgica, 1997. **139**(9): p. 804-817.
105. de Boorder, M.J., J. Hendrikse, and J. van der Grond, *Phase-Contrast Magnetic Resonance Imaging Measurements of Cerebral Autoregulation With a Breath-Hold Challenge: A Feasibility Study.* Stroke, 2004. **35**(6): p. 1350-1354.
106. Lindholm, P. and C.E. Lundgren, *The physiology and pathophysiology of human breath-hold diving.* Journal of Applied Physiology, 2009. **106**(1): p. 284-292.
107. Thomas, B., et al., *Assessment of cerebrovascular reactivity using real-time BOLD fMRI in children with moyamoya disease: a pilot study.* Child's Nervous System, 2013. **29**(3): p. 457-463.

108. Lin, Y., et al., *Physiological and conventional breath-hold breaking points.* Journal of applied physiology, 1974. **37**(3): p. 291-296.
109. Birn, R.M., et al., *The respiration response function: the temporal dynamics of fMRI signal fluctuations related to changes in respiration.* Neuroimage, 2008. **40**(2): p. 644-654.
110. Birn, R.M., et al., *Separating respiratory-variation-related fluctuations from neuronal-activity-related fluctuations in fMRI.* Neuroimage, 2006. **31**(4): p. 1536-1548.
111. Brosch, J.R., et al., *Simulation of human respiration in fMRI with a mechanical model.* Biomedical Engineering, IEEE Transactions on, 2002. **49**(7): p. 700-707.
112. Mckay, L.C., et al., *Neural correlates of voluntary breathing in humans.* Journal of Applied Physiology, 2003. **95**(3): p. 1170-1178.
113. G, G., *Autoregulation of cerebral blood flow in newborn babies.* Early Hum Dev, 2005. **81**(5): p. 423-8.
114. Magon, S., et al., *Reproducibility of BOLD signal change induced by breath holding.* Neuroimage, 2009. **45**(3): p. 702-712.
115. Thomason, M.E. and G.H. Glover, *Controlled inspiration depth reduces variance in breath-holding-induced BOLD signal.* Neuroimage, 2008. **39**(1): p. 206-214.
116. Ances, B.M., et al., *Regional differences in the coupling of cerebral blood flow and oxygen metabolism changes in response to activation: Implications for BOLD-fMRI.* Neuroimage, 2008. **39**(4): p. 1510-1521.
117. Bulte, D., et al., *Measurement of cerebral blood volume in humans using hyperoxic MRI contrast.* Journal of Magnetic Resonance Imaging, 2007. **26**(4): p. 894-899.
118. Urbano, F., et al., *Impaired cerebral autoregulation in obstructive sleep apnea.* Journal of Applied Physiology, 2008. **105**(6): p. 1852-1857.
119. Binder, K., et al., *Heat stress attenuates the increase in arterial blood pressure during isometric handgrip exercise.* European journal of applied physiology, 2013. **113**(1): p. 183-190.
120. Weiner, R.B., et al., *The impact of isometric handgrip testing on left ventricular twist mechanics.* J Physiol, 2012. **590**(20): p. 5141-5150.
121. Hartwich, D., et al., *Differential responses to sympathetic stimulation in the cerebral and brachial circulations during rhythmic handgrip exercise in humans.* Experimental Physiology, 2010. **95**(11): p. 1089-1097.
122. Ikemura, T., N. Someya, and N. Hayashi, *Autoregulation in the ocular and cerebral arteries during the cold pressor test and handgrip exercise.* European journal of applied physiology, 2012. **112**(2): p. 641-646.
123. Willie, C.K., et al., *Regional brain blood flow in man during acute changes in arterial blood gases.* J Physiol, 2012. **590**(14): p. 3261-3275.
124. Traon, A.P.-L., et al., *Dynamics of cerebral blood flow autoregulation in hypertensive patients.* Journal of the Neurological Sciences, 2002. **195**(2): p. 139-144.
125. Panerai, R., P. Eames, and J. Potter, *Variability of time-domain indices of dynamic cerebral autoregulation.* Physiological measurement, 2003. **24**(2): p. 367.
126. Marmarelis, V., et al., *Time-Varying Modeling of Cerebral Hemodynamics.* 2014.
127. Marmarelis, V., D. Shin, and R. Zhang, *Linear and nonlinear modeling of cerebral flow autoregulation using Principal Dynamic Modes.* The open biomedical engineering journal, 2012. **6**: p. 42.
128. Marmarelis, V.Z., *Nonlinear dynamic modeling of physiological systems*. Vol. 10. 2004: John Wiley & Sons.
129. Mitsis, G.D., et al., *Modeling of Nonlinear Physiological Systems with Fast and Slow Dynamics. II. Application to Cerebral Autoregulation.* Annals of Biomedical Engineering, 2002. **30**(4): p. 555-565.
130. Zhang, R., et al., *Transfer function analysis of dynamic cerebral autoregulation in humans.* American Journal of Physiology-Heart and Circulatory Physiology, 1998. **274**(1): p. H233-H241.

131. Goode, S.D., et al., *Precision of Cerebrovascular Reactivity Assessment with Use of Different Quantification Methods for Hypercapnia Functional MR Imaging.* American Journal of Neuroradiology, 2009. **30**(5): p. 972-977.
132. Kassner, A., et al., *Blood-oxygen level dependent MRI measures of cerebrovascular reactivity using a controlled respiratory challenge: Reproducibility and gender differences.* Journal of Magnetic Resonance Imaging, 2010. **31**(2): p. 298-304.
133. Chin, K.Y. and R.B. Panerai, *Comparative study of Finapres devices.* Blood Pressure Monitoring, 2012. **17**(4): p. 171-178 10.1097/MBP.0b013e328356e1b3.
134. Markus, H. and M. Harrison, *Estimation of cerebrovascular reactivity using transcranial Doppler, including the use of breath-holding as the vasodilatory stimulus.* Stroke, 1992. **23**(5): p. 668-673.
135. Brodie, F., et al., *Reliability of dynamic cerebral autoregulation measurement using spontaneous fluctuations in blood pressure.* Clinical science, 2009. **116**: p. 513-520.
136. Wszedybyl-Winklewska, M., A.F. Frydrychowski, and P.J. Winklewski, *Assessing changes in pial artery resistance and subarachnoid space width using a non invasive method in healthy humans during the handgrip test.* Acta Neurobiol Exp, 2012. **72**: p. 80-88.
137. Heyn, C., et al., *Quantification of Cerebrovascular Reactivity by Blood Oxygen Level–Dependent MR Imaging and Correlation with Conventional Angiography in Patients with Moyamoya Disease.* American Journal of Neuroradiology, 2010. **31**(5): p. 862-867.
138. Van den Aardweg, J.G. and J.M. Karemaker, *Influence of chemoreflexes on respiratory variability in healthy subjects.* American journal of respiratory and critical care medicine, 2002. **165**(8): p. 1041-1047.
139. Rout, C.C., D.A. Rocke, and E. Gouws, *Leg elevation and wrapping in the prevention of hypotension following spinal anaesthesia for elective Caesarean section.* Anaesthesia, 1993. **48**(4): p. 304-308.
140. Vianna, L.C., A.R.K. Sales, and A.C.L. da Nóbrega, *Cerebrovascular responses to cold pressor test during static exercise in humans.* Clinical physiology and functional imaging, 2012. **32**(1): p. 59-64.
141. Imholz, B.P., et al., *Non invasive continuous finger blood pressure measurement during orthostatic stress compared to intra-arterial pressure.* Cardiovascular research, 1990. **24**(3): p. 214-221.
142. Phillips, A., et al., *Comparing the Finapres and Caretaker systems for measuring pulse transit time before and after exercise.* International journal of sports medicine, 2012. **33**(2): p. 130.
143. Baruch, M.C., et al., *Pulse Decomposition Analysis of the digital arterial pulse during hemorrhage simulation.* Nonlinear biomedical physics, 2011. **5**(1): p. 1.
144. Bos, W.J.W., et al., *Reconstruction of brachial artery pressure from noninvasive finger pressure measurements.* Circulation, 1996. **94**(8): p. 1870-1875.
145. Wesseling, K., *Finger arterial pressure measurement with Finapres.* Zeitschrift fur Kardiologie, 1995. **85**: p. 38-44.
146. IMHOLZ, B.P., et al., *Continuous non invasive blood pressure monitoring: reliability of Finapres device during the Valsalva manoeuvre.* Cardiovascular research, 1988. **22**(6): p. 390-397.
147. Maestri, R., et al., *Noninvasive measurement of blood pressure variability: accuracy of the Finometer monitor and comparison with the Finapres device.* Physiological measurement, 2005. **26**(6): p. 1125.
148. van der Velde, N., et al., *Measuring orthostatic hypotension with the Finometer device: is a blood pressure drop of one heartbeat clinically relevant?* Blood pressure monitoring, 2007. **12**(3): p. 167-171.
149. Sesso, H.D., et al., *Systolic and diastolic blood pressure, pulse pressure, and mean arterial pressure as predictors of cardiovascular disease risk in men.* Hypertension, 2000. **36**(5): p. 801-807.
150. Dawson, S.L., R.B. Panerai, and J.F. Potter, *Critical closing pressure explains cerebral hemodynamics during the Valsalva maneuver*. Vol. 86. 1999. 675-680.

151. Jenkinson, M., et al., *Improved optimization for the robust and accurate linear registration and motion correction of brain images.* Neuroimage, 2002. **17**(2): p. 825-841.
152. Smith, S.M., *Fast robust automated brain extraction.* Human brain mapping, 2002. **17**(3): p. 143-155.
153. Worsley, K., *Statistical analysis of activation images.* Functional MRI: an introduction to methods, 2001. **14**: p. 251-270.
154. Abbott, D.F., et al., *Brief breath holding may confound functional magnetic resonance imaging studies.* Human Brain Mapping, 2005. **24**(4): p. 284-290.
155. Martin Bland, J. and D. Altman, *Statistical methods for assessing agreement between two methods of clinical measurement.* The lancet, 1986. **327**(8476): p. 307-310.
156. Buxton, R.B., *Interpreting oxygenation-based neuroimaging signals: the importance and the challenge of understanding brain oxygen metabolism.* Frontiers in neuroenergetics, 2010. **2**.
157. Winn, H., R. Rubio, and R. Berne, *Brain adenosine production in the rat during 60 seconds of ischemia.* Circulation research, 1979. **45**(4): p. 486-492.
158. Shah, P.J., et al., *Cortical grey matter reductions associated with treatment-resistant chronic unipolar depression. Controlled magnetic resonance imaging study.* The British journal of psychiatry, 1998. **172**(6): p. 527-532.
159. Triantafyllou, C., et al., *Comparison of physiological noise at 1.5 T, 3 T and 7 T and optimization of fMRI acquisition parameters.* Neuroimage, 2005. **26**(1): p. 243-250.
160. Liu, P., et al., *A comparison of physiologic modulators of fMRI signals.* Human Brain Mapping, 2012.
161. Helms, G., H. Dathe, and P. Dechent, *Quantitative FLASH MRI at 3T using a rational approximation of the Ernst equation.* Magnetic Resonance in Medicine, 2008. **59**(3): p. 667-672.
162. Li, D., et al., *Magnetic resonance imaging of coronary arteries.* Coronary artery disease, 1995. **6**(5): p. 368-376.
163. Marstrand, J.R., et al., *Cerebral hemodynamic changes measured by gradient‐echo or spin‐echo bolus tracking and its correlation to changes in ICA blood flow measured by phase‐mapping MRI.* Journal of Magnetic Resonance Imaging, 2001. **14**(4): p. 391-400.
164. Spilt, A., et al., *MR assessment of cerebral vascular response: a comparison of two methods.* Journal of Magnetic Resonance Imaging, 2002. **16**(5): p. 610-616.

Study	Journal	year	Number of subjects	Age (mean±SD) or range	Gender	method/s to measure CA	Features
Katsogridakis et al,	ISCBFM	2012	n=30 C	(31±12)	F=13	TCD	500Hz
Panerai et al,	AJP	2003	n=14 C	Range (21-43)		TCD	2-MHz (QVL-120-SciMed)
Willie et al,	J.Phyysiology	2012	n=26 C	(22±3.2)	F=10	TCD+extracranial U/S	2MHz+10MHz
Mitsis et al,	IEEE	2009	n=12 C	(29±6)	F=3	TCD	2MHz
katsogridakis et al,	Physiol.Meas.	2012	n=10 C	Range (27-63)	F=1	TCD	2MHz
Brodie et al,	clinical science	2009	n=10 C	M=37.5 (21-56)	F=5	TCD	2MHz
Mitsis et al,	IEEE	2004	n=10 C	(30.4±20.1)		TCD	2MHz
Vianna et al,	Clin Physiol Funct Imaging	2012	n=8 C	(25±2)	F=0	TCD	2MHz
Wszedybyl-Winklewska	ACTA Neurobiology	2012	n=26 C	29.3 ± SE 4.0	F=18	TCD	2MHz
Hartwich et al,	Exp Physiology	2010	n=9 C	(22±5)	F=1	TCD	2MHz&8MHz
Ikemura	Eur J Applied Physiology	2012	n=11 C	(26±5)	F=6	TCD	2MHz

Table11: TCD tables healthy control

C=healthy control, F=female, TCD=Trans cranial Doppler ultrasound,

Study	Interventions	Physiological measurements	Tools used for physiological measures	Anatomical localization	Method/s
Katsogridakis et al,2012	Hypercapnia, TCR	ABP, Continuous BPM,ECG, Capnograph	PRBS (OMRON 705C),FP(Finapres), Capnograph(Datex Normocap 200)	MCA	Eighth-order Butterworth low-pass filter (cutt-off frequency 20Hz), Welch averaged periodogram method (estimation of auto& cross-power spectral densities) 102.4s window, 512 samplea&50%overlap.
Panerai et al,2003	(30 s on-off)word generation test	ABP, ECG, PET CO2	FP (Finapres 2300-Ohmeda), Capnograph (Novo matrix),Digital Audiotape(PC-108,Sony)	MCA	transfer function analysis of ABP-CBFV(i.e. input-output)
Willie et al,2012	hypercapnia+hypocapnia	BP,HR,PACO2,IRABG, pressure & analysis(pH,PAO2,PACO2 and Sao2)	FP(Finometer),AN/DG (Power lab/16SPML795,AD Instruments),ABG-analysis system	MCA,PCA,ICA,VA	CVC indices(MAP/mCBV) (MCAv &PCAv)or flow (ICA&VA)
Mitsis et al,2009	Valsalva &Trimethapan drug(ganglionic blockade),LBNP (0-5 mmHg, 0.05Hz)	MABP,HR,PETco2	FP(Finapres),ECG, Nasal cannula, mass spectrometer	MCA	Transfer function analysis ABP-CBFV(i.e. input-output)

Table12: TCD data healthy controls/methods

TCR=thigh cuff release, ABP=arterial blood pressure, BPM= blood pressure monitoring, PRBS=pseudo-random binary sequence, MCA=middle cerebral artery,

PCA=posterior cerebral artery, ICA=internal carotid artery, VA=vertebral artery, CBFV=cerebral blood flow velocity, IRABG= intra-radial arterial blood gas analysis,

PACO2=partial pressure of CO2, HR=heart rate, LBNP=lower body negative pressure, FP=finger plethysmograph, MABP=mean arterial blood pressure.

Study	Interventions	Physiological measurements	Tools used for physiological measures	Anatomical localization	Method/s
katsogridakis et al,2012	TCR	ABP,CBFV	FP(Finapres)	MCA	fourth-order Butterworth(cut off freq. 20Hz), modified periodogram Welch method(spectral density ABP,CBFV,TCIS)
Brodie et al,2009	NON	BP,RR-interval, HR.	Brachial cuff(ANDUA767),FP (Finapres),ECG		inter& intra-subject comparison of ARI, CBFV, RAP& CrCP
Mitsis et al,2004	Hypercapnia	ABP, PETCO2, PETO2, Respiratory volumes.	FP (Finapres), Turbine volume transducer (Sensor Medics. VWM Series), Mass spectrometer(MGA3000)	MCA	Laguerre–Volterra network methodology
Vianna et al, 2012	IHGT&CPT	HR, BP, CO,SV	ECG, FP(Finapres)	MCA	CVCi(mean MCAv/MABP)
Wszedybyl-Winklewska et al, 2012	IHGT	HR, BP, Sub-arachnoid space width & pial artery pulsation	FP(Finapres), NIR-T/BSS	Lt. ACA,SAS, Pial artery response	CBFV , RI
Hartwich et al, 2010	IHGT&CPT	HR,BP,SV,CO,PETCO2	ECG,FP(PortaPress)	Lt. MCA	CBFV & CVCi, FVC.
Ikemura et al, 2012	IHGT&CPT	HR,BP	ECG,FP(FINAPRES)	MCA, STRA,ITRA&RCV	MCA v mean, CVCi

Table13: TCD data healthy controls/methods

IHGT=isometric hand grip test, CPT= cold presser test, Lt. ACA= left anterior cerebral artery, ARI= autoregulatory index, RAP=resistance area product, CO=cardiac output, SV=stroke volume, CVCi= cerebrovascular conductance indices, MCAv= middle cerebral artery velocity, NIR-T/BSS= near infra-red, Trans illumination/ back scattering sounding, RI= resistance index, FVC= forearm vascular conductance, STRA= superior temporal retinal artery, ITRA= inferior temporal retinal artery, RCV=retinal choroidal vasculature, CrCP=critical closing pressure, SAS=sub arachnoid space.

Study	Statistics	Results	Significance
Katsogridakis et al,2012	Shapiro-wilk, ANOVA, paired t-test.	Thigh-cuff ↑ ABP & CBV variability (normocapnic p=0.59)(hypercapnic p=0.96)	Thigh-cuff improved CA impairment sensitivity and specificity AUC increased from 0.746 to 0.859(p=0.031)
Panerai et al,2003	ANOVA, Post hoc comparisons with Shceffe's test, significance level p<0.05 for all tests	during activation coherence function <0.5Hz was significantly increased for Rt MCA (0.36±0.16 vs. 0.26±0.13,p<0.05)& Lt MCA (0.48±0.23 vs. 0.29±0.16,p<0.05)	Brain activation led to changes in the temporal pattern of CBFV. Data suggests that transfer function analysis suggests important changes in dCA during mental activation tests.
Willie et al,2012	one-way ANOVA& Shapiro-Wilk normality(compare ICA - PACO2).Dunnet's post hoc(comparisons to baseline blood gases)	With (35mmHg) hypoxia the relative ↑ in VA diameter was 50% >other vessels (+9% of original). ICA change in diameter (~25%) positively related to changes in PACO2. (R2,0.63±0.26;P<0.05).* P<0.01 **p<0.05	Hypocapnia reactivity was larger in VA than ICA, MCA&PCA, and similar reactivity response to hypercapnia. MCAv& PCAv show smaller reactivity and estimates of flow than VA&ICA
Mitsis et al,2009	non-linear multivariate modeling approach	MABP mmHg (base line 85.7±2.4)(GB 79.4±3.4)(GB+LBNP 73.9±4.5*) MCBFV cm/s (Base line 64.3±4.4)(GB 60.2±3.5**)(GB+LBNP 58.11±3.9) PETCO2 mmHg (Base line 39.7±0.8) (GB 37.0±1.4) (GB+LBNP 36.0±1.6)	MABP& MCBVFV ↓ during ganglionic blockade
katsogridakis et al,2012	Shapiro-wilk (normality), two-way ANOVA (effects of TCIS&MTCP on ABP&HR, ARI estimates), paired t-test. All p<0.05	↑ ABP (P=0.001), CBFV variability (p=0.026).mean HR (p=0.108), HR variability (p=0.350)	No significant difference in CBFV step response (no distortion of autoregulatory parameters from TCIS) no significant sympathetic response elicited.
Brodie et al,2009	ICC	CV of SEM (1.7% CBFV)(100% RAP), ICC was <0.5 for ARI, rising to >0.8 for CBFV& diastolic BP	data demonstrate excellent absolute & relative reliability of CBFV, but ARI is of comparable reliability to heart rate

Table14: TCD data healthy controls/results

MCBFV=middle cerebral blood flow velocity. GB= ganglionic blockade, LBNP=lower body negative pressure, PETCO2=partial pressure of end tidal carbon dioxide, AUC=area under the curve, MCAv=middle cerebral artery velocity, PCAv=posterior cerebral artery velocity, TCIS=thigh cuff inflation sequence, ICC=intra correlation coefficient,

Study	Statistics	Results	Significance
Mitsis et al,2004		MABP (77.2±9.1), PETCO2 (40.0±1.9), MCBFV (59.1±12.3).all PETCO2 power < 0.1Hz which is significantly lower than MCBFV power <0.3Hz.	Data suggests that the CA is strongly non-linear (frequency dependent). Non-linearity is mainly active in low freq. range <0.4Hz. PETCO2 fluctuation, &non-linear interactions between pressure and PETCO2 have considerable effects in <0.4 Hz freq range.
Vianna et al, 2012		MCAv ↑ during IHGT (18.5±2%, P<0.05 vs. rest), ↑ during IHGT+CPT (19.6±2%, p<0.05 vs. rest), not changes during CPT. CVCi evoked by CPT (15 ± 2%, P<0Æ05 versus rest), CVCi reduced by IHGT (8 ± 2%, P<0Æ05 versus CPT).	CVCi reduced during CPT, while that reduction decreased by adding IHGT
Wszedybyl-Winklewska et al, 2012		MABP& HR ↑ (+34.8%, P<0.0001 and +7.9%, P<0.0001, respectively). CBFV not ↑ significantly (+1.0%), RI ↑↑(+12.0%, P<0.05	IHGT evoked a significant increase in pial artery resistance, with a simultaneous decrease in the width of the SAS. With no significant change in CBFV.
Hartwich et al, 2010		HR, FBF, FVC and mean MCAv increased (P <0.05 versus rest), while MAP and CVCi were unchanged and PETCO2 fell slightly (P <0.05 versus rest).	The small reduction in CVCi with cold presser test was similar at rest and during handgrip (approximately −5%).
Ikemura et al, 2012	ANOVA,F value, Dunnet's post hoc test p<0.05	RCV BFV ↑ by 19 ± 9% from resting baseline level during the CPT (P<0.05), while blood flow in the STRA, ITRA and MCAv showed no changes. The CI of the MCA decreased. RCV, ITRA blood flow& mean MCAv ↑ by (8 ± 1%), (9 ± 3%) and (11 ± 4%), respectively, during the IHGT (P<0.05). STRA BF unchanged.	Data suggests that cerebral blood flow velocity was maintained during the CPT, but autoregulation does not work well in the RCV during the CPT and HG

Table15: TCD data healthy controls/results

SAS=sub arachnoid space, CVCi= Cerebro-vascular conductance indices, BF=blood flow, FBF=forearm arterial blood flow, IHGT=isometric hand grip test, CPT=cold presser test, MCAv=middle cerebral artery velocity, FVC=forearm vascular conductance, RCV=retino choroidal vasculature, STRA BF=superior temporal retinal artery blood flow, ITRA=inferior temporal retinal artery, PETCO2=partial pressure end tidal carbon dioxide.

study	year	journal	number of subjects	Gender	Mean (age/yr. ±SD) or(age range)	Scanner	Field strength	sequence
Bright et al,	2013	NeuroImage	n=12 C	F=5	(32±6) years	GE HDx	3T	BOLD
Murphy et al,	2011	NeuroImage	n=12 C	F=5	(29±4.6) years	GE HDx	3T	BOLD
Thomason et al,	2007	NeuroImage	n=13 C	F=6	m=30 range(23-64)	GE	3T	T2*
Boorder et al,	2004	Stroke	n=20 C	F=10	range (22-32)	Philips	1.5T	2D PC MRI
Meckel et al,	2012	Neuroradiology	n=20 C	F=9	range (20-27)	Siemens	3T	2D&4D PC MRI vs. TCD/TCCD
Horsfield et al,	2013	PlOS ONE	n=12 C	F=4	(58±13) range(41-75)	Siemens	3T	Gradient-echo EPI
Saeed et al,	2010	ISCBFM	n=10 C	F=3	(59±15) range (31-75)	Siemens	1.5T	GE- EPI
Magon et al,	2009	NeuroImage	n=11 C	F=6	(31.7±8.3) range(20-42)	Siemens	3T	T2* GE EPI

Table16: MRI data healthy controls demography

2D PC MRI=two dimensional phase contrast MRI, 4D PC MRI= four dimensional phase contrast MRI, GE-EPI= Gradient echo EPI,

study	year	journal	number of subjects	Gender	(Mean age± SD) or(age range)	Scanner	Field strength	sequence
Goode et al,	2009	AJNR	n=16 C	F=7	M=27.7 range(19-34)	Siemens	1.5T	BOLD
Leontiev et al,	2007	NeuroImage	n=10 C	F=5	(32±8)	GE	3T	Simultaneous BOLD and Perfusion(PICORE, PICORE QUIPSS II)
Emir et al,	2008	Physiol.Meas.	n=4 C	F=1	(25±1)	Siemens	1.5T	T2* GE EPI BOLD+ FNIRS
Nöth et al,	2008	NMR Biomed	n=19 C	F=0	(25±2) range(21-28)	Siemens	3T	PCASL+T2* GE EPI
Bulte et al,	2007	JMRI	n=6	F=2	(29±3.7)	Siemens	3T	PASL(Q2TIPS),BOLD
Bright et al,	2009	Neuroimage	EX1 n=9, EX2 n=8	EX1 F=3, EX2 F=3	EX 1(24-54), EX2 (23-32)	GE	3T	BOLD
Kassner et al,	2010	JMRI	N=19 C	F=9	M=(25-42)	GE	1.5T	T2* GE EPI
Ances et al,	2008	NeuroImage	n=13 C	F=9	(21-56)	GE	3T	BOLD & ASL

Table17: MRI data healthy controls demography

EX=experiment, BOLD= blood oxygen level dependent MRI, ASL= arterial spin labeling MRI, PICORE=proximal inversion with a control for off resonance effects, QUIPSS II=quantitative imaging of perfusion using single subtraction (version 2), pCASL= pseudo pulsed arterial spin labeling MRI, PASL=pulsed arterial spin labeling, FNIRS=functional near infrared spectroscopy,

Study	Interventions	Physiological measures	Tools used for physiological measures	Areas of brain covered	TR	TE	Resolution	FOV
Bright et al, 2013	BHT ()	HR, ECG	Finger plethysmograph, nasal cannula, gas analyzer (AEI Technologies, PA)	GM, Insula, thalamus, Putamen, FC,PC,TC,OC,	2000	35	3.5×3.5×4.0	22.4 cm
Murphy et al,2011	BHT exp.(30s PB-20s BH), SENS	Base line end-tidal CO2,	Nasal-cannula, gas analyzer(AEI Technologies, PA)	pre motor cortex, pre-SMA, PCC	3000	35		20.5 cm
Thomason et al,2007	BHT insp.(13.5s SPB-3s prep.-13.5s BH)	Respiration monitor	respiratory monitoring belt(TSD 201, biopac system)	GM Parietal, temporal, PCC)	2000	30		22 cm
Boorder et al,2004	BHT Insp.(30s BH-1 min rest-30s BH)	Respiratory monitor	pressure sensor+ respiratory band	BA, ICAs, SSS and sinus rectus	16	9		250×250 mm
Meckel et al,2012				ICA(C5,C7), MCA, BA	4D(6.8-7.0), 2D(5.3)	4D(4.0-4.4), 2D(2.83_2.86)	2D(0.9×0.7)	4D &2D(220×176)

Table18: MRI studies healthy controls/features

BHT=breathe hold test, BH= breathe hold, SPB= self-paced breathing, GM=grey matter, PC=parietal cortex, TC=temporal cortex, FC=frontal cortex, PCC=posterior cingulate cortex, pre-SMA=pre-supplementary motor area, SSS=superior sagittal sinus, insp=inspiratory, ICA=internal carotid artery, MCA=middle cerebral artery, BA=basilar artery,

Study	Interventions	Physiological measures	Tools used for physiological measures	Areas of brain covered	TR	TE	Resolution	FOV
Horsfield et al, 2013	TCR	base line BP, continuous BP monitoring	Omron BP cuff, non-invasive arterial blood volume clamping(Finapres)	Whole brain	1000	40	3.45*3.45	
Saeed et al, 2010	TCR	base line BP, continuous BP monitoring	Omron BP cuff, non-invasive arterial blood volume clamping(Finapres)	Whole brain, GM	1000	40	3.45*3.45	
Magon et al,2009	BHT Insp.(BH9,BH15,BH21)+42 SPB	respiratory monitoring	Respiratory belt	GM cortex	3000	30		192×192 mm
Goode et al,2009	hypercapnia 10%CO2	continuous BP,HR,AB-Po2	(invivo,siemens,malvern,Pa)MRI compatible	GM,WM, Supratentorial brain, GM-MCA territory	3500	60		192×192 mm
Leontiev et al,2007	5%CO2 hypercapnia, visual stimulus.	PR, RR, PETCO2	Pulse Oximeter, Respiratory Band, gas meter)	GM, primary visual cortex VI.	2000(all sequences)	TE1 9.4-TE2 30)ASL, TE 30 EPI	EPI 3-mm isotropic resolution	EPI 19cm, ASL 24cm.

Table19: MRI data healthy controls/features

TCR=thigh cuff release, GM= grey matter, MCA=middle cerebral artery, WM=white matter, RR=respiratory rate, PETCO2=partial pressure end tidal CO2, SPB=spontaneous paced breathing, BHT=breathe hold test, BH=breathe hold.

study	Interventions	Physiological measures	Tools used for physiological measures	Areas of brain covered	TR	TE	Resolution	FOV
Emir et al,2008	BHT(90s SPB-30s exp.BH)	RR, hbO& hbR (cerebral)		Pre frontal cortex	2000	TE1 9.4-TE2 30)ASL, TE 30 EPI	128×128	192
Nöth et al,2008	Hypercapnia+ Hypoxia	PETO2,PETCO2,SaO2	Gas Analyzer(AE, CD-A and S-3A),pulse oximeter(NONIN 8600FO)	GM	2300-65	TE1 9.4-TE2 30)ASL, TE 30 EPI	3.5mm-3mm	
Bulte et al, 2007	Hyperoxia FiO2 (0.5)	PETO2,PETCO2	Gas Analyzer (CD-3A)(S-3A) AEI Technologies	GM, WM	4500	TE1 9.4-TE2 30)ASL, TE 30 EPI	4×4×6	
Bright et al, 2009	CDB , Hypercapnia 4%CO2, BH	ET gas monitoring	Gas Analyzer(CD-3A)(S-3A)AEI Technologies	MCA and PCA Territories	EX1(2000), EX2(1250)	TE1 9.4-TE2 30)ASL, TE 30 EPI	EX1(2.3×2.3×5), EX2(3.5×3.5×5)	EX1 (220), EX2(225)
Kassner et al,2010	Hypercapnia 8%CO2- Hypocapnia	ET gas monitoring	Capnograph(Capnomac Ultima),(dataq.akron.oh)	GM,WM	2240	TE1 9.4-TE2 30)ASL, TE 30 EPI	200	
Ances et al ,2008	Hypercapnia (5%CO2+21%O2)	PR, respiratory excursions	pulse Oximeter, Resp. Band, gas meter)	subcortical (Lentiform nuclei) cortical(VC)	2500	(TE1 9.4-TE2 30)ASL		24 cm

Table20: MRI data healthy controls/features

BHT=breathe hold test, CDB=cued deep breathing, SPB=Spontaneous paced breathing, RR=respiratory rate, hbO=oxy hemoglobin, hbR=deoxy hemoglobin, SaO2= base line arterial oxygen saturation, FiO2= fractional oxygen concentration, ET= end tidal, VC=visual cortex,

study	software/s	Method/s for analysis and regression	ROI /masks	Statistics method/s	Results	Significance
Bright et al, 2013	AFNI	ROI, GM-CVR (voxel based), BHM (20s linear ramp, Time-scaled ramp, PETCO2).	GM(TC,FC,OC,PC, Insula, putamen, thalamus)	ICC (repeatability of CVR for each BH),paired t-test	ICC values for (20s- LR=0.43) (TS-ramp=0.45) (ETCO2=0.82) Significant (p<0.05). ICC results are equal in all ROIs.	PETCO2 regressors resulted in excellent repeatability (ICC<0.82)in GM, & acceptable repeatability in smaller regions analyzed(ICC<0.4)
Murphy et al,2011	AFNI(3dDeconvolve),FSL(rest, block& event)	Voxel based, BHM(9 regressers), RSfMRI(SBA)	block-fROI (Visual, motor, auditory), RSfMRI-(LMA,pre-SMA,PCC)	paired t-test	Base line PETCO2 (m=39.7, range (35.8-44.4)), BH PETCO2 (m=39.3±8.5) range (26.3-55.7), sine-cosine-model (t-test t=4.36.p=0.001).	Spatial extend of stimulus-evoked activation is improved by expressing BOLD-BH response as a percentage signal increase with respect to absolute PaCo2 (mmHg) change.
Thomason et al,2007		Voxel based, activation maps sine-cosine correlated (signal amplitude).	Whole-brain mask, ROI(TC,PC,PCC)GM	paired t-test	Activation (C-BH 10061±3250%) (UC-BH 9081±3455%) Significant ↑ 10.8 %(t (10) =2.5, p<0.05). BH-Signal intensities (UC-BH 3.96±0.55%)(C-BH 4.16±0.61%)(non-sig↑ 4.8%)(t(10)=1.7,p=0.12)	
Boorder et al,2004		Quantitative flow volume, Max flow velocity.	ICA, BA, Sinus Rectus, SSS)	t-test, Bland-Altman	No sig. diff. in flow and velocity between the first& sec BH. Flow↑ (59% Rt. ICA BHI=1.96) (66% Lt ICA BHI=2.19) (71%BA BHI=2.35) (65%Sinus Rectus BHI=2.16) (62%SSS BHI=2.06). Velocity on BH, (Rt. ICA 48% BHI=1.59)(Lt. ICA 53% BHI=1.76)(BA 47% BHI=1.56)(Sinus Rectus 41% BHI=1.36)(SSS 75% BHI=1.59)	CV=18% for total CBF ↑ (BA& ICA) BETWEEN 1ST and 2nd BH. Combination of PCMRI & BH allows fast, reproducible measurement of VMR.
Meckel et al,2012	EnSight, Matlab	Mean velocity PSV,EDV	ICA(C5,C7), MCA, BA	two-tailed test, CI, Bland-Altman	Mean velocity ± SD (m/s), 4D PC MRI (MCA (M1), PSV 0.88 (0.13), EDV 0.38 (0.08). BA, PSV 0.78 (0.19), EDV 0.36 (0.11). ICA (C5), PSV 0.83 (0.12), EDV 0.35 (0.06). ICA (C7), PSV 0.98 (0.14) EDV 0.44 (0.09). PSV 0.88 (0.13)	Significant for both PSV &EDV in ICA C7 segment, but only for PSV in C5 segment.

Table21: MRI data healthy controls/results

20S-LR = all 20 second ramps, TS-ramp= time scaled ramp, ETCO2= end-tidal CO2 ramps, AFNI=Analysis of functional neuro image, CVR=Cerebro vascular reserve, PC=parietal cortex, TC=temporal cortex, FC=frontal cortex, PCC=posterior cingulate cortex, BHI=breath hold index, LMA=left motor area, SMA=supplementary motor area, RSfMRI=resting state MRI, PC MRI=phase contrast MRI, BH=breath hold, PSV=peak systolic volume, EDV=end diastolic volume, C-BH= controlled breathe hold, UC-BH= un controlled breathe hold, BHM= breathe hold model, fROI=functional region of interest, VMR=vaso-motor reactivity, ICC= inter correlation coefficient

study	software/s	Method/s for analysis and regression	ROI /masks	Statistics method/s	Results	Significance
Horsfield et al, 2013	FSL 4.1.7	ARI, voxel based (MRARI, Signal drop).	Whole-brain, GM-Excluding cerebellum, WM-Excluding cerebellum.	t-test, ANOVA	TCD (↓ of signal whole brain (19%±11%)), MRI, No difference between Rt. And Lt. Hemisphere signal drop. Significant difference between GM and WM signal drop,(GM 1.81%±0.67%),(WM 1.18%±0.59% p<0.001,d=1.75).WM-MRARI(0.702±0.067), GM-MRARI(0.672±0.066 p=0.009 d=0.97), cortices (1.87%±0.72%),cerebellum(1.55%±0.67,p=0.003,d=0.95)	WM exhibited faster recovery than GM (MRARI=0.702vs. 0.672,p=0.009), cerebral cortex showed faster recovery than cerebellum(MRARI=0.669 vs. 0.645.p=0.016)
Saeed et al, 2010		4D Sets(3 Spatial dimensions+240 time point),signal intensity in 8ROI/240-sec.	8 ROI, GM	Z-transformation, ANOVA, C-C values, CoV.	TCD (↓ ABP 19%±11 %(9.3%-59.2%) & ↓CBFV (24%±7 %(4.5%-64.8%). Intra-MRI C-C (Lt. 0.85±0.08) (Rt. 0.83±0.07*). Intra-MRI CoV (Lt. 9.7±5.7) (Rt. 9.2±7.0*). Intra TCD C-C(Lt. 0.70±0.14)(Rt. 0.60±0.17) CoV(Lt. 21.1±14.5)(Rt.30.5±15.1)	No significant amount of motion detected during the 4 min scan MRI-TCR, more consistent results for Intra-MRI results. Sig(Rt hemisphere).MRI C-C show ↑ Intra-subject reproducibility (↓CoV).sig Difference only Rt hemisphere(ANOVA P=0.022)
Magon et al,2009	Voyager QX 1.9.10,Matlab 7.0,SPSS13	4D Volume time course, ROI (cortical GM).	GM-ROI	ANOVA. CoV Intra & inter- subject variability	PSC (BH9, 0.43±0.24) (BH15, 0.80±0.27) (BH21, 1.17±0.25). Volume(BH9, 4.59±4.34)(BH15, 33.54±22.64)(BH21, 61.09±18.54).TTP (BH9,25.95±3.81)(BH15, 31.09±4.3)(BH21, 34.36±3.32) *P<0.05,**P<0.01,***P<0.001	The reproducibility of MRI signal change depends on BH duration, BH21 associated with lowest dispersion of the magnitude of BOLD.
Goode et al,2009	FSL,SPSS 15,STATA	Boxcar & Automated regression model-ETCO2. PSC	WB(Supratentorial), GM, GM-MCA territory, WM.	Student t-test(parametric)&Mann-Whitney U test(non-parametric).CoV	PSC higher for GM than WM. PSC Boxcar (Non-norm GM 2.93±0.68, WM 2.65±0.43) (norm GM 0.42±0.13 mmHg, WM 0.38±0.13 mmHg) Auto (non-norm GM 2.73±0.48, WM 2.54*±0.29) (norm GM 0.40±0.16 mmHg, WM 0.37±0.14 mmHg)p<0.5*.Significant linear correlation PSC&ET CO2 for both methods(Boxcar R2=0.244(P=0.001),(Auto. R2=0.18(P=0.003).	Qualitatively symmetric ↑BOLD signal intensity during Hypercapnia. Linear correlation PSC&ET CO2. no significant non-linear relationship between(PSC& ETCO2) (QUADRATIC TERM)
Leontive et al,2007	AFNI, Matlab	%CBF &%BOLD response to CO2 and FA	6 ROI(according activated voxels)	correlation coefficient	CRC,V1 (8.3±2.1),PICORE-BOLD (C-C=0.5)(8.5±2.7),PICORE-CBF(C-C=0.4)(8.4±2.1),QUIPSS II CBF(C-C=0.5)(9.0±2.7)	The reproducibility was best for CBF-activated method. Among all measures, CMRO2 during activation was the most robust and substantially more stable within individual subjects (CV=7.4%) than across subject pool (CV=36.95%)

Table22: MRI data healthy controls/results

C-C=correlation coefficient, ARI=autoregulatory index, MRARI=MRI derived ARI, ETCO2=end tidal CO2, CoV=coefficient of variation, CMRO2=cerebral metabolic rate of oxygen, TCR=thigh cuff release, PSC= percentage signal change, PICORE=proximal inversion with a control for off resonance effects, QUIPSS II=quantitative imaging of perfusion using single subtraction, MRARI=MRI derived ARI, CV=coefficient variation, WB= whole brain

study	software/s	Method/s for analysis and regression		ROI /masks	Statistics method/s	Results
Emir et al,2008	AFNI	Balloon model, Boxcar, BOLD amplitude	ROI(pre-frontal cortex)	paired t-test	BOLD signal changes varied (0.5%-2.2%) during BHT. The ↑hbR is temporally coincide with post-stimulus undershoot and occurs later than BOLD peak	Data suggests inverse relationship between BOLD amplitude and PaCO2 obtained from the model
Nöth et al,2008	SPM2	Quantitative GM-CBF map		two-tailed student's t-test	↑ In GM-CBF (7.0±2.9) (mean± SEM)/10% ↓ in SaO2. (Positive CBV responders 70%). GM-CBF ↑ by (5.8±0.9%)/1 mmHg ↑ PETCO2.	Data suggests that CBF response to hypoxia is highly variable. Both ↑CBF&↓CBF detected with hypoxia.
Bulte et al, 2007	Matlab , FAST	Voxel wise-global CBV map, GM & WM specific CBV	GM & WM mask+ SSS		Mean CBV (3.77+1.05)mL/100g, GM-CBV (3.93+0.90)mL/100g, WM-CBV (2.52+0.78)mL/100g. Mean GM/WM=1.56	Results are comparable with previous studies
Bright et al, 2009	fsl FLIRT	voxel based BOLD percentage change			BOLD signal change (~0.5-3.0% GM).	Putamen& bilateral medial cortex reached Max signal change several seconds earlier than rest of cortical GM
Kassner et al,2010	FNI, SPM9sigmentation)	pixel by pixel CVR maps(slope of BOLD signal and PETCO2)	GM&WM	ICC	excellent within-day CVR reproducibility GM(ICC=0.92),WM(ICC=0.88),excellent between-day reproducibility in WM(ICC=0.66)	Different gender CVR responses, males exhibited greater CVR by (22%±2%) in GM and (17%±2%)in WM.
Ances, et al 2008	Comparing M & n between cortical and subcortical regions. ROI, CRC	GLM(cardiac and respiratory fluctuation data)	putamen and Globus Pallidus ROI,VC parietal-occipital sulci	paired t-test Sidak correction, p<0.05 & Post hoc Cohen's test	M was similar in both regions (~5.8%), differences in n produced substantially weaker responses (~3.7×)	strong sensitivity to n, suggests, BOLD response amplitudes cannot be interpreted as a quantitative reflection of underlying metabolic changes, particularly when comparing cortical and sub-cortical regions

Table23: MRI data healthy controls/results

GLM=general linear model, CBV=cerebral blood volume, VC=visual cortex, ICC=inter correlation coefficient, CBF=cerebral blood flow, hbR=deoxy hemoglobin concentration, M=a scaling parameter reflecting base-line deoxyhemoglobin, n= ratio of fractional changes in CBF to CMRO2

Study	Year	Journal	Number of subjects	Gender	(Mean age±SD)or (age range)	Pathology	Scanner	Field Strength	Sequence	TR	TE	Resolution	FOV
Heyn et al,	2010	AJNR	n=11 PG	F=7	(10-48)	Moyamoya Disease	GE	3T	BOLD		40	3.75×3.75×4.5	
Donahue et al,	2010	JCBFM	n=8 C, n=7 M-ICAs, n=10 S-ICAs		C(29±5), M-ICAs(72±8), S-ICAs(73±8)	ICA Stenosis	Siemens	3T	iVASO-DS,TOF,DWI	TOF(22), DWI(4.400)	iVASO(18),TOF(43),DWI(93)	iVASO(2.4×2.4×5),TOF(0.75×0.75×1),DWI(1.6×1.6×3.0)(b=1000)	iVASO(240)
Hattingen et al,	2008	Neuroradiology	n=15 C , n=51 PG-SAH	F=34	C 51.3 (19-73),PG 52.1 (30-88)	Aneurysmal SAH	Siemens	1.5T	PW-MRI, DWI, axial T2, axial T2*	TR	PWI(60.7) DWI(123)	Resolution	PWI&DWI(230)

Table:24: MRI patient data/demography

PG= patient group, c= healthy controls, C-C= correlation coefficient, *n*= the ratio of calibrated CBF to the CMRO2), *M*=a scaling parameter reflecting baseline deoxyhemoglobin, iVASO-DS= inflow vascular-space-occupancy with digital subtraction, DWI=diffusion weighted imaging, TOF=time of flight, PWI=perfusion weighted imaging, SAH=sub arachnoid hemorrhage, M-ICA=mild stenosis internal carotid artery, S-ICA= severe stenosis internal artery stenosis,

Study	Comparative study	Method/s	Software/s	ROI /masks	Statistics method/s	Results	Significance	Interventions	Physiological measures	Tools used for physiological measures	Areas of brain covered
Heyn et al, 2010	Angiography(Suzuki score)	Voxel based CVR. least squares regression analysis	AFNI,PRISM	ACA,MCA,PCA	one-way ANOVA, unpaired t-test., C-C	Pearson C-C CVR& Suzuki score MCA (0.7560) ACA (0.6140) P<0.001. ↑Mean CVR (territories with collateral) M+P+ (0.021±0.013), M+P- (0.068±0.031), ↓ mean CVR (terr. Without collateral) (0.20±0.017)	Mean CVR scales non-linearly with extend of vascular steal.	Gas blend (PETCO2 40-50 mmHg)	ET Gas monitoring	Capnograph	ACA, MCA, PCA
Donahue et al,2010		iVASO-DS CBF maps(aCBV, DSC-CBF,DSC-CBV,DSC-MTT)	MCFLIRT, PErfusioN GUI (Penguin)	GM &WM mask	student t-test p<0.01, nonparametric permutation p<0.01	aCBV controls(Rt 1.60±0.10)(Lt 1.61±0.20)no asymmetry, severe stenosis(ips 1.58±0.20) asymmetry (p<0.01)in 41% patients.	iVASO-DS was significantly correlated with DSC-CBF (R=0.67,P<0.01) after accounting for TT discrepancies				GM,WM
Hattingen et al, 2008	DSA	CBF &CBV parameter maps	STROKETOOL 2.0, STATISTICA 7.1	MCA,ACA&BG	Spearman rank C-C	Rt. ACA significant difference between SAH (severe CVS) and Controls (P=0.029). NO significant difference between SAH& Control in MCA, BG significant difference between controls &non-CVS (rCBF, p=0.029) (rCBV, p=<0.001), and with moderate-CVS (rCBF, p=0.017) (rCBV, p<0.01), and sever CVS (p=0.003), between mild and severe CVS (p=0.030).	SAH, rCBV↓ with ↑degree CVS & ↓CBF. ↑rCBV&↑rCBF controls>SAH	IV-contrast(0.1 mmol/kg Gd-DTPA)			ACA, MCA, BG

Table25: MRI patient data/results

aCBF=arterial cerebral blood flow volume, iVASO= inflow vascular-space-occupancy, CVR=Cerebro vascular reactivity, iVASO-DS= inflow vascular-space-occupancy with digital subtraction, rCBF=regional cerebral blood flow, DSC-CBF=industrial standard dynamic susceptibility contrast-CBF, TT=transient time, SAH=sub arachnoid hemorrhage, MTT=mean transit time. BG=basal ganglia, ACA=anterior cerebral artery, MCA=middle cerebral artery, ET=end tidal. M+P- =presence of Moyamoya collaterals but the absence of pial collaterals, M+P+ = presence of Moyamoya and pial collaterals.

Study	Journal	year	Number of subjects	Age (mean+SD) or range	Gender	Method/s to measure CA	Feature	Pathology/ Diagnosis	Interventions	Physiological measurements
Budohoski et al	JCBFM	2013	n=66 PG-SAH	54(33-75)	F=43	TCD, SPECT		DCI	carotid artery short compression	ABP
Troan et al,	Neurological sciences	2002	n=21 C n=21 PG-HTN	PG-HTN (48.9±13.6)	F=8 C&PG	TCD	2MHz	Treated HTN.		ABP, RR, ET respiratory volumes.
Urbano et al,	J.applied Physiology	2008	n=26 C N=26 PG-OSA	C(41±2) PG-OSA(47±2)	C(F=17), PG-OSA(F=3)	TCD	2MHz	OSA	Squatting standing test, 5%CO2(2min)	ABP, PETCO2, Base line poly somnography.
Panerai et al,	Physiol Meas.	2008	n=27 CAA	(61±11)	F=1	TCD	2MHz	Stroke		BP, ET CO2,BPao

Table26: TCD patient data/demography

PG=patient group, C= healthy control, SPECT=Single Photon Emission Computed Tomography, TCD=Trans cranial Doppler, DCI=delayed cerebral ischemia ABP=arterial blood pressure, PETCO2=partial pressure end tidal carbon dioxide, OSA= obstructive sleep apnea, ET=end tidal, BPao=aortic blood pressure

Study	Tools used for physiological meaures	anatomical localization	method/s of analysis	statistics	Software/s	results	significance
Budohoski et al 2013	FP(Finapres)	MCA	THRT, Sxa &Toxa	Parametric testes(Shapiro-wilk test)(significance level 0.05)	SPSS	-ve THRT (Sxa AUC, 0.788.95% CI:0.723 TO 0.854)(TOxa AUC, 0.82, .95% CI:0.769 to 0.885), all three indices accurate in predicting DCI(0-5 day data) (THRT AUC: 0.801,95% CI:0.660 to 0.942)(Sxa AUC: 0.857,95% CI:0.731to0.984)(TOxa AUC: 0.796,95% CI:0.658 to0.934)	Both Sxa and TOxa showed good accuracy in predicting CA. combining all three indices 100% specificity for predicting DCI
Troan et al,2002	FP(Finapres), nasal sensor(Datex Norma-cap, helsiniski)	MCA	CR slope(CR/second during BP decrease)CR(MABP/MCAv	Mann-Whitney test	HEM(Notochords system, France)	similar T1&T2 between two groups(HTN&C)& between HTN groups(treated& non-treated) (controls T1:11.3±3.1s, T2:12±5.9s; HTN T1:11.7±2.5s, T2:10.7±4.5s)	↑BP squatting>supine ($p<0.01$). No significant changes in mean MCA FV between two groups (HTN&C) in squatting and supine. PETCO2 showed lower values in controls significantly in squatting position.

Table27: TCD patient data/results

THRT=transient hyperemic response test, Sxa =TCD based CA indices, Toxa= NIRS based CA indices, TCD= Trans cranial Doppler ultrasound, AUC=area under the curve, MCA=middle cerebral artery, FP=finger plethysmograph, CR=Conductance.

Study	Tools used for physiological measures	anatomical localization	method/s of analysis	statistics	Software/s	results	Significance
Urbano et al, 2008	FP(Finapres), (Beckman-medical Gas-analyzer), Computerized Grass data acquisition system(Astro-Med, west Warwick-RI)	MCA	CR slope, CBFV/MAP (CVC)	F-test (slopes),unpaired t-test between parameters)	MacLab 400	Mean CBFV significantly ↓ in OSA (48±3) controls (55±2) cm/s; P<0.05, OSA has lower rate of recovery of conductance/ given↓ in BP. (OSA 0.06±0.02)(controls 0.20±0.06) cm.s-2.mmHg-1; P<0.05. No evidence of CVR response to CO2 changes.	OSA patients have ↓ CBFV &delayed CVR response to changes in BP but not CO2.
Panerai et al,2008	FP(Finapres),(Millar catheter,BPao),(TINA, Radiometer)	MCA	ARMA(autoregressive moving-average applied to 60s moving average), ARI (0-9)	Non- linear regression, paired t-test (ARI), F-test (intra-subject variability), Pearson C-C&Z-test.		highly significant correlation between continuous ARI of Rt& Lt MCA (Finapres r=0.60±0.20;BP (AO) r=0.56±0.22)& also between continuous ARI estimates derived from Finapres& BP(AO)(Rt. MCA r=0.70±0.22; Lt MCA r=0.74±0.22)	surrogate data showed that the continuous ARI was highly sensitive to the presence of noise in the CBFV signal(bias &dispersion of estimates increased for lower values of continuous ARI

Table28: TCD patient data/results

CVC=Cerebro vascular conductance, C-C=correlation co efficient, CBFV=cerebral blood flow velocity, ARI=autoregulatory index, OSA=obstructive sleep apnea, AO=aorta, BPao=aorta blood pressure, CR=conductance

Appendix 2

Healthy volunteers consent form v1.1 25.1.12

University of Nottingham,

School of Clinical Sciences,

Division of Radiological and Imaging Sciences

Title of Project: **Development and optimisation of novel MRI techniques**

Name of Investigators: **Dr RA Dineen, Prof DP Auer, Dr H Faas, Dr A Awwad**

Dr L Condon, Dr J Dixon, Dr D Rodriguez, A French,

Dr S Reid, Dr S Schwarz, Dr N Altaf

Healthy Volunteer's Consent Form

Please read this form and sign it once the above named or their designated representative, has explained fully the aims and procedures of the study to you

☐ I voluntarily agree to take part in this study.

☐ I confirm that I have been given a full explanation by the above named and that I have read and understand the information sheet given to me which is attached.

☐ I have been given the opportunity to ask questions and discuss the study with one of the above investigators or their deputies on all aspects of the study and have understood the advice and information given as a result.

☐ I agree to comply with the reasonable instructions of the supervising investigator and will notify him immediately of any unexpected unusual symptoms or deterioration of health.

☐ I authorise the investigators to disclose the results of my participation in the study but not my name.

☐ I understand that information about me recorded during the study will be kept in a secure database. If data is transferred to others it will be made anonymous. Data will be kept for 7 years after the results of this study have been published.

☐ I understand that I can ask for further instructions or explanations at any time.

☐ I understand that I am free to withdraw from the study at any time, without having to give a reason for withdrawing.

☐ I confirm that I have disclosed relevant medical information before the study.

☐ In the unlikely event of the imaging showing a significant incidental abnormality, I authorise the investigators to disclose the details of the findings to me and to my General Practitioner, and will provide details of the scan findings to my General Practitioner so that any further investigations or referrals can be made.

Healthy volunteers consent form v1.1 25.1.12

Name: .....

Address: .....

Telephone number: .....

Signature: ..... **Date:** .....

I confirm that I have fully explained the purpose of the study and what is involved to:

.....

I have given the above named a copy of this form together with the information sheet.

Investigators Signature: ..... **Date**: .....

Investigators Name:.....

Study Volunteer Number: .....

University of Nottingham Medical School MR Scanners

Application for use of the Division of Radiological and Imaging Sciences **Protocol Development Ethics (B12012012a) Notes**

1. Maximum 20 volunteers per protocol development project. Please indicate if participants will be scanned more than once per project, and if so, how many times each.

2. Inclusion criteria:

- Adult (age ≥ 18 years)
- Healthy
- Able to fully comprehend the informed consent procedure

Exclusion criteria:

- Inability to complete MRI safety questionnaire and / or informed consent process
- Known contraindication to MRI scanning (for example pacemaker / implanted defibrillator, intracranial vascular clip, implanted programmable device, intra-ocular metallic fragment, etc)
- Current or previous neurological, neurosurgical, psychiatric, cognitive or mood disorder
- Other significant medical condition (specific details to be reviewed by the PI prior to inclusion)
- Claustrophobia
- Pregnant
- Cranioplasty, craniofacial reconstruction, fixed dental brace or other craniofacial metalwork that is likely to cause significant image degradation or artefact

3. Please include relevant info for your project this could include scanning sequences to be used or developed, fmri paradigm design, required equipment etc. If easier, you may attach previously written documents. For fmri paradigms please attach a diagram to show the timings of events and indicated number of repetitions of cycle shown in diagram, total length of scan and how many repeats of the whole scan are necessary. **Please indicate areas for which you anticipate that you will require specialist input in protocol design.**

4. Info on RF coils / visual / buttons response / EEG etc.

The University of Nottingham

MR Volunteer Safety Screening Questionnaire:

NAME	Date of Scan	Date of Birth
ADDRESS	Volunteer Number	
	Ethics Code	
Phone number	Weight	Height if applicable

MR scanning uses strong magnetic fields. For your own safety and the safety of others it is **very important** that you do not go into the magnet halls with any metal in or on your body or clothing. Please answer the following questions carefully and ask if anything is not clear. All information is held in the strictest confidence.

1. Do you have any implants in your body? e.g. replacement joints, drug pumps Y/N
2. Do you have aneurysm clips (clips put around blood vessels during surgery)? Y/N
3. Do you have a pacemaker or artificial heart valve? *(These stop working near MR Scanners)* Y/N
4. Have you ever had any surgery? Please give brief details over. Y/N
   (We do not need to know about uncomplicated caesarean delivery, vasectomy or termination of pregnancy)

5. Do you have any foreign bodies in your body (e.g. shrapnel)? Y/N
6. Have you ever worked in a machine tool shop without eye protection? Y/N
7. Do you wear a hearing aid or cochlear implant? Y/N
8. Could you be pregnant? (Pregnancy tests are available in the female toilets) Y/N
9. Have you ever suffered from tinnitus? Y/N
10. Do you wear dentures, a dental plate or a brace? Y/N
11. Are you susceptible to claustrophobia? Y/N
12. Do you suffer from blackouts, epilepsy or fits? Y/N
13. Do you have any tattoos? (If yes, you may be asked to read and sign another form) Y/N
14. Do you have any body piercing jewellery that cannot be removed? Y/N
15. Do you have any skin patches (trans-dermal patches)? Y/N
16. Do you have a coil in place (IUD) for contraception? Do you know what type? Y/N
17. Do you have any condition that may affect your ability to control your temperature ?
    (e.g. Do you have a fever, cardiovascular disease, hypertension, diabetes or cerebrovascular disease?)
    Y/N
18. Will you remove all metal including coins, body-piercing jewellery, false-teeth, hearing aids etc. before entering the magnet hall? *(lockers available by the changing rooms)* Y/N

Appendix 3

Summary of the Caretaker output files

Several files are saved automatically under the selected directory after activating "save results" option on the GUI control system. These include:

(ETC (asc) __ (time_date).dat contains raw data

ETC (press) __ (time_date).dat contains pressure information data

ETC (log) __ (time_date).dat contains time information and comments written during acquisition process

ETC(Results) __ (time_date).datcontain BP and all necessary information

The files (log) and (Results) are containing the necessary information for recorded physiological data.

The log file contains the time marks and notes that have been set by the operator.

The Results file contains all the necessary BP component information including; the results of the analysis of the data stream, interbeat interval, systole, diastole, time positions (time stamped based on the computer's clock with millisecond resolution), as well as parameters that the algorithm calculates.

Appendix 4

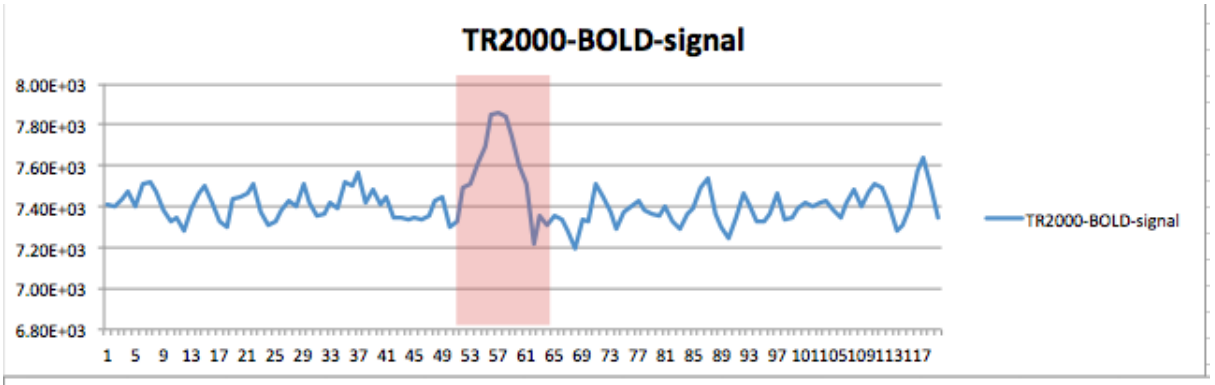
TR2000-BOLD-signal
8.00E+03
7.80E+03
7.60E+03
7.40E+03
7.20E+03
7.00E+03
6.80E+03
1 5 9 13 17 21 25 29 33 37 41 45 49 53 57 61 65 69 73 77 81 85 89 93 97 101105109113117
TR2000-BOLD-signal

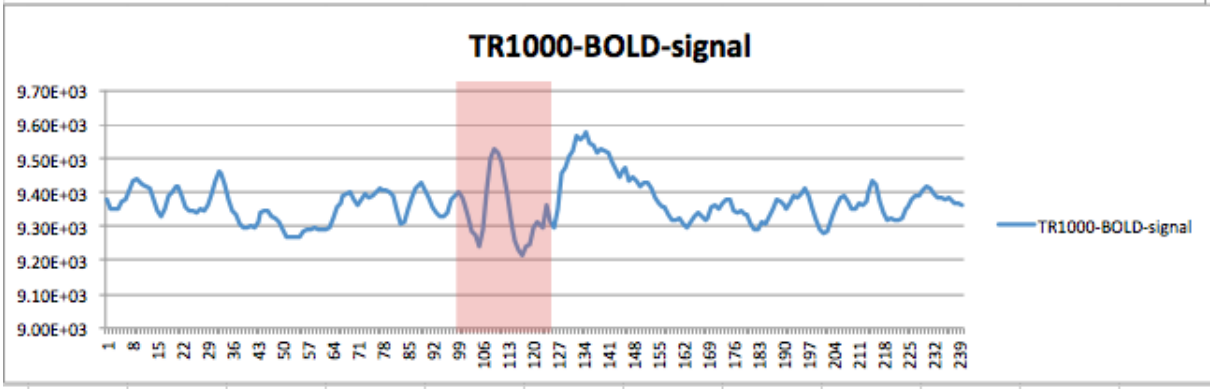
TR1000-BOLD-signal
9.70E+03
9.60E+03
9.50E+03
9.40E+03
9.30E+03
9.20E+03
9.10E+03
9.00E+03
1 8 15 22 29 36 43 50 57 64 71 78 85 92 99 106 113 120 127 134 141 148 155 162 169 176 183 190 197 204 211 218 225 232 239
TR1000-BOLD-signal

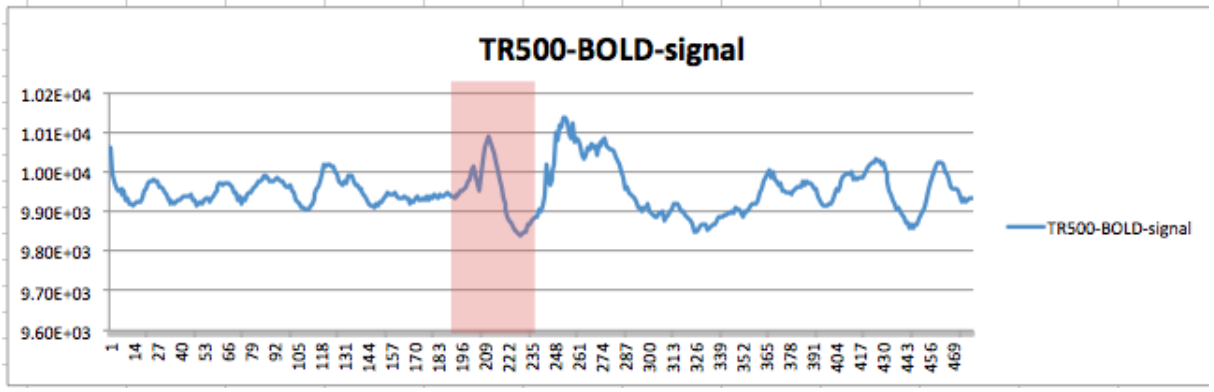
TR500-BOLD-signal
1.02E+04
1.01E+04
1.00E+04
9.90E+03
9.80E+03
9.70E+03
9.60E+03
1 14 27 40 53 66 79 92 105 118 131 144 157 170 183 196 209 222 235 248 261 274 287 300 313 326 339 352 365 378 391 404 417 430 443 456 469
TR500-BOLD-signal